U.L.

UNIVERSITY OF LONDON

Imperial College of Science and Technology

Technical Optics Section

THE VISUAL SIZING OF NON-PERIODIC OBJECTS BY MICROSCOPY

by

William Neil Charman

Thesis submitted for the
Ph.D. (Tech. Optics) degree
1961.

ABSTRACT

A general survey is given of the methods of estimating the size of small objects using visual microscopy. The limitations of such techniques set by the physical and physiological optical arrangements employed are discussed in terms of such theoretical and experimental data as are available. The desirability of further experimental work using objectives of high numerical aperture is stressed.

The production of circular test objects of known diameters in the range 0.1 to 2.8 microns is described. Details are given of the construction of an apparatus to measure the visual size of the image of a test object and the physical light intensity distribution in the image. Results are shown relating the visual size to the true size of the object. Further experimental work shows the dependance of the visual size upon the pre-adaptation of eye and the luminance and angular subtense of the image, these results being discussed in relation to the image light intensity distribution and the characteristics of the eye.

Conclusions are drawn regarding the optimum conditions for high-resolution visual sizing work.

TABLE OF CONTENTS

		Page
CHAPTER 1.	A SURVEY OF THE METHODS OF VISUAL SIZING OF NON-PERIODIC OBJECTS BY MICROSCOPY.	
	1.1. General Introduction	7
	1.2. Introduction to the Methods of Visual Sizing by Microscopy	9
	1.3. Methods Involving the Projection of a Scale onto the Object	12
	1.4. Eyepiece Graticule Methods	13
	1.5. Projection Methods	15
	1.6. Sheared Image Methods	19
	1.7. Methods Involving Mechanical Movement of the Stage or Object	21
	1.8. Count Methods	22
	1.9. Variable Phase Microscope Method	24
	1.10. Miscellaneous Depth Measurement Methods	25
	1.11. Summary of Visual Sizing Methods	28
CHAPTER 2.	THE OPTICAL ERRORS IN SIZING BY VISUAL MICROSCOPY.	
	2.1. Introduction to Sizing Errors	30
	2.2. Factors Affecting the Diffraction Image	32
	2.3. The Diffraction Image of an Opaque Edge	34
	2.4. The Diffraction Images of Circular Objects	37
	2.5. The Visual Assessment of the Diffraction Image	41

		Page
	2.6. High Resolution Sizing Errors	47
CHAPTER 3.	TEST OBJECT PREPARATION	
	3.1. General	49
	3.2. The Production of Circular Apertures of Known Diameter	51
	3.3. The Production of Opaque Discs of Known Diameter	56
CHAPTER 4.	AN APPARATUS TO MEASURE IMAGE INTENSITY DISTRIBUTION AND VISUAL SIZE	
	4.1. General	61
	4.2. The Light Source and Supply	64
	4.3. The Monochromator	64
	4.4. The Microscope	65
	4.5. The Scanning Block Unit	67
	4.6. The Detector and Indicator	71
CHAPTER 5.	OPTICAL DETAILS OF THE APPARATUS	
	5.1. Monochromator Design	73
	5.2. Monochromator Bandwidth	74
	5.3. The Testing of the Microscope Objective	79
	5.4. The Properties of the Scanning Blocks	82
	5.5. Linearity of Image Movement	83
	5.6. Aberrations Introduced by the Blocks	86
	5.7. Geometrical Quality of the Scanning Blocks	89

Page

CHAPTER 6. THE IMAGES OF CIRCULAR APERTURES

6.1. General 93

6.2. Causes of Error in the Experimental Image Profiles 94

6.3. The Effects of Tubelength Variation 99

6.4. The Influence of Condenser Aperture 103

6.5. The Images of Circular Apertures under Full-Cone Illumination 106

CHAPTER 7. THE VISUAL SIZE OF APERTURE IMAGES

7.1. General 114

7.2. The Effect of the Adaptation of the Eye 115

7.3. The Dependance of Visual Size upon Magnification 128

7.4. The Influence of Image Luminance 135

7.5. The Effect of Condenser Aperture 139

CHAPTER 8. THE IMAGES OF OPAQUE DISCS

8.1. General 142

8.2. The Influence of Condenser Aperture 143

8.3. The Occurrence of the Mach Effect 147

8.4. Disc Images Under Full-Cone Illumination 152

Page

CHAPTER 9. DISCUSSION AND CONCLUSIONS

9.1. The Diffraction Images of Small Objects 157

9.2. The Optimum Conditions for Visual Sizing 159

9.3. The Limitations and Errors of Visual Sizing 163

9.4. The Influence of the Observer 168

9.5. Conclusions 169

CHAPTER 1

A SURVEY OF THE METHODS OF VISUAL SIZING OF NON-PERIODIC OBJECTS BY MICROSCOPY

1.1. General Introduction.

Since the earliest days of microscopic observation, those who use the microscope have realised that the size, in terms of the dimensions of the object, as well as the details of the magnified image seen must be recorded. Thus Hooke (1665) in his 'Micrographia' already includes linear scales giving the dimensions of the object with many of his drawings. With the steady increase in use of the microscope, not only in research but also as a tool for controlling industrial processes, the accurate specification of object size in terms of length, area or volume has become an important branch of microscopy in its own right, as well as an inseperable adjunct to other applications.

The need for this size specification in obvious. In industrial chemistry the dimensions of the individual grains of a powder may strongly affect its reactivity and the size of airborne industrial dust is of particular significance in determining the health hazard that it constitutes. In biology too, the relative dimensions of different portions of a structure play a central part in growth experiments, while in metallurgy or mineralogy the relative volumes of the different constituent grains in a specimen strongly affect its mechanical and physical properties. In fact, the

size of an object constitutes one of its most important properties and the optical microscope is one of the few instruments which can measure this parameter for small objects, it being unique in also giving the shape of the object.

However, the microscope can only accurately specify size within certain limits of error, these being imposed by the fact that the image is formed under the laws of physical optics and is not a pure point-to-point magnified geometrical image of the object. Thus each point of the object is imaged as a diffraction pattern, the edges of the object appearing as lines having a finite width, the exact form of the diffraction structure depending upon the degree of coherence of the illumination as well as the nature of the object and objective. There is therefore an uncertainty in the position of the geometrical image of the edge of an object, leading to a corresponding lack of precision in the dimensions of the object as deduced from its image. This uncertainty is of about the same order of magnitude as the resolution limit of microscope objective employed. When the objects are large compared to this resolution limit the proportional error in the estimated object size is small but it becomes of great significance when the objects to be sized approach a micron or less in diameter, when the possible error becomes an appreciable fraction of the true size, even when a high-aperture objective is used. It will be shown that there is a general tendency for the diffraction image to appear

slightly larger than the ideal geometrical image, the exact effect depending not only upon the physical laws governing the formation of the diffraction image but also upon the physiological response of the eye to the image during the visual sizing process.

From the survey of visual sizing methods that follows it will be apparent that almost all of these are affected by this limitation, those which escape it being restricted in their application by other shortcomings.

1.2. Introduction to the Methods of Visual Sizing by Microscopy.

As has been indicated, the size of a small object is one of the most important parameters that a microscope can yield. However the form of the information on the specimen size that is desired from the microscope depends greatly upon the specimen itself and upon the use to which that information is to be put. It is therefore not surprising to find that a variety of sizing techniques have been developed to yield dimensional information on different types of object.

When a limited number of objects are to be sized, either their linear dimensions or their areas are normally measured directly to the degree of accuracy required. With particulate specimens, such as fine powders, pigments or dust particles, where the size of the particles varies considerably, it becomes necessary to specify either an average particle dimension or to determine the size distribution of

the particles, this normally being found in the form of a histogram comprised of a finite number of size groups. For this purpose a 'statistical' diameter is normally taken, generally either Martin's or Feret's. Martin (1923) suggested that the line used as the diameter of each particle should be drawn in one direction so as to divide the area of each particle image in half. He claimed that if a large enough number of randomly orientated particles were taken and if all the lengths were measured parallel to one another, then the same average size would be found as if they were spheres. However the number of particles involved in determining the average is the number in each size-class. Thus at either end of the size-frequency distribution curve where the numbers of particles involved is small, the error in Martin's diameter will be large if the departure from particle sphericity is great. Feret's (1931) statistical diameter is given by the distance apart of two tangents on opposite sides of the particle image, the diameters for different particles all being measured in the same direction. Other methods of expressing particle size include the mean projected diameter, this being the diameter of a circle having an area equal to that of the projected image of the particle and the diameter of the circle of equal perimeter. The mean projected diameter approximates closely to Martin's diameter. Heywood (1945) has suggested that the mean projected diameter is a useful estimate of size when using

eyepiece graticules and that Martin's diameter is a convenient measure of the size when the image is projected onto a screen.

Feret's diameter has been criticised by several authors as leading to gross errors in the sizing of elongated particles, although Walton (1948) has shown that Feret's diameter averaged over all particle orientations is equal to the particle perimeter divided by π, provided that the particle profile is not re-entrant in form. Other discussions of essentially the same statistical aspects of particle sizing include those of Green (1927), Loveland and Trevelli (1927), Heywood (1937) and Chamot and Mason (1958a).

One feature which is common to most methods of visual sizing is the need for calibration with an object of known size. Stage micrometers, consisting of lines ruled at known intervals, are normally used for this purpose and these may be in error. The calibration process should therefore be checked with several micrometers, or the correctness of the micrometer rulings should be verified interferometrically. Brumley and Richardson (1950) have investigated the production of stage micrometers and have devised a technique for their accurate manufacture. A periodic object of this type can be used for calibration since the diffraction images of each part of the periodic structure are the same, so that the intervals between similar parts of the diffraction images can be correctly measured, unlike the dimensions of non-periodic objects.

The various visual methods for the sizing of non-periodic objects using the microscope may be subdivided into the following groups:

Methods involving the projection of a scale onto the object : section 1.3.

Eyepiece graticule methods : section 1.4.

Projection methods : section 1.5.

Sheared image methods : section 1.6.

Methods involving mechanical movement of the stage or microscope : section 1.7.

Count methods : section 1.8.

Variable phase microscope method : section 1.9.

Miscellaneous depth measurement methods : section 1.10.

1.3. Methods involving the Projection of a Scale onto the Object.

The image of an external scale of any type can be projected by the microscope condenser into the plane of the object. In this method, described by Clendinnen (1910), the image of the scale is calibrated in terms of the object size by means of a stage micrometer, which is then replaced by the object. Since the object and scale image are in the same plane, the value of the scale image divisions will be unaffected by any changes in the microscope system used to view the object, provided that the distance between the external scale and the condenser is not altered. By varying this distance, the image divisions can be adjusted to a

convenient number of microns.

The method permits any type of scale to be viewed simultaneously with the object but the condenser must be of good enough quality to give a distortion-free image of the scale and the object must be sufficiently transparent and free of scattering to allow the scale divisions to be seen clearly.

1.4. Eyepiece Graticule Methods.

One of the simplest techniques for measuring the size of an object which is smaller than the field of view of the microscope, applicable at any magnification, is to compare the size of the image of the object with a high-contrast linear scale on a reticle in the focal plane of the eyepiece. The eyepiece scale is calibrated using a stage micrometer. As an alternative to a fixed scale a filar micrometer with a moving crosswire may be used, this giving measurements of greater precision at any point in the field of view. With individual objects, dimensions in any desired direction may be measured, but with particulate specimens Martin's or Feret's diameters are normally taken, these being easily measured in the direction of crosswire movement.

Direct linear measurements of this nature on a large number of individual particles are however tiring and a particulate sample is generally classified into a limited number of size groups. Blacktin (1946) has described a simplified linear graticule divided into squares, whose sides correspond to 1, 2, 5 and 10μ, these being used

both to define counting field and to group the particle lengths into five size ranges.

A more rapid technique for particle size grouping involves the use of the mean projected diameter as the parameter of particle size. Here the areas of the particle images are compared with the standard areas of a series of either transparent or opaque circles engraved on an eyepiece graticule. The earliest graticule of this type was that described by Patterson and Cawood (1936), designed for use with a 2mm, x100 objective. The ten globes and circles of the graticule then corresponded to diameters of 0.2, 0.4, 0.6, 0.8, 1.0, 1.25, 1.5, 2.0 and 2.5μ. A rectangular counting field was also included. Fairs (1943, 1951) has suggested many different types of graticule based on the Patterson-Cawood design, and emphasises that little improvement in sizing precision is to be gained by using a progression of circles of common ratio less than $\sqrt{2}$. May (1945) has described a similar graticule with the addition of a series of parallel lines whose separation from a given line increased in a $\sqrt{2}$ progression, so that Martin's and Feret's diameters could also be measured. Watson (1952) has simplified the Patterson-Cawood graticule by including only three globes and circles, corresponding to diameters of 0.5, 2 and 5μ, the particulate sample thus being classified into four size groups. Hamilton et al (1954) further modified Watson's graticule by changing the 2μ to a 2.5μ diameter circle and adding a 1μ diameter circle. In an investiga-

tion into the ease and accuracy of measurement with this graticule, a Patterson-Cawood type and a line graticule similar to May's, they found that the observers expressed a definite preference for the simplified globe and circle type on the grounds that it was easier to use, although the three types of graticule gave equal counting consistency. Heywood (1945) states that there seems to be a general tendency to overestimate particle size when using a globe and circle graticule, although this diminishes with experience. Holdsworth et al (1954) have shown that by standardising techniques and comparing the results of regular cross-checks it is possible to maintain good agreement between well-trained observers in different laboratories when using the globe and circle graticule. Watson and Mulford (1954) using a particle profile test strip were able to show that the sizing bias varied from individual to individual when using the globe and circle graticule and were able to give a quantitative assessment of this bias.

Loveland (1952) has suggested that if all the objects to be sized have a shape that is hexagonal, cubic or otherwise regular in form then it is valuable to make the reference areas of the graticule have the same form.

1.5. Projection Methods.

Many workers prefer projection techniques to 'down the tube' viewing although the American Society for Testing Materials (1951) only recommends this for particles above 2 μ in size. Dunn (1930) and Brown and Yant (1935) are

unanimous in suggesting that projection techniques offer significant improvements in sizing accuracy.

Back or front projection viewing may be used, although direct measurements on the screen with front projection are difficult. At small magnifications with back projection screens the grain size of the screen may make measurements difficult, while at higher magnifications the light intensity may be low. Welford (1961) has suggested the use of two ground and etched glass screens rotating with respect to one another to give an effectively grainless screen of high brightness, this being a development of an earlier suggestion by MacAdam and Taylor (1946). Loveland (1952) emphasises that for protracted measurements observer comfort is of great importance and recommends the use of a sloping desk-like screen in front of the observer, the images being projected from below.

Green (1921) and Loveland both recommend the use of photomicrography as an intermediate stage when using projection methods, the image first being photographed at one magnification and then projected at a higher magnification, the magnification being determined accurately at each stage. This allows the image contrast in the photomicrograph to be improved during the development process and adequate light intensity in the projected image is easy to obtain even at high magnifications. Wavelengths can be selected outside the visible range to give the best differential absorption of the specimen or short wavelength radiations can be used

to give improved optical resolving power. Photomicrographic methods however suffer from the serious disadvantage as compared with visual methods in that the focus is determined at the time the photograph is made, it being impossible to focus up and down on the particles during their measurement. It is therefore only useful when the particles lie substantially in one plane and where the particle depth does not significantly exceed the depth of focus of the objective.

Whether or not the intermediate stage of photomicrography is used, the object size may either be determined by direct measurement on the screen image or by projecting the image of an eyepiece graticule, as described in section 1.4., simultaneously with the image of the object, lower screen magnifications normally being used in the latter technique. Fairs (1951) has described a method where a graticule is inscribed directly onto the screen and Loveland (1952) recommends that the graticule should be drawn on a transparent plate which can then be moved about on the screen so that the outlines of the standard graticule areas can be superimposed directly on the image. Circles, hexagons or other shapes appropriate to the objects being sized can be used as standard areas.

Where irregular areas, as are frequently found in biological or metallurgical studies, are to be measured a series of graph-like cross hatchings may be superimposed upon the image, the squares covered by the image of the object being counted to give its area. As an alternative

to this rather tedious method a technique due originally to Delesse (1847) may be used. A sheet of uniform transparent material is placed over the screen image, and the outline of the structure whose area is required is drawn round and then cut out, the area of the structure being proportional to the weight of the cut-out tracing. This method has been compared with the square-counting technique by Mainland (1929) and with the use of a planimeter by Scammon and Scott (1927), all three investigators concluding that it was the easier and more rapid method.. Mainland however points out that for small areas of about 5 square mms the cross-hatch method is both quicker and more accurate although for larger areas it rapidly loses efficiency. Loveland (1952) states that a planimeter, though slow, may be used as a calibration check for other methods and advocates for the tracing technique the use of very thin Kodaloid as the transparent sheet material, the outlines being traced round with a hotpoint etching tool to eliminate the extra cutting-out process. Watson and Cruise (1954) used a similar method for determining irregular areas with a Vickers projection microscope. The image outlines were traced with a hard sharp pencil onto tracing paper, particles being focussed in depth to give the maximum boundary. These outlines were then blacked in with indian ink and the areas found by measuring the reduction in the current of a photocell having a strictly linear relationship between the fall in current and the opaque area of the tracing.

As a variation on the straightforward projection technique, a camera lucida may be used to view simultaneously the images of the object and of an external graduated scale. Frechette and Sephton (1949) used this method for particle sizing, the image of one of three scales being viewed with the sample. The scales were designed for use with 2 mm, 4 mm and 8 mm objectives and the particles were grouped according to their Martin's diameters into eleven size ranges from below 1 μ to above 72 μ.

1.6. Sheared Image Methods

In methods based on this principle two indentical coplanar images of the object are produced, the separation of the centres of the images being variable, this distance being equal to the diameter of the object when the two images are arranged to touch. In the apparatus due to Timbrell (1952), designed mainly for sizing spherical particles, the two sheared images are produced by means of a mirror set at 45° to the optical axis of the microscope and sending light into a horizontal eyepiece. The mirror is vibrated about a perpendicular to the optical axis at about 50 c/s, the light source flashing at the extremities of the vibration to give the two laterally sheared images. The magnitude of the shear can be calibrated in terms of the amplitude of the vibration. Timbrell suggests that repeated readings differ from their mean by less than 3% for 1 μ particles and less than 1% for particles greater

than 10μ. McGinn (1956) has used birefringent elements to give the two sheared images, although the magnitude of the displacement is smaller. Barer (1960) uses an optical system similar to the Mach-Zehnder interferometer, the mirror in one arm of the interferometer being rotatable. Two sheared images are thus produced, one by the fixed and one by the moving arm, the magnitude of the separation depending upon the tilt of the moving mirror. Dyson (1960) has described a similar device based on the Mach-Zehnder interferometer in which two identical prism blocks, each consisting of one rhomboidal and one right-angled prism cemented together with a half-silvered interface, are used in each arm of the interferometer, this being inserted between the objective and eyepiece. Relative rotation of the two prism blocks gives a lateral shear between the images from each arm of the system.

All these instruments are best suited to measuring near-spherical particles, it being possible to obtain a direct size distribution in Timbrell's method by modulating the energising current which controls the amplitude of the mirror's vibration with a low frequency square wave. Integrated size distribution curves can be obtained from all the methods by setting the separation at a series of fixed values and counting the number of particles whose sizes lie above and below these values. By altering the direction of the shear the shape and dimensions of an object can be plotted in polar coordinates.

1.7. Methods Involving Mechanical Movement of the Stage or Microscope.

For objects which are larger than the field of view of the microscope, one of the simplest ways of measuring the object size is to use a travelling microscope, the microscope generally being traversed horizontally across the specimen. Crosswire settings are made on the edges of the object and the extent of the movement of the microscope and hence the size of the object is read off on a micrometer drum. Alternatively, a vernier mechanical stage can be used to move the object with respect to the fixed microscope. This technique finds particular application in the use of integrating stages for the assessment of the relative areas of the various components in a rock or metal section, as described by Chamot and Mason (1958b). A series of equally spaced lateral traverses are made across the section and the distances traversed across each grain are recorded on micrometers, a separate micrometer being used for each constituent. The total reading of each micrometer drum corresponds to the total intercept length, this being proportional to the total area of each constituent in the section, providing enough grains are measured.

In these methods the accuracy is restricted by the precision of the mechanical parts to about ten microns. Dunbar (1934) extended this technique to measure objects down to less than 1μ in size by using a mechanical stage with a very fine movement, the motion being measured in

terms of the movement of a system of interference fringes. He also adapted his microscope to measure depth to a similar degree of accuracy.

1.8. Count Methods

These methods only give the average size of a system of particles and are hence normally used for particulate samples whose size range is small or unimportant or for particles which are below the resolution limit of the microscope. The principle is simple. A volume of fluid containing a known weight of the dispersed material is taken and the number of particles in it are counted under the microscope. The weight of the material is then divided by the number of particles to give the average weight $\bar{w}$. Then if the density ρ is uniform throughout the particle dispersion the volume $\bar{v}$ of the average particle is $\frac{\bar{w}}{\rho}$, this being expressed in terms of the diameter of the sphere of equal volume if a linear dimension is required. In practice, if the material is a powder, a known mass is obtained by weighing out, or if it is already in suspension by physical or chemical analysis. The material is then uniformly dispersed in a known volume, the number of particles in an aliquot of this volume being counted.

The average size of any particulate specimen can be determined under normal brightfield conditions, providing the objective is capable of detecting the smallest particles present. The volume in which the particles are counted is

normally measured with an eyepiece counting grid to define the area together with a cell of known depth, or alternatively the microscope may be focussed downwards through a known depth to give the third dimension, allowance being made for the refractive index of the suspending medium.

Very small particles below the detection limit under normal brightfield conditions are counted either using the ultramicroscope described by Seidentopf and Szigsmondy (1903) or a darkfield condenser in conjunction with a cell of known depth. In both these techniques the field appears like the night sky with a grid of squares from the eyepiece graticule superimposed on it, these corresponding to known areas by calibration. In the Szigsmondy ultramicroscope an observing microscope is used to view the cell containing the suspension, this being illuminated from the side by a ribbon of light, particles within the beam scattering light into the observing microscope, where they are counted. The volume in which the count is made is determined by the dimensions of the illuminating beam. Since most of the light is scattered forwards, a very intense light source is required and a further disadvantage is that the edges of the illuminating beam are not sharp, leading to an error in the volume determination. The method is however the most convenient one for many specimens and has found wide application, especially for aerosols.

The alternative technique is to use a darkfield condenser, generally of the cardioid or Cassegrain type, in

conjunction with a cell of known depth, as described by Gehmann and Morris (1932) in their investigations into the average particle size of fine pigments, these condensers allowing far better collection of the scattered light. With very fine particles, cell depths of 2 - 10 μ are used, the important dimension of cell depth being best measured with a channelled spectrum interferometer as described by Gamble and Pfund (1933). In order to eliminate the effect of Brownian movement, either snap counting or a photographic exposure using a xenon flash lamp, as described by Loveland (1952), must be used to 'stop' the motion. These darkfield counting techniques can be used to size particles down to 5 μ but suffer from the disadvantage that extraneous dirt particles cannot be distinguished from the system under observation and that only under exceptional conditions is any shape information given. Their efficiency falls off if any coarse particles, as well as the fine ones, are present, since these scatter larger amounts of light, thus lowering the contrast and making the finer particles difficult to detect.

1.9. Variable Phase Microscope Method.

Osterberg and Pride (1950b) have described a method of measuring the area of unresolved single particles of uniform thickness by variable phase microscopy. The particles must have an effective radius of less than half the Airy limit of the microscope objective, and the method is basically photometric. The particle is viewed with a variable phase-

contrast microscope, such as those described by Osterberg (1947) and Payne (1950, 1954), where the amplitude transmission ratio h and the phase difference δ of the two zones of the diffraction plate are variable, the appearance of the particle image varying with these two parameters. It can be shown that it is possible to find a setting h_1, δ_1 for these two quantities such that the energy density at the centre of the diffraction image of the unresolved particle is zero, or that it can be made to have a minimum value for a system scattering light. If the particle is not opaque, two sets of readings in different refractive index embedding mediums must be taken unless the refractive index of the particle is known. From a knowledge of the parameters h_1 and δ_1 for the particle, it is claimed that the projected areas of particles whose effective radii approach .05 of the Airy limit of the microscope objective can be measured. Since the usual assumptions of scalar diffraction theory are made in the derivation of the theory of this method it is only strictly applicable to low aperture microscope systems.

1.10. Miscellaneous Depth Measurement Methods.

Most methods of object sizing can only measure the dimensions of the object in a plane perpendicular to the axis of the microscope. However in some cases the dimensions of an object parallel to the microscope axis may be required. If it is possible to focus separately on the top and bottom of the object a travelling microscope may be used if the

object is large, or the fine focus calibration of the microscope may be utilised for smaller objects. This technique has been criticised by Galbraith (1955), since the refractive indeces of the object or its surround must be known accurately and he recommends that other methods should be used wherever possible. Richards (1959) points out the poor accuracy of most microscope fine focus calibrations and their lack of linearity of movement. He states that the adjustment should be calibrated at the time of use using an interferometer as described by Beck (1924) or England (1957). This is done simultaneously in the microscope attachment described by Dunbar (1934). Robins (1952, 1954) has described a method of measuring the thickness of fine particles in the range 3 - 76 μ in which a quartz lens is brought into contact with the object slide. By measuring the distance from the contact point of the lens and slide, located by the Newton ring pattern, to where the particle just touches both lens and slide, the thickness of the particle can be calculated with about a 10% error using the spherometer formula and knowing the radius of curvature of the lens. Huitt (1954) has utilised a shadowing technique similar to that used in electron microscopy for the three dimensional measurement of sand grains. The grains are observed under low magnification on a opaque white surface, collimated light being directed obliquely onto them They are then photographed and the dimensions in the plane of the image measured in the normal way, the depth dimension being calculated from the length

of the shadows, an object of known height and shape being used to give the shadowing angle. This method has been further developed by Wright (1957) for the measurement of fine-grained sediments, using evaporated gold as the shadowing material and 20 - 30μ spheres as the standard objects to give the shadowing angle, this being about 20°. This method suffers from the disadvantage that the shadow length depends partly upon the shape of the particles, ellipsoidal particles giving shorter shadows than cubes of the same depth, so that a knowledge of the particle shape is necessary before accurate measurements can be made.

Small differences in height of opaque specimens can be measured by using one of the many interference microscopes designed for the purpose, as reviewed, for example, by Hale (1958). These instruments are also applicable to thickness measurements on transparent specimens providing their optical path length compared with their surround does not exceed a few wavelengths and that the various refractive indeces are known. A very precise method of measuring small differences in height or thickness is the multiple-beam technique due to Tolansky (1948) where fringes are produced between the specimen and an optical flat. It is claimed that differences in surface height of as little as 5 Å can be measured.

1.11. Summary of Visual Sizing Methods

All the methods described in sections 1.3 to 1.7 where measurements are made on the plane of the object lying perpendicular to the optical axis of the microscope are finally limited in their accuracy by the way in which the eye assesses the diffraction image of the edge of the object whose size is required. Of the other methods, the count technique is limited to determining the average size of a large number of similar objects and the variable phase-contrast method is only applicable to objects smaller than the resolution limits of the microscope objective, the objective having to be of low aperture. The depth-measuring techniquesdescribed in section 1.10 are limited to sizing particulate specimens above 3μ in size, with the exception of the multiple beam technique which is best adapted to the measurement of surface irregularities on an extended object. Thus for general visual sizing work with the microscope it is fair to say that the limiting accuracy of the sizing process, assuming that all other errors inherent in the various methods could be eradicated, this being in principle possible, is set by the correct assessment by the eye of the geometrical position of the edges of the object whose size is required with respect to the diffraction image of the edge given by the microscope. This applies both in the case of area or length determinations, an error in linear dimensions giving an error in area dimensions. It will be shown in

Chapter II that the literature contains surprisingly little information on the amount of error inherent in estimating the edge position under various conditions, a description of a series of experiments to investigate some of these effects constituting the remainder of this thesis.

CHAPTER 2

THE OPTICAL ERRORS IN SIZING BY VISUAL MICROSCOPY.

2.1. Introduction to Sizing Errors.

It has long been realised that, since microscope objectives have a finite aperture and utilise light of a finite wavelength, diffraction effects will occur in the image, these not only r-estricting the resolution obtainable with the objective, but also causing a steady gradation of intensity at the edge of an image, giving the edge a hazy appearance. One of the earliest attempts to assess the influence of diffraction upon visual sizing work was that of Nelson (1903, 1904) who noted that a minute hair appeared appreciably larger under dark-field illumination than under bright-field conditions, when viewed with an objective of the same numerical aperture. This he attributed to the diameter of the central disc of the Airy diffraction pattern being added to the true diameter of the hair in one case and subtracted in the other, a theory which, although an obvious over-simplification of the observed facts, nevertheless was of value in stressing the importance of the conditions under which the object was observed. Surprisingly little work followed this early investigation, although Spitta (1920) noted that any measurement on a microscope image must be uncertain within limits comparable to the resolution limit of the objec-

tive employed. Bishop (1934), when using a projection technique for determining the diameter of glass spherules observed that the refractive index of the mounting medium affected the measured size, the size increasing when the refractive index of the mounting medium was decreased. Schelding (1958) investigated quantitatively the differences between the real and apparent sizes of spheres when photomicrography and ultra-violet light were used and found a constant oversize of about a third of the resolution limit of the objective employed. The use of photomicrography however introduces its own sizing errors, quantitative observations on these having been made by Loveland (1952). As far as can be ascertained, no quantitative work using visual methods only has been published, although Loveland states that such work is in progress, using very thin hexagonal platelets as the test objects. Heywood (1945) has however noted that there is a tendency to oversize particle images when using area comparison graticules, Hawkesley (1952) and Loveland agreeing that as the object size approaches the limit of resolution its image tends to appear appreciably larger than the true size of the object. The only attempts to relate the data obtained on the physiology of the eye to the problems of visual observation with the microscope would appear to be those of Hartridge (1954), who discussed the general properties of the eye in relation to the microscope, and Ronchi (1957, 1958), who pointed out the effect of visual factors upon the resolving

power of the microscope and eye when considered as a single system. In addition Fleury (1951) has stressed the dependance of the contrast perception of the eye, and hence its ability to discern details in an image, upon a wide range of visual parameters and Fleury and Matthieu (1956) give details of the results of Arnulf for the visual resolution of Foucault-type test objects as a function of their contrast and luminance when viewed with an ideal objective of N.A = 1.

It can be seen that the field for investigation, though large, is as yet relatively unexplored. In order to understand the factors controlling the apparent size of objects seen with the microscope, two aspects of the visual sizing process must be considered, firstly the form of the physical light intensity distribution in the image and secondly the subjective sensation produced at the eye by that intensity distribution.

2.2. Factors Affecting the Diffraction Image.

The physical light intensity distribution in the image produced by a microscope objective depends on a) the illuminating conditions b) the object and c) the objective.

a) The parameters which define the illuminating conditions are the spectral composition of the light used and its coherence, this depending in effect upon the size of the source used and upon the numerical aperture of the condenser. Hopkins and Barham (1950) have shown that, providing the back aperture of the condenser is evenly illuminated

and that the numerical apertures of the condenser and objective have the same values in both cases, the images formed under Kohler or critical illumination are identical. b) The refractive indeces and absorptions of the object and its surround as well as the three-dimensional geometry of the object affect the intensity distribution in the image. c) The numerical aperture of the objective controls the form of the image, the focal length only affecting its lateral dimensions. Any aberration present in the objective or defects of focus will manifest themselves by causing a change in the distribution of light in the image.

It is not surprising to find that no one general expression has been derived to express the image intensity distribution in terms of all these factors. In fact, all the theoretical investigations that have been made so far have concerned objects of simple shape, that is, straight edges between opaque and transparent areas and objects of circular symmetry, the objects having negligible thickness. The calculations are extremely laborious and the theory as applied is small angle diffraction theory, this only being strictly applicable where the angles of diffraction do not exceed 0.1 radians, the physical theory also being simplified by the assumption that the light disturbance can be represented by a single scalar variable. Since in high-resolution microscopy the objective and condenser may take in cones of light of semi-angles greater than $\frac{\pi}{3}$ radians, the theoretical results so far produced can only be regarded

as being of limited usefulness. However it does appear that there is approximate qualitative agreement between scalar theory and the results obtained with high-aperture systems.

Several authors, including Steel (1953) Marechal (1953) and Slansky (1955), have discussed microscope imagery for certain types of object in terms of the contrast at the centre of the object image, the illumination having varying degrees of coherence. However, in relation to visual sizing work the significant theoretical results are those giving the full intensity distribution in the image.

2.3. The Diffraction Image of an Opaque Edge.

The distribution of light flux in the image of a straight edge between opaque and transparent fields has been calculated for the case of slit-shaped condenser and objective pupils by Canals-Frau and Rousseau (1958). Qualitatively similar, but practically more useful, results have been obtained by Welford (1960a) for the case of circular pupils, using the approximations of scalar diffraction theory. The results of his calculations are shown in figure 2.1. The light flux in the image is normalised in terms of the flux transmitted by the transparent area of the object. The image dimensions are given in terms of 'diffraction units', these being a dimensionless measure of object or image size defined as follows: let η be a dimension in the object plane, then the same dimension in

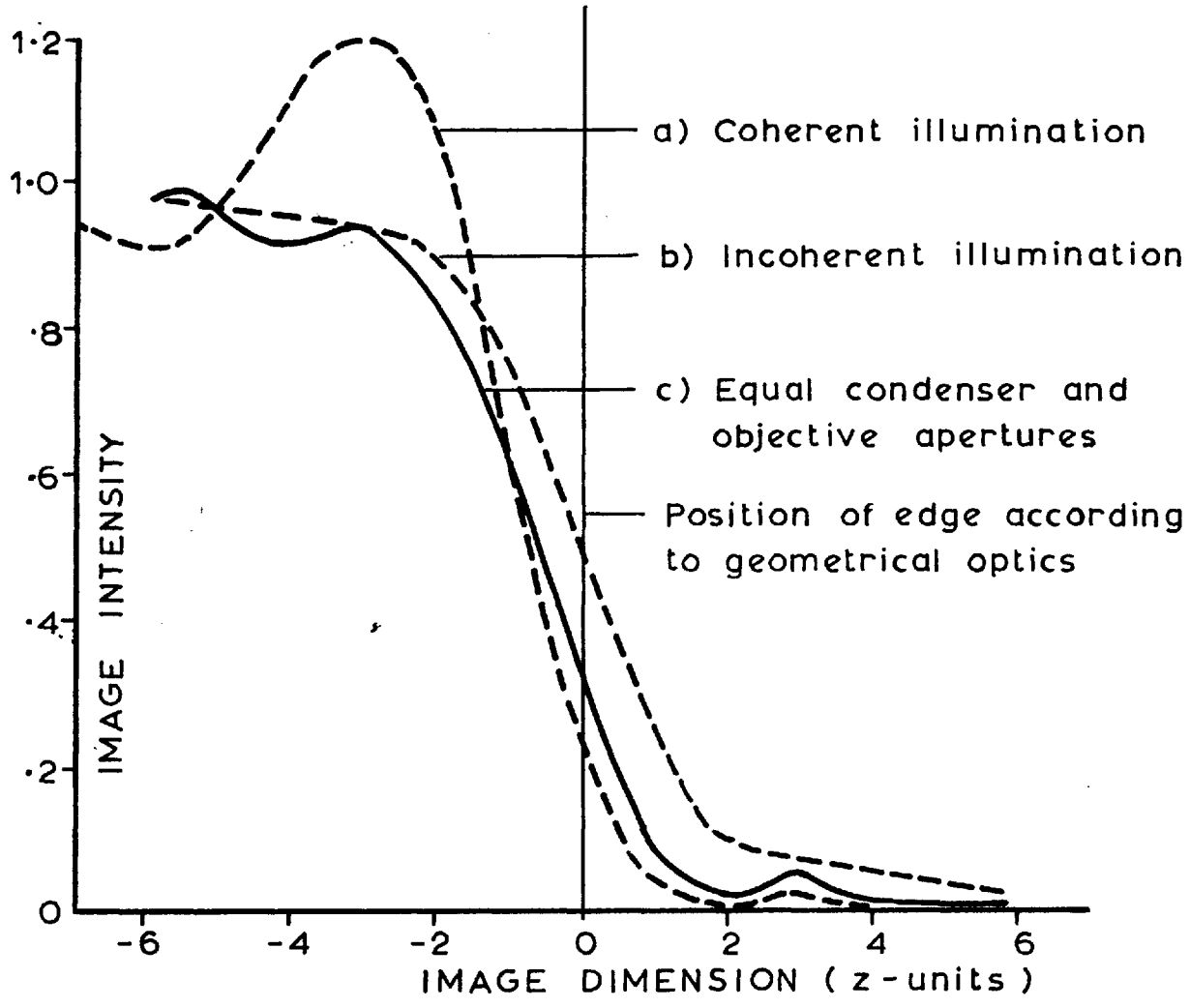

FIG. 2.1 THE DIFFRACTION IMAGE OF A STRAIGHT EDGE (AFTER WELFORD)

diffraction units is denoted by $\underline{Z}$ where

$$\underline{Z} = \frac{2\pi}{\lambda} \; n \sin u \, . \eta$$

λ being the wavelength of the illuminating light in vacuo, $\underline{n}$ the refractive index and $\underline{u}$ the convergence angle of the axial pencil of rays in the object space. The quantities η and λ must be measured in the same units, when $\underline{Z}$ will be dimensionless. Image dimensions can clearly be specified in exactly the same way using the quantities appropriate to the image space.

The three curves shown are for

a) Axial coherent illumination, where the condenser aperture approaches zero.

b) Incoherent illumination, corresponding to a condenser of infinitely large numerical aperture.

c) Conditions where the numerical apertures of the condenser and objective are equal.

The significant feature of these curves is their differing positions with respect to the true geometrical image of the edge of the border. Thus, supposing the distribution of intensity in the image of such an object could be measured, only in the case of incoherent illumination would the true edge correspond to the half-intensity point, such illumination rarely being attained in practice. It can be seen too that there is no one point common to all the curves that can be related to the true edge position. Thus it is clear that the degree of coherence of the illumination will affect any sizing process conducted with the

microscope, the coherence given with an extended source generally being specified in terms of the ratio of the numerical apertures of the condenser and objective, this being the 'S' value of Hopkins and Barham.

2.4. The Diffraction Images of Circular Objects.

The distribution of light intensity in the image of a single uniform opaque or transmitting circular particle in a uniform transmitting surround when the object is illuminated by a narrow cone of axial illumination has been extensively investigated by Osterberg and Pride (1950a). The theory again as applied is scalar diffraction theory, the objective being taken as having uniform transmission across its pupil. Their results are given in terms of the parameters of the particle radius, its optical path difference from its surround and the ratio of its transmission to that of the surround. Fig. 2.2 shows their results for particles of radii 1.15, 2.30, 3.45 and 3.83 z - units for the cases a) where the particles have zero amplitude transmission and b) where their amplitude transmission is the same as that of their surround, but where their optical thickness differs from the surround by half a wavelength. The results have been replotted to give the image dimensions in z-units, the intensity being normalised in terms of that obtained with the surround alone.

Weinstein (1955) has calculated the light flux distribution in the images of incoherently illuminated circular bright and opaque discs. Completely incoherent illumina-

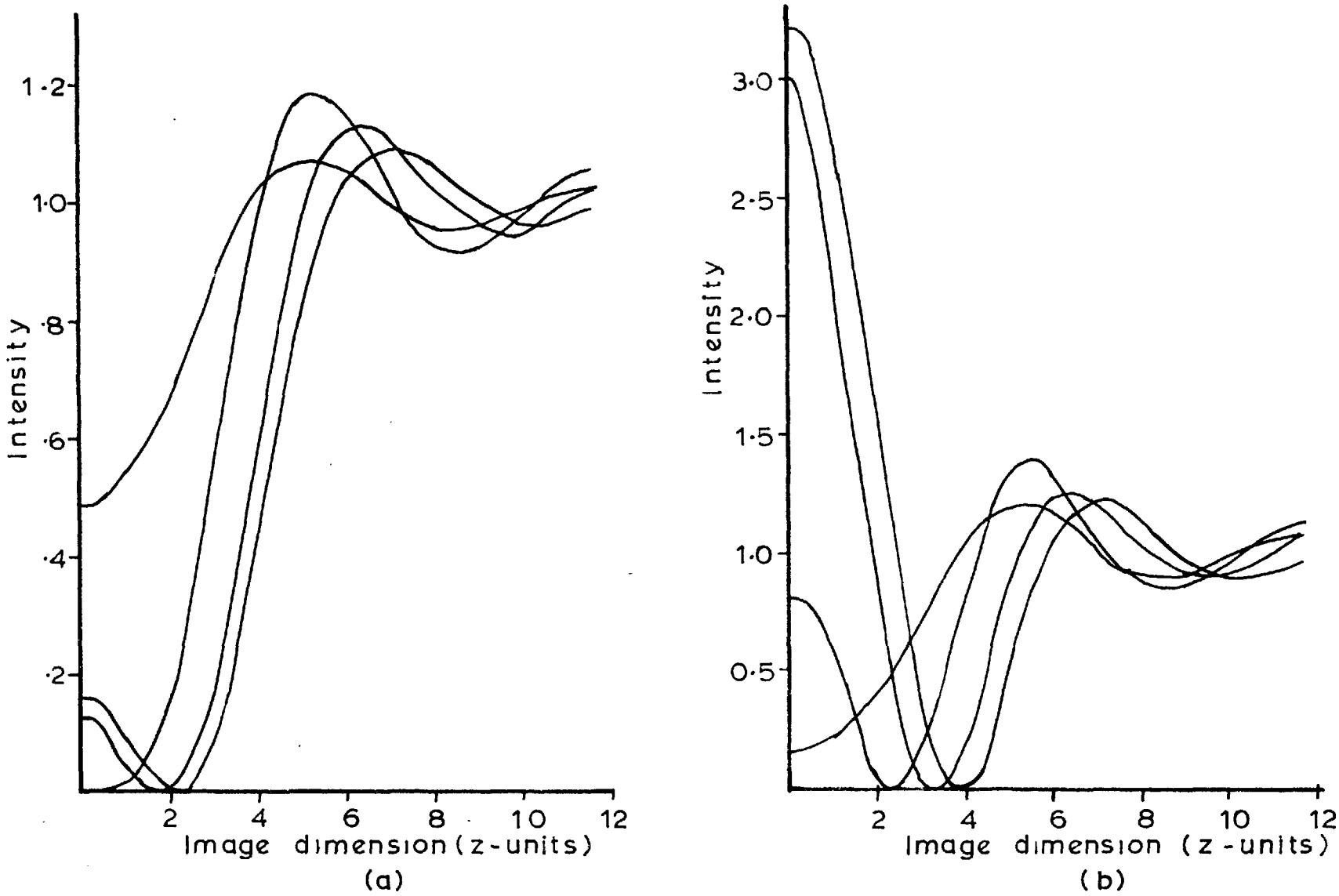

FIG. 2.2 DIFFRACTION IMAGES OF CIRCULAR OBJECTS IN NARROW-CONED AXIAL ILLUMINATION (AFTER OSTERBERG AND PRIDE)

tion rarely exists in microscopy however, so the results are of limited usefulness.

Osterberg and Smith (1960) have extended scalar diffraction theory to cover the case of thin disc-shaped particles in a uniform surround, their solution holding for equal condenser and objective numerical apertures, although the diffraction integrals are stated for any value of condenser aperture. Smith (1960) in a following paper, has computed the energy densities for various types of disc-shaped particle using these results. Examples of Smith's computations are replotted, using the same units as before, in fig. 2.3. a) for the case where the surround is opaque and b) where the particle is opaque and the surround transparent. The results are for particles having radii 0.77, 1.53, 2.30, 3.07, 3.83, 4.60, 5.36 and 7.66 z-units, Smith's results, like those of Osterberg and Pride, being in terms of Airy units, one Airy unit being the radius of the first dark ring of the Airy diffraction pattern i.e. 3.83 z units. This is of course the usually accepted value for the resolution limit of an objective. The interesting features of the curves shown in fig. 2.3 are the comparatively regular form of the image intensity distributions under these conditions and the way in which the intensity at the geometrical images of the edges of the particles, indicated in the figure by the short vertical lines, varies with the particle size. It is clear that as the particle size increases in these two cases, the geometrical image of the edge

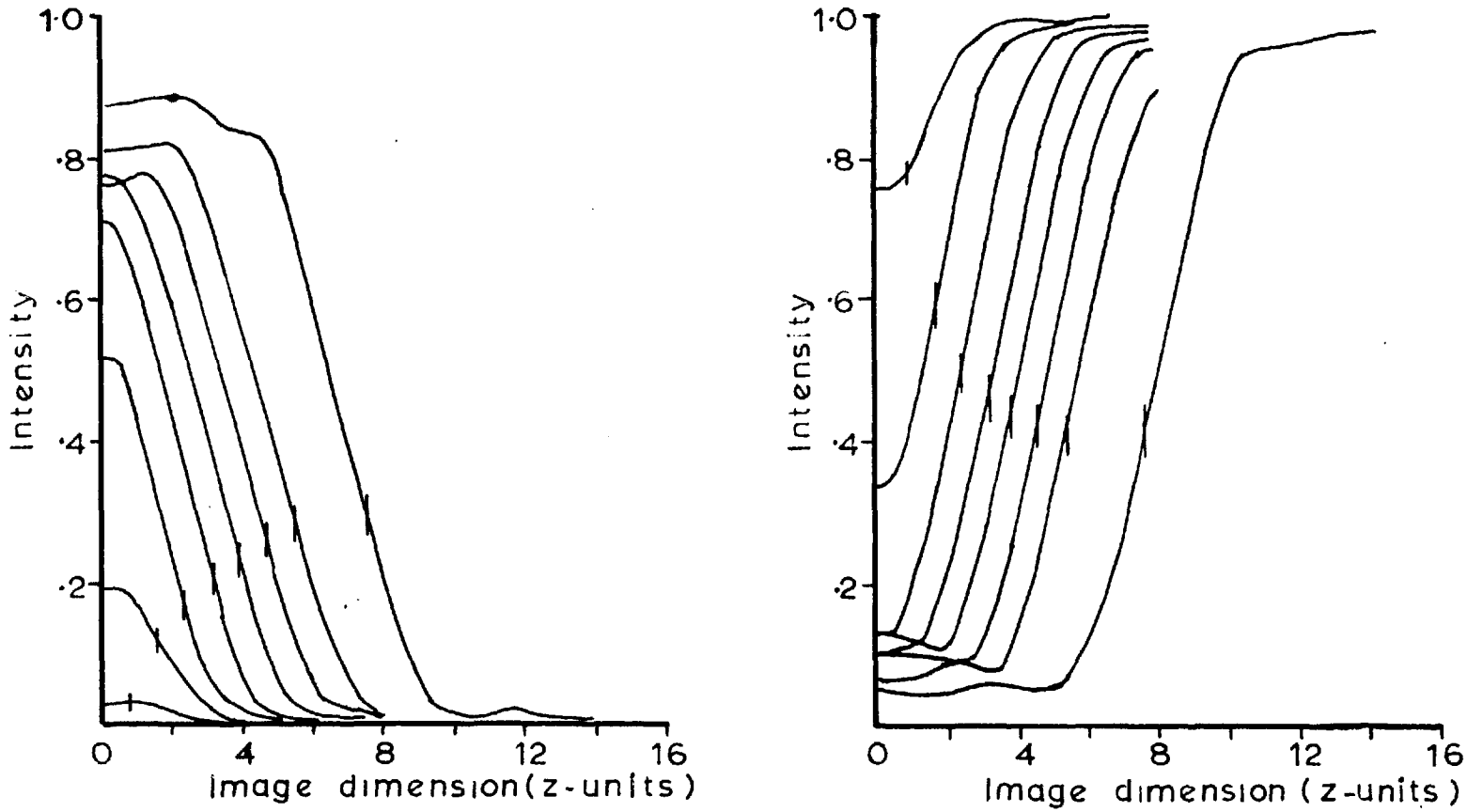

FIG. 2.3 DIFFRACTION IMAGES OF CIRCULAR OBJECTS IN FULL-CONE ILLUMINATION (AFTER SMITH)

appears to be tending towards one-third of the intensity obtained with a transmitting field alone, this being the edge intensity value found by Welford for the case of a straight edge between transparent and opaque fields under the same conditions. Smith has also calculated the form of the diffraction images of particles differing from their surround only in optical thickness or absorption.

Canals-Frau and Rousseau (1958) have calculated the variation in image contrast with the ratio, S, of the numerical aperture of the condenser to that of the objective for opaque discs having radii in the limited range 0.2 to 2 z-units, S varying from 0 to 5. These authors also investigated the case where the object consists of an opaque parallel-sided strip against a clear background when the condenser and objective have slit-shaped apertures. Both types of object were found to show the highest contrast in coherent illumination, a fairly rapid fall in contrast occurring down to S values of about 1.5, further decrease of coherence having little effect on the image contrast.

2.5. The Visual Assessment of the Diffraction Image.

It is evident from the results of diffraction theory described in the preceding sections that the edge of the image of an object will in general show a gradient of intensity, the form of this gradient and its relation to the geometrical image of the object depending upon the

nature of the object and the optical conditions. If now the eye observes such an image, normally with the aid of an eyepiece, it will be presented with a luminance distribution of the same form as the intensity distribution. The subjective impression received by the observer however will be a distribution of brightness that will not, in general, correspond to the luminance distribution of the image.

Before discussing the factors governing the form of the brightness distribution, the criteria to be used for judging visually where the edge of the image lies must be considered. Three types of setting are possible for images in monochromatic light, the 'visual edge' being set at

a) The point where the brightness of the edge gradient is just perceptibly different from that of the object surround

b) The point where the brightness of the edge gradient is just perceptibly different from that at the centre of the image of the object.

c) The point lying midway between the settings a) and b), that is the setting 'midway through the diffuse region' at the edge of the image that has been challenged by Soper (1954). The principle of these three types of setting is shown in fig. 2.4, the luminance distribution given corresponding to that obtained with the image of a straight edge between transparent and opaque fields, as shown in fig.2.1(b). Similar types of setting can obviously be made with the images of other types of object. It is clear from the examples of diffraction images shown previously that none

FIG. 2.4. POSSIBLE CRITERIA FOR JUDGING THE 'VISUAL EDGE.'

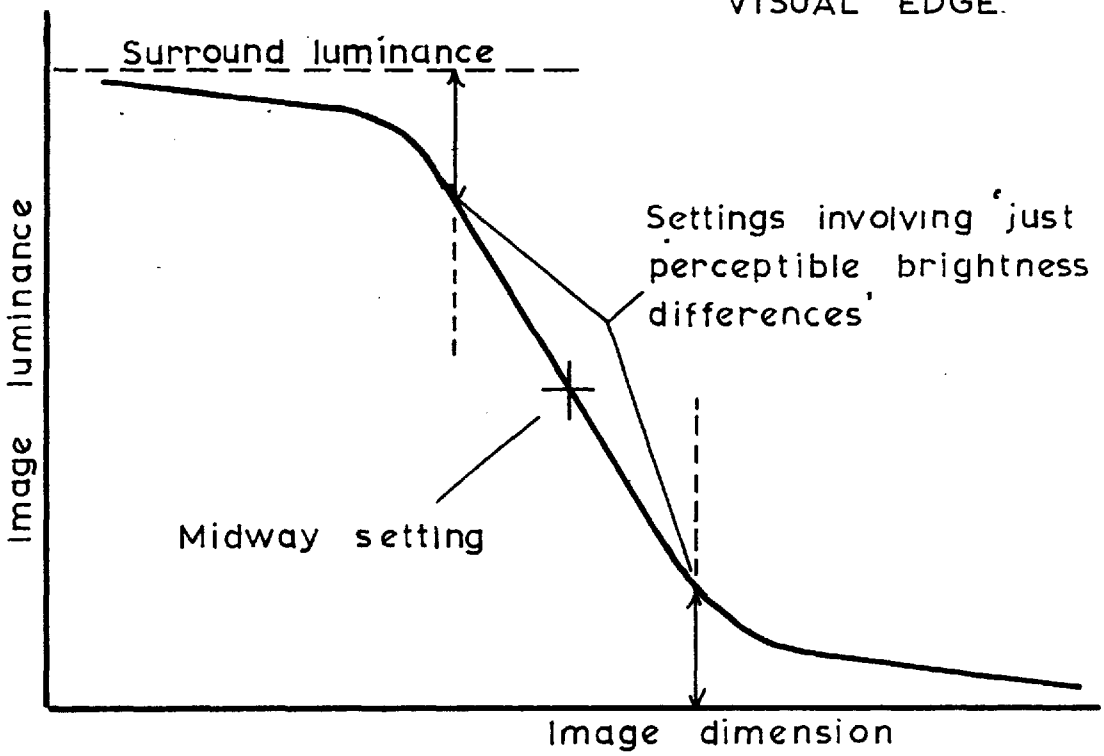

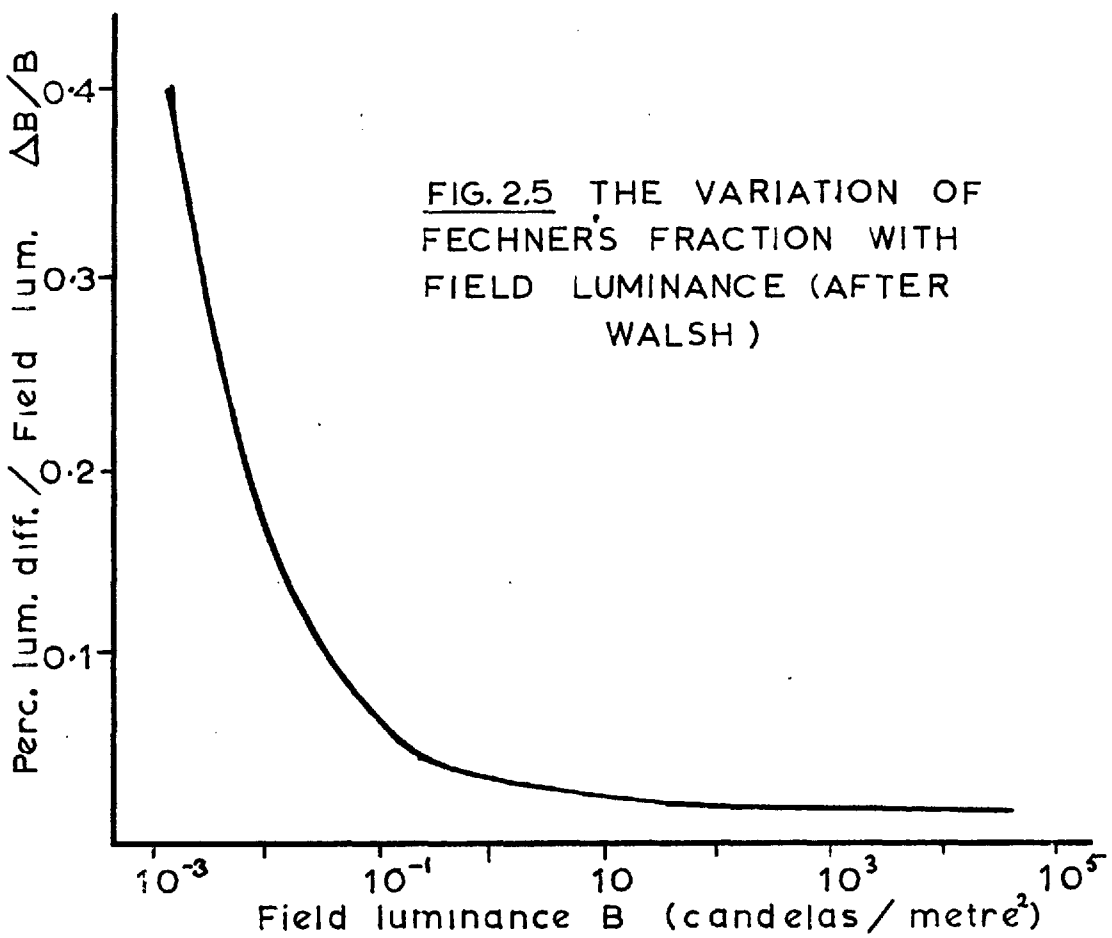

FIG. 2.5 THE VARIATION OF FECHNER'S FRACTION WITH FIELD LUMINANCE (AFTER WALSH)

of these criteria is likely to give a 'visual edge' position corresponding to the geometrical edge. However, if a consistent visual edge position is given for a particular type of object, this having a fixed relationship to the geometrical edge under defined conditions, then it becomes possible to introduce a correction factor into the results obtained. Thus an object can be sized visually and the true object size deduced by adding a correction term appropriate to the conditions under which sizing is carried out. The factors affecting the visual edge as defined by the brightness discrimination criteria suggested must therefore be considered.

The main features governing the luminance discrimination of the eye have been widely investigated and although the subjective sensation of brightness is not necessarily linked in a simple manner with the variation in field luminance, the results will obviously be qualitatively applicable to the problem of brightness discrimination.

The variation of the ratio of the just perceptible luminance difference ΔB of a small test field to the luminance of its surround B with B is shown in figure 2.5, taken from Walsh (1953, p,62). Although the exact values involved vary with different observers and with the viewing conditions, the form of the curve is typical of all cases. The significant feature is that the Fechner fraction $\Delta B/B$ remains constant down to a luminance level of about 10 candelas/metre^2 (10^{-3} stilbs), below which it rises

rapidly. We may therefore expect that the same visual edge criterion under otherwise constant conditions is likely to give constant visual sizing results at values of field luminance above a certain level, but that the visual size given will depend critically upon the exact value of the field luminance at lower luminance levels.

The value of the Fechner fraction also rises when the size of the test-patch is decreased, this being shown in fig. 2.6, taken from the work of Hunt (1953) who used the results of several authors in plotting the curve. It can be seen that the Fechner fraction tends to a constant value providing the size of the test field is large enough, so that we may anticipate that there will be a tendency towards a constant visual size, assuming that other conditions are kept constant, if the angular subtense of the image is made large enough.

A complicating factor when attempting to compare the luminance of the image with the subjective brightness distribution seen, is the occurrence of the Mach effect when two uniform fields of differing luminance separated by a graded field are observed. This effect, which has been investigated qualitatively be various authors including McDougall (1903), Thouless (1922), and Fry (1948) and quantitatively by Fiorentini et al (1955,57,58) consists essentially in the subjective perception of a bright band between the higher luminance field and the graded field and a dark band between the lower luminance field and the

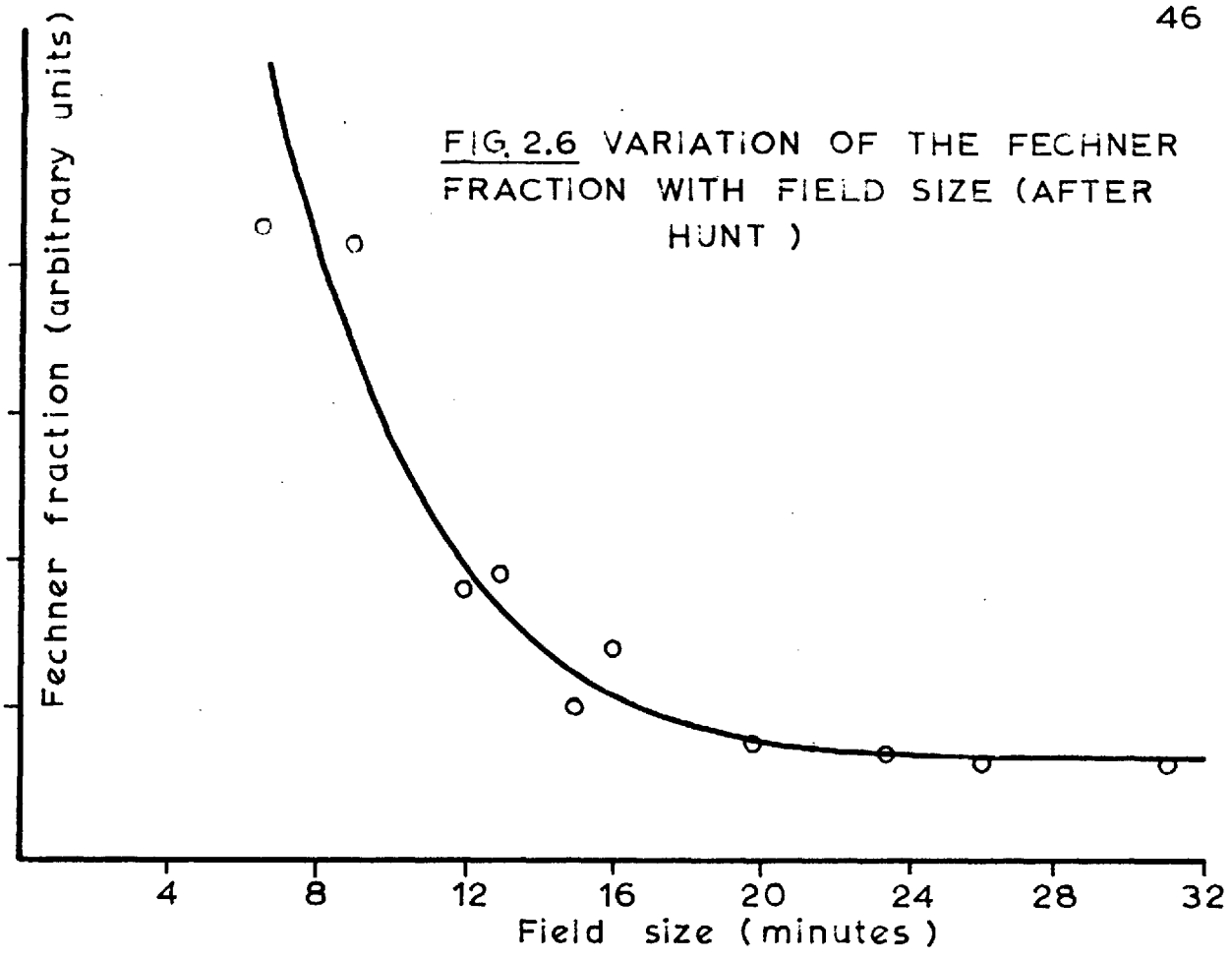

FIG. 2.6 VARIATION OF THE FECHNER FRACTION WITH FIELD SIZE (AFTER HUNT)

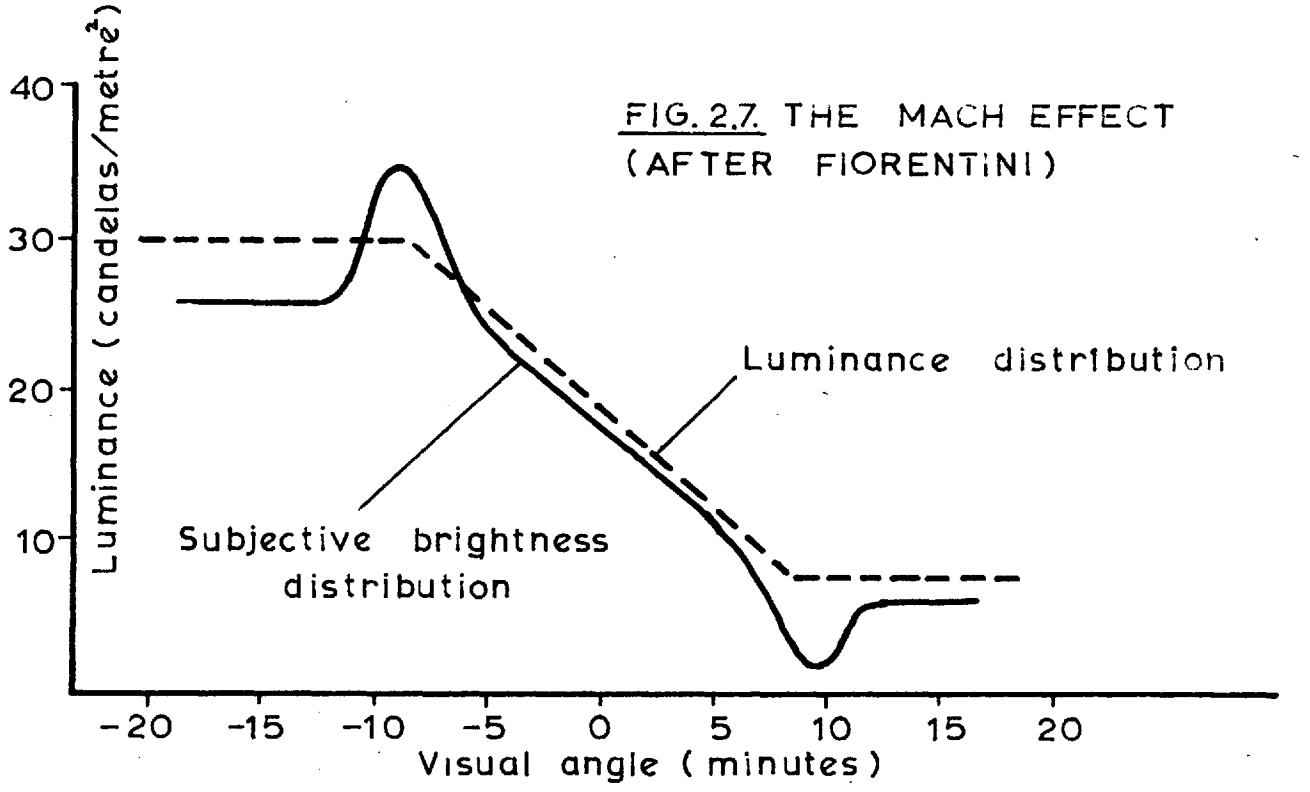

FIG. 2.7. THE MACH EFFECT (AFTER FIORENTINI)

graded field. Further bands may also be seen. A typical example of the difference in form between the subjective brightness and luminance distributions is shown in fig. 2.7, taken from Fiorentini (1958), although the exact brightness distribution seen varies considerably with different observers and viewing conditions. Since many of the diffraction images discussed exhibit luminance distributions approaching this form, it is likely that the Mach effect will be observed when sizing by visual microscopy. In general its influence will be to increase the subjective contrast of the edge, but it is clear that attempts to predict the movement of the 'visual edge' in terms of the luminance alone of the image cannot be completely valid.

Other factors, including the state of adaptation of the eye and the size of its effective entrance pupil will also affect the visual assessment of the image. The colour of the light used is obviously of great importance too, but the effects of using heterochromatic radiation are beyond the scope of this thesis. If monochromatic radiation is used, then allowance must be made for the variance in the properties of the visual system with wavelength.

The effect of all these parameters on the visual size of an image will be further discussed in later Chapters.

2.6. High Resolution Sizing Errors.

If objects below ten microns are to be sized using the microscope, a high aperture objective must be employed, this

normally being of the immersion type. A cone of light of semi-angle of the order of $\pi/3$ radians may be admitted by the objective, so that the angles of diffraction are far larger than those for which the scalar diffraction theory, whose results have been described previously, is valid.

Any investigation into the errors involved in high-resolution sizing work must therefore be related to experimentally determined image intensity distributions for objects of known size and shape, although these distributions may well correspond qualitatively to those predicted by scalar diffraction theory.

The preparation of suitable test objects is therefore discussed in the following chapter while in the succeeding chapters 4 and 5 an apparatus is described which enables the image intensity distribution to be found with all types of objective and object under varying optical conditions. The visual sizes of the objects for these conditions can also be determined as can the variation of the visual size with the visual conditions of observation.

CHAPTER 3

TEST OBJECT PREPARATION

3.1. General.

It is clear from the preceding chapter that the first requirement in any investigation into the factors affecting visual sizing is for objects of known size and shape to be available as standard test objects. These should be of as simple a form as possible, that is they should be thin, sharp-edged and of uniform transmission across their area. The most useful type of object is one where either the object itself or its surround is completely opaque.

If experimental results are to be compared with the predictions of diffraction theory, then the test objects must have forms corresponding to those for which the theoretical results were discussed in chapter 2, that is, they should either be straight edges or circular objects. Straight edges provide considerable difficulties in the location of the true edge with respect to the visual edge and image intensity distributions, and the form of their image may also depend upon the polarisation of the illuminating light. Circular objects however are free from these difficulties since they have circular symmetry and dimensions can be measured between opposite ends of a diameter. A further advantage is that the production of circular apertures in an opaque film has been extensively investigated by Slater (1958, 1960). The size range of greatest

interest is where the object radii lie between 1 and 10 diffraction units since theoretical results have been obtained within these extremes.

As prepared, the test objects are either circular apertures in an opaque film or opaque discs, both types of object having the same radii as a series of mono-disperse polystyrene spheres. These are manufactured by the Dow Chemical Company and have already found wide use as sub-standards in electron microscopy. The quality and size of the original batch of spheres (lot G-580) have been investigated by several authors, notably Backus and Williams (1948,1949), Scott (1949), Gerould (1950), Ming Feng (1951) and Bradford (1952). More recently, Dow's have prepared a range of polystyrene spheres by a carefully controlled emulsion polymerisation technique, a statistical analysis of the diameter of each batch of latex having been made by Bradford and Vanderhoff (1955) using an electron microscope. The diameters of the batches of spheres, as determined from their measurements, are given in table 3.(i) below. $\underline{S}$ is the standard deviation from the mean $\bar{x}$ of $\underline{n}$ measurements.

Table 3(i). The diameters of the polystyrene spheres used in the test-object preparation.

$\bar{x}$ Å	S Å	n
880	80	1164
1380	62	526
1880	76	1065
2640	60	577
3400	52	415
3650	79	438
5120	74	359
5570	108	373
8140	105	357
11720	133	315
* 18300	180	not known
* 27900	1500	not known

The two starred sizes are more recent additions to the range and do not appear in the original paper. It will be observed that the sphere diameters range from approximately 2 to 40 diffraction units for a typical oil immersion objective used in the visible region of the spectrum, which overlaps well with the size range for which theoretical results have been obtained.

By courtesy of the Dow Chemical Company, 25 ml samples of the above latexes were obtained and from these aperture and disc test objects were prepared by the methods to be described.

3.2. The Production of Circular Apertures of Known Diameter.

The technique used to produce aperture test objects from spheres of known diameter has been fully described by

Slater (1958, 1960).

The procedure is a development of the technique of Hamilton and Phelps (1956) who shadowed dust particles with evaporated aluminium at normal incidence to produce, on removal of the particles, transparent apertures in an opaque film having the same profile as the original objects. Slater's method may be summarised as follows.

A microscope slide is first thoroughly cleaned with hydrogen peroxide and alcohol and a small amount of a dilute suspension of the spheres is placed on it and allowed to dry. Spectroscopically pure aluminium is then evaporated at normal incidence onto the slide at a pressure of about 5×10^{-5} mm of mercury until an opaque layer sufficiently thick to prevent the white-hot source being seen through it is given on the slide. On removal of the spheres by a jet of distilled water directed at grazing incidence onto the slide, circular apertures of a diameter equal to that of the spheres are given, a cover slip cemented over the aluminised portion of the slide allowing the ap-ertures to be used as test objects for microscopy.

Bond (1954) has stated that the thickness of an aluminium film necessary to render it opaque is 300 Å, but measurements using a Zeiss interference microscope on typical opaque aluminium films prepared under the conditions described suggest that the film thickness may frequently be much higher thanthis. Fig. 3.1(c) shows a typical example having a thickness of about 800 Å, a displacement of one

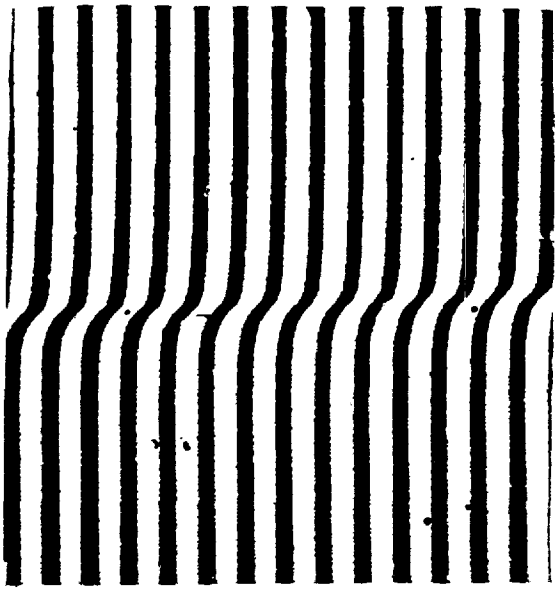

a) Rock salt film
(1900 Å thick)

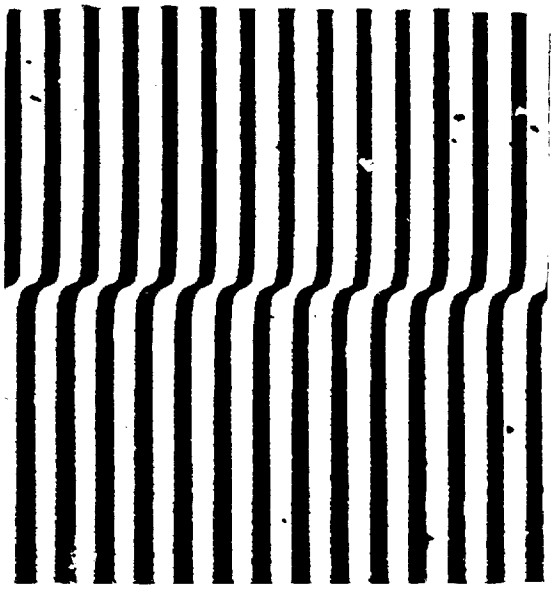

b) Silver film
(1600 Å thick)

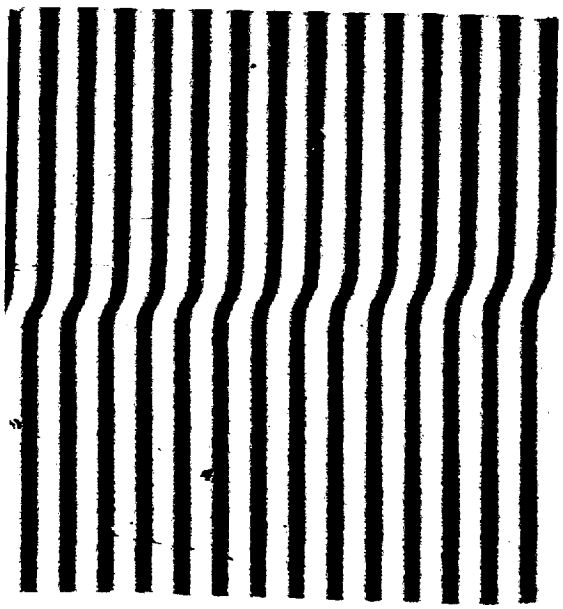

c) Aluminium film
(800 Å thick)

FIG. 3.1 TYPICAL FILM THICKNESSES MEASURED WITH ZEISS INTERFERENCE MICROSCOPE

fringe at the film boundary representing a step height of 2700 Å, a second film of aluminium of uniform thickness having been applied to both the original film and the glass substrate to give uniform reflectivity and to avoid the occurrence of different phase changes on reflection from the two surfaces.

The finite source size and source-substrate distance will result in two effects. There will be a penumbral region which is partly aluminised around the edge of the apertures and the apertures will be elliptical by an amount depending upon the cosine of the angle between the slide surface and the line joining the sphere with the source.

With a source diameter of 1 cm and a source-substrate distance of 30 cm, the penumbra will have a width of about 3% of the radius of the sphere. This becomes of increasing significance as the sphere diameter rises. Fortunately, when the larger sizes of apertures were being prepared a taller bell-jar became available for the vacuum plant, allowing the source-substrate distance to be increased to 40 cm, with a corresponding reduction in the width of the penumbra. Some variation in the width of the penumbra will occur when using a V as opposed to a spiral basket tungsten source, but provided thesource dimensions are minimised this effect has been found to have no practical significance, there being no detectable differences between the images of apertures prepared using either source.

The effect of the aluminium molecules not striking the

slide at exactly normal incidence is small, since, for a 1% increase in the projected sphere diameter, the angle of incidence must be 8° or 0.14 radians, so that smaller angles than this yield only very slightly deformed apertures. In practice, the line joining the centre of the sphere-covered area to the source is always arranged to be normal to the slide. With a source-substrate distance of 30 cms and a sphere-covered area of radius 3 cms, the maximum angle of incidence, assuming that the source is a point, is therefore 6°, this being increased slightly with a source of finite size. These dimensions are never exceeded in the preparation of the objects, so that the effect of the incidence angle not being exactly zero is always small compared with the penumbral effect due to the finite source size.

Slater has compared, using an electron microscope, the aperture diameters with those of the original spheres, the relative sizes being measured from the electron micrographs with a travelling microscope. He found that the agreement of sphere and aperture sizes was within $\pm$ 1.5%, this being of the same order of accuracy as that of the measuring technique and the standard deviation of the sphere size. He concluded that the penumbra produced was no greater than that predictable from the geometry of the arrangement used during evaporation, that there was no scattering of aluminium molecules by the inside of the bell-jar to fall inside the apertures and that no damage occurred to the apertures during the removal of the spheres.

3.3. Preparation of Opaque Discs of Known Diameter.

Knowing the ease with which transparent apertures could be produced from the spheres, it was felt that it should be possible to extend the method to produce opaque discs having the same diameter, using a similar evaporation technique.

The original method tried was as follows. The spheres were deposited on a slide in the normal way and a thin film of rock salt was evaporated onto the slide from a molybdenum boat, the evaporation geometry being the same as that used with the aluminium in the previous section. The spheres were then removed from the slide by a high pressure jet of oxygen directed onto the surface at grazing incidence, this giving circular apertures in the rock salt film. On evaporating an opaque film of aluminium over this first rock salt layer, the aluminium was in direct contact with the slide where apertures existed in the rock salt film and elsewhere was separated from the slide by a rock salt layer. Hence it was hoped that, when the slide was gently slid into distilled water, the rock salt layer would dissolve, so that the aluminium on its surface would fall away from the slide, leaving behind those portions of the film that adhered directly to the glass, that is, circular discs of aluminium.

In practice however, the aluminium films appeared to strip off in one piece. This was probably due to the finite source size yielding a thin 'linking layer' of aluminium between the film on top of the rock salt and that on the slide, the strength of this layer being greater than

the adhesion of the small areas of aluminium to the glass, so that the film stripped off in one piece.

No greater success was experienced when using silver as the material for the second film, although at one stage discs apparently were given. On closer examination however, using the large 2.79 μ spheres as the starting material, these could be seen to be spheres with a hemispherical cap of the coating metal.

It is possible that a careful control of the thickness of the rock salt layer might have improved the results since too thick a rock salt layer would result in the spheres becoming embedded in the film. The small refractive index difference between the slide and rock salt makes such monitoring of the film thickness difficult although this could be done using a piece of high index glass as a control. In addition, the use of a collimating aperture above the source would reduce the thickness of the linking layer of aluminium.

On balance however the prospects of success were felt to be small and a second technique has therefore been developed which has been found to allow circular opaque discs of known diameter to be produced relatively easily, these appearing perfect when viewed under the optical microscope.

The spheres are first spread on a clean slide in the usual way and a film of rock salt followed by an opaque film of silver is evaporated at normal incidence from a small source at a distance of about 30 cms. Suitable shaping of

molybdenum boats from which the rock salt and silver are evaporated keeps the source diameter down to about 6 mm, resulting in a penumbra around the apertures produced having a width of about 2% of the sphere radius. The use of the taller bell jar allows the source-substrate distance to be increased to 40 cm with a corresponding decrease in the width of the penumbra, although more evaporations may be necessary.

The slide is then slid gently into distilled water when the rock salt layer dissolves, so that, with care, the silver film, containing apertures which are accurate projections of the spheres, floats off in one piece and can be caught on a second clean microscope slide.

The silver film is allowed to dry and any remaining spheres are gently brushed or blown off, their removal being checked by examination of the slide with a dry 4 mm microscope objective. A few scratches are made in the film, these facilitating focussing later. A second opaque layer of silver is then evaporated on top of the first film, this new layer adhering strongly to the slide where apertures or scratches exist in the first film, but only taking poorly to the first silver layer, so that the strength of the thin linking layer between the two types of area is small. Thus when a gentle current of distilled water is allowed to fall onto the slide, the first film comes away, taking all the second film with it except for those parts which adhere directly to the glass. Accurate discs are therefore left

with additional streaks of silver which makes it considerably easier to focus on the plane of the slide.

This method removes most of the difficulties experienced with the earlier technique. The only limitation in the preparation of the first silver layer with its apertures is that the combined thicknesses of the silver and rock salt layers must be less than the radius of the spheres. Although the rock salt film thickness is not controlled exactly, measurements on typical films using a Zeiss interference microscope gave thicknesses in the range 1 - 2000 Å, the same range of thicknesses being found for the silver films, as is shown in fig.3.1(a) and (b), an aluminium layer of constant thickness having been applied to all surfaces. Taking the extreme values of film thickness, apertures of the same diameter as the spheres will only be given if the sphere radius exceeds 0.4 μ. Careful monitoring of the rock salt layer can probably reduce its thickness to about 100 Å. The first silver film need not be completely opaque, but for it to come off the slide in one piece it must have a completely connected structure, Sennett and Scott (1950) having shown that this requires a thickness of at least 500 Å, depending upon the speed at which the evaporation is carried out. It would therefore appear that the method is in practice limited to spheres having an absolute minimum diameter of about 0.2 microns.

This conclusion is reinforced by the fact that the second silver film has a minimum thickness of 0.1 μ, so

that the objects are in fact short cylinders rather than discs of negligible thickness. It seems reasonable to expect therefore, in view of the comparatively rough treatment that they receive, that the practical lower limit of the diameter of the objects that can be prepared would be between 0.2 and 0.5 μ .

Aluminium, in spite of the obvious advantage that it possesses over silver of needing a smaller thickness to give an opaque film, was not found to be suitable for either of the metal evaporations used in the disc preparation. When used as the first film, the aluminium frequently failed to float off from the slide and when forming the second film the requisite separation of the discs from the rest of the film failed to occur.

Although the techniques discussed for the preparation of circular test objects have referred exclusively to the case where either the object or its surround is completely opaque, it is clear that the same methods could equally well be applied to produce circular objects having greater or lesser amplitude transmission than their surround or having the same amplitude transmission but differing optical thickness. The experimental work performed however has been entirely concerned with the opaque type of object.

CHAPTER 4

AN APPARATUS TO MEASURE IMAGE INTENSITY DISTRIBUTION AND VISUAL SIZE.

4.1. General.

In chapter 2 it was concluded that an investigation into the process of visual sizing and its errors must relate three properties of the object: its true size, the physical light intensity distribution in the image and the visual size, the variation of these latter properties with optical and visual conditions also being of importance.

An apparatus was therefore constructed to allow the interrelation of these properties to be studied, using the test objects discussed in the previous chapter. Essentially the apparatus consists of a normal microscope equipped with a monochromator, the image of an object either being directed to enter a filar eyepiece, where its visual size may be measured, or focussed upon a pinhole whose dimensions are very much smaller than those of the smallest resolved detail in the image. The light flux passing through the pinhole can be measured using a photomultiplier connected to a sensitive microammeter, so that by moving the image across the pinhole in a known fashion its light flux distribution can be determined. The image movement is achieved by the use of rotating parallel-sided glass blocks, these acting as optical micrometers. The general arrangement of the apparatus is shown in figs. 4.1 and 4.2, a more detailed description

FIG. 4.1 OPTICAL LAYOUT OF APPARATUS

A Tungsten ribbon filament lamp
B Condenser
C Monochromator entrance slit
D Achromatic lens
E 60° Prism
F Plane mirrors
G Achromatic lens
H Monochromator exit slit
I Achromatic condenser
J Object slide
K Apochromatic objective
L Scanning blocks
M Removable mirror
N Micrometer eyepiece
O Six micron pinhole
P Photomultiplier

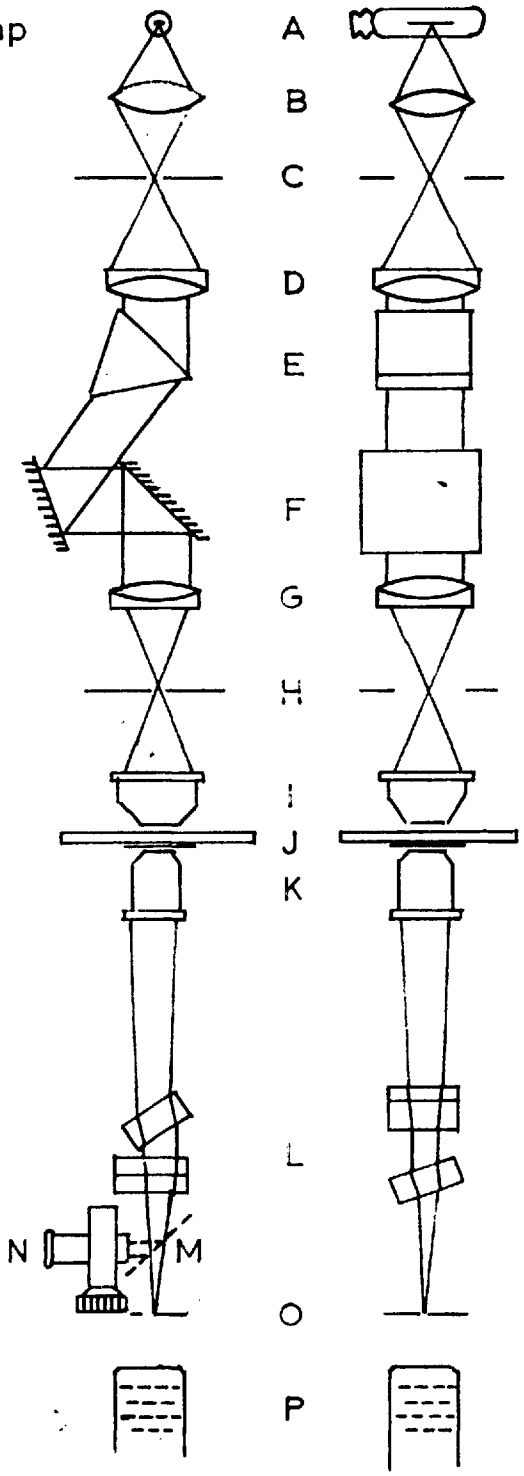

PLAN ELEVATION

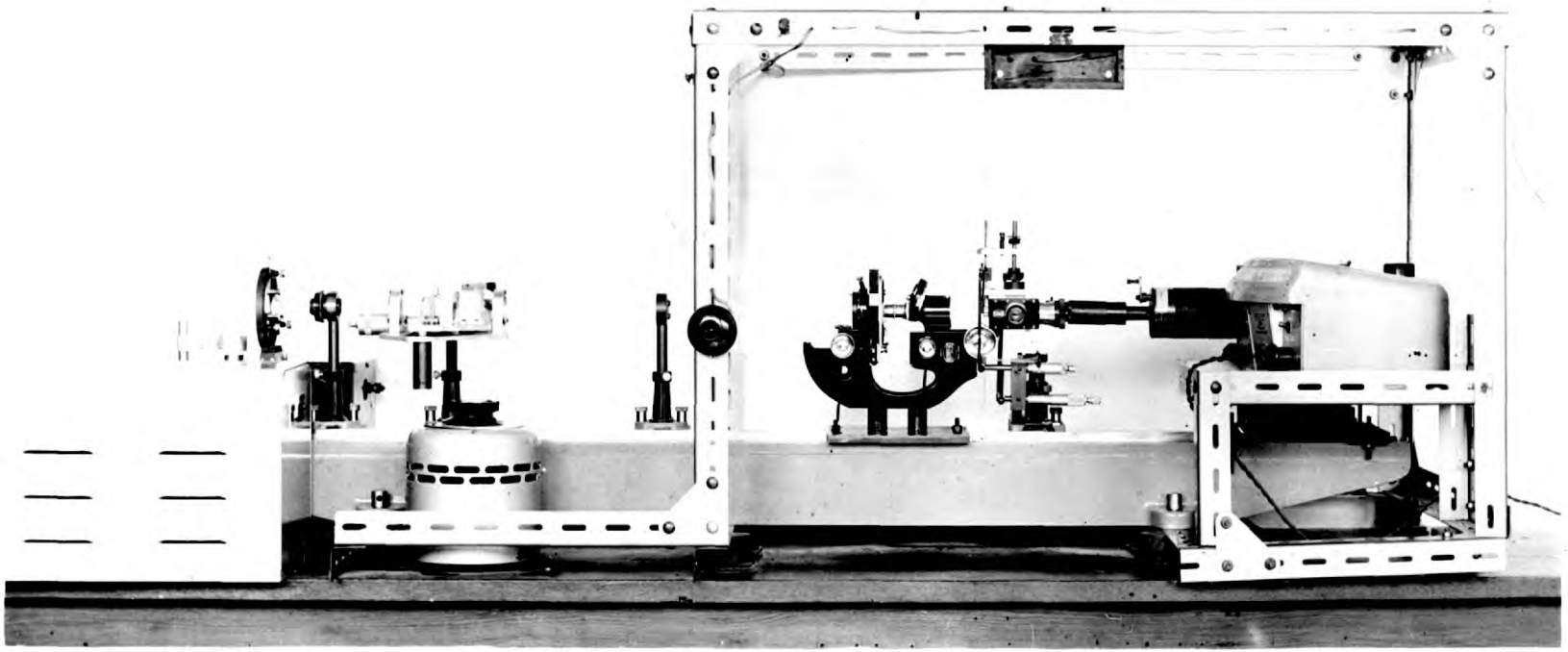

FIG. 4.2 GENERAL VIEW OF THE APPARATUS

of the individual components being given below. The design, selection and testing of some of the components will be further discussed in Chapter 5.

4.2. The Light Source and Supply.

The light source used is a tungsten ribbon filament lamp (6V, 18A) with a colour temperature of about 2850°K at its full working voltage. The mains supply is stabilised to ± 0.5% and is connected to the lamp via a rheostat and transformer, the output of the lamp thus being variable over a wide range by suitable adjustment of the rheostat.

Since the lamp is run off the A.C. mains without rectification, the light intensity emitted has a 100 c.p.s. ripple superimposed on a D.C. level. Fortunately this is very much faster than the critical flicker frequency of the eye, so that visual results are unaffected, while the use of a microammeter with a slow response time to measure the output of the photomultiplier allows the small ripple in the signal to pass undetected.

4.3. The Monochromator.

The light from the tungsten lamp is focussed onto the adjustable entrance slit of a monochromator based on a modification described by Strong (1938) of a type originally devised by Wadsworth (1894). The arrangement of the monochromator is shown in fig. 4.3, the essential features being an achromatic collimating lens, a 60° prism and plane mirror arranged to rotate together about an external axis, a second

fixed mirror to bring the light at minimum deviation parallel to the axis of the collimating lens again and a final achromatic doublet to focus the resultant spectrum in the plane of the exit slit. With a proper choice of the axis of rotation of the moving prism and mirror, the least deviated ray will always emerge parallel to the axes of the collimator and telescope lenses, although its wavelength will depend upon the position of the rotating components, this being controlled by a micrometer screw. Details of the design of the monochromator, its calibration and bandwidth are given in Chapter 5.

4.4. The Microscope.

This is a Beck London Model (48 LI), the limb carrying the condenser, stage and objective being detached from its normal foot and bolted rigidly to a heavy base plate attached to the 1½ metre optical bench that carries all the components. The angular aperture of the illuminating beam from the monochromator is sufficiently large to evenly fill the back aperture of the condenser with light, as is necessary if the experimental results are to be compared with diffraction theory. By means of a calibrated iris diaphragm mounted in approximately the back focal plane of the condenser, the numerical aperture of the illuminating cone can be varied from 0.2 to 1.3, the calibration being performed using an apertometer designed by Spencer and Welford (1961). The condenser is focussed by the usual rack and

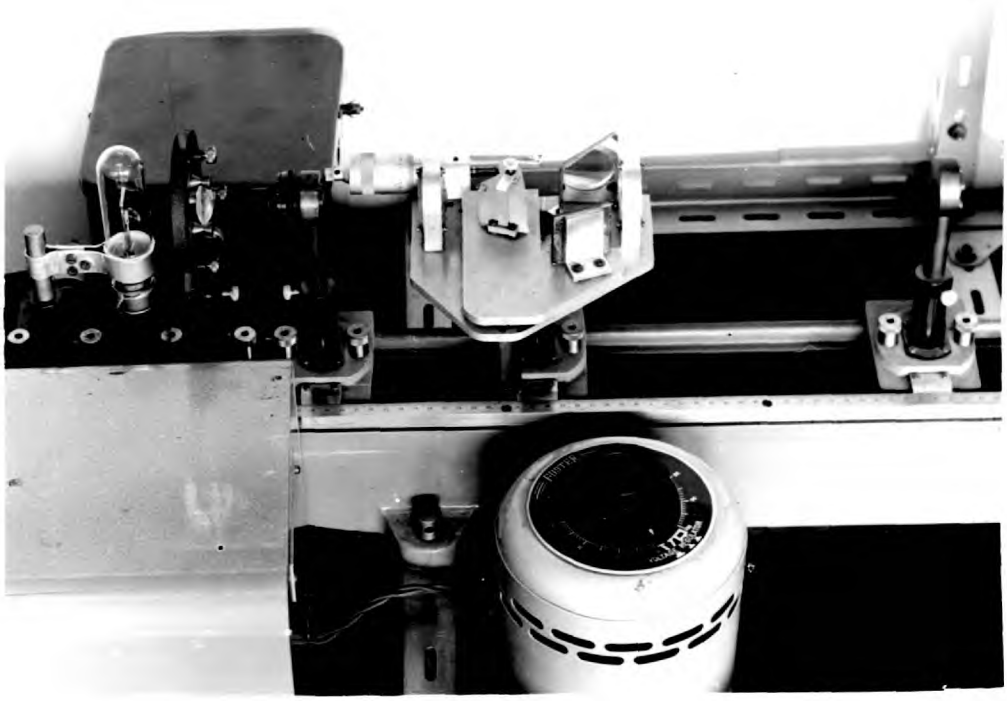

FIG.4.3 THE MONOCHROMATOR

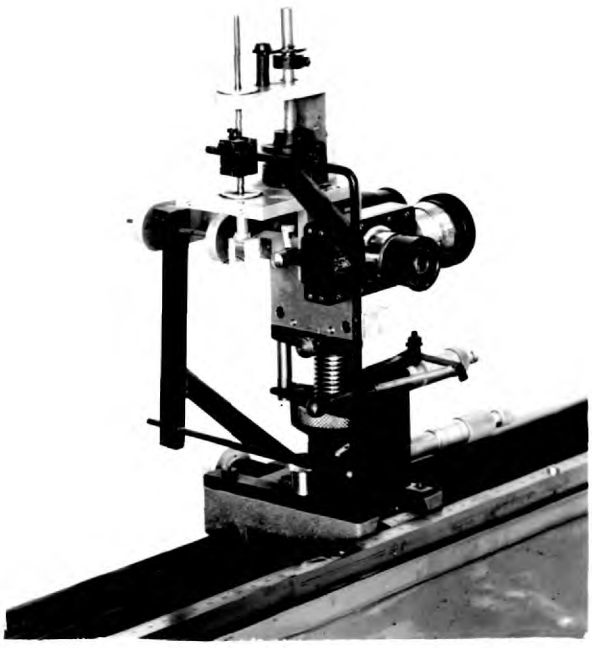

FIG.4.4 THE BLOCK UNIT

pinion, more precise control being given by the use of a lever instead of the normal knurled head.

A rectangular precision mechanical stage fitted with a rotating slide carrier supports the object, any portion of which can thus be brought into the field of view and orientated to any desired direction.

The objective, whose selection and testing will be discussed in a subsequent chapter, is carried on a rotatable nosepiece so that a field may first be searched using a lower power objective before the sizing objective is swung in. Coarse focussing is again by rack and pinion, the fine focus, which incorporates an anti-crash device to prevent damage to the objectives through mishandling, being sufficiently smooth and free from backlash to ensure precise focussing with a high aperture objective. As in the case of the condenser, a lever attached to the focussing knob allows a more delicate control of the focussing to be obtained.

4.5. The Scanning Block Unit.

The unit designed to incorporate the eyepiece for visual sizing, the scanning blocks, the scanning pinhole and the removable mirror is shown in figs. 4.5 and 4.6. The incorporation of all these components in a single optical bench unit greatly facilitates any adjustments in optical tube-length for different objectives.

The two scanning blocks (A), whose principal is the same as that of the optical micrometer, are arranged to move

the image in two mutually perpendicular directions. Since they work in a low aperture beam the tolerances on their manufacture are not too severe, these being discussed in the following chapter. The blocks were cut with a diamond saw from $\frac{3}{8}$" thick Pilkington plate glass of refractive index 1.52. Each block is mounted on a spindle (B) turning in two ball races, the axes of their rotation being perpendicular to the axis of the microscope. The angle through which each spindle turns is controlled by a lever connected at right angles to the spindle. A phosphor bronze ball brazed onto the free end of each lever is kept in contact by a weak spring (C) with the free end of an inch micrometer head (D), movement of this micrometer resulting in a rotation of the block.

A front-aluminised plane mirror (E) can be placed in the optical train to direct the light into a Beck filar eyepiece, the light otherwise passing straight down the microscope axis to reach the photomultiplier pinhole. The mirror unit (F) is lowered into a kinematic mount when required, three steel balls engaging in three V-slots in a steel ring (G) to ensure precise positioning. The mirror mount is designed to allow rotation about the two axes shown in fig. 4.6 so that an image centralised on the photomultiplier pinhole can be brought to a known position with respect to the fixed cross wires in the filar eyepiece. The mirror can be lifted vertically out of the optical train and secured by a catch when not required.

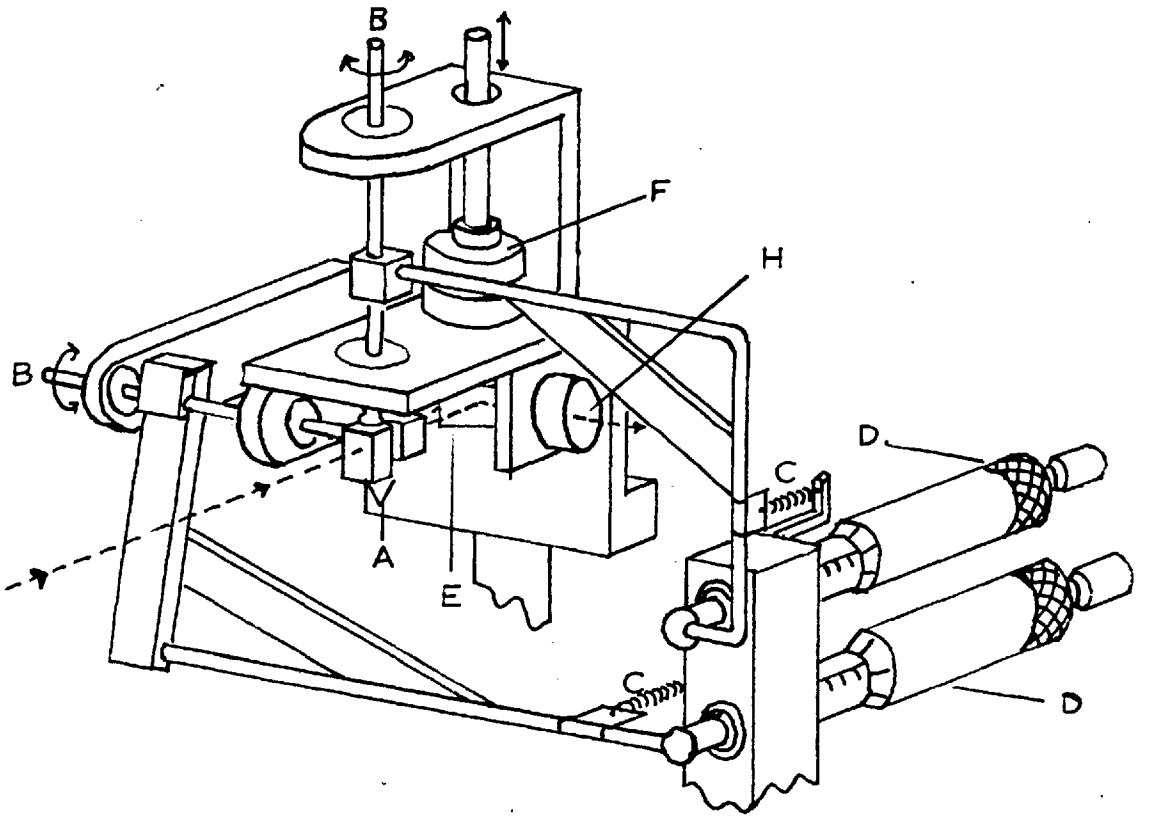

FIG. 4.5 THE SCANNING BLOCK UNIT

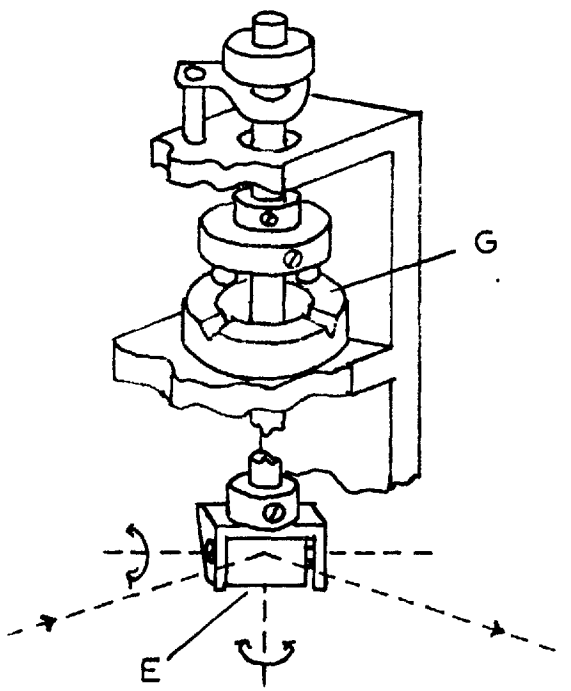

FIG. 4.6 THE MIRROR UNIT

The Beck filar eyepiece for visual sizing fits into a short length of tube (H) of the standard eyepiece diameter attached to the basic block unit, a lock screw securing the eyepiece in position. Rotation of a graduated micrometer drum results in the movement of a single crosswire with respect to a fixed graticule, the latter enabling objects to be brought to the same place in the field of view every time. Suitable modifications allow positive eyepieces of any power to be focussed on the plane of the crosswire and graticule.

A second eyepiece tube fitting takes the holder for the photomultiplier pinhole. The dimensions of this pinhole must be small compared with those of the detail in the image, since the photomultiplier signal is proportional to the integrated light flux over the area of the image which falls upon the pinhole. Provided however that the pinhole diameter is very much smaller than the actual diameter of the Airy disc, the effect of the finite size of the pinhole is fairly small. That used, a 6μ electro-formed hole in copper, manufactured by Smethurst High-Light Ltd. as an aperture for an electron microscope objective, has an effective diameter of about one diffraction unit in the image plane when used with green light and a 1.28 N.A., x 100 objective. Reference to the diffraction images given in Chapter 2 shows that the effect of integrating the image flux over a circle of this diameter is unlikely to cause any radical difference between the scanned and true image flux distributions. The effect of the finite pinhole size

however will always be to 'smooth' any abrupt changes in the image flux distribution.

By suitable adjustment of the lengths of the eyepiece and pinhole mounts, the image can be arranged to be precisely in focus in the plane of either the eyepiece graticule or the pinhole, depending upon the mirror position. Movement of the whole mount along the optical bench results in an equal increment in the optical tubelength in both cases, and the mirror, eyepiece and pinhole mounts can be moved as a single unit in two mutually perpendicular directions to the optical axis by suitable movements in the optical bench fitting.

4.6. The Detector and Indicator.

The photomultiplier used as a detector is an E.M.I. type 6094 B, the photo-cathode being of antimony-caesium on glass having a maximum spectral response at a wavelength of about 4000 Å. Photoelectrons from the photo-cathode are multiplied by a system of eleven dynodes supplied through a suitably decoupled potential divider. Since the gain varies as a high power of the overall voltage, a highly-stabilised power supply is used, this being a Panax type 3000 power pack whose output is variable from 0 to $\pm$ 3 KV, - 2 KV normally being employed. The average interstage potential after the first stage is about 165 volts, so that the collector current is proportional to the incident light intensity up to at least 1 mA. The dark current is less than 0.1 μA and by the use of suitable screening round the

apparatus stray light is kept to a minimum.

A Pye galvanometer functioning as a microammeter registers the photomultiplier current. Since its period is about 2 secs., the 100 c.p.s. ripple in the light source is not detected. The full scale deflection on the least sensitive range (X.01) corresponds to about 45 μA, most measurements being taken on the X.1 scale.

CHAPTER 5

OPTICAL DETAILS OF THE APPARATUS

5.1. Monochromator Design.

The geometry of the modified Wadsworth monochromator described in the previous chapter must be such that equal angular rotations of the prism and moving mirror about the same external axis (fig. 5.1) result in the rays for which the condition of minimum deviation is satisfied striking the collimating lens parallel to its axis. In order that the aperture of the collimator should be equally filled with light at all wavelengths, there must also be no lateral movement of the minimum deviated beam perpendicular to the axis of the collimator when the wavelength is changed.

The ray at minimum deviation has its direction altered by an angle $(180 - 2\alpha)$ by the prism and moving mirror, where α is the angle between the bisector of the prism angle and the mirror. A value of $\alpha = 45^{\circ}$ thus means that the fixed mirror must be placed at 45° to the telescope axis to bring the least deviated ray parallel to the collimator and telescope axes.

The condition that there should be no lateral movement of the ray at minimum deviation on rotating the moving parts of the system is found as follows. Consider (fig. 5.1) the ray striking the prism at a point such that the line joining the point of incidence to the centre of rotation of the moving system is perpendicular to the collimator axis.

Suppose the ray is at minimum deviation and passes through a prism thickness $\underline{t}$ and an air path $\underline{l}$ before striking the mirror. Then if the angle of incidence on the prism is I degrees and the moving system is rotated through a small angle ΔI radians, the rotation being in such a direction as to increase I, the lateral movement L of the least deviated ray in the direction shown is given by

$$L = x\Delta I - t\Delta I \sin (I-30) - l\Delta I \sin (2I-60) - \left[l\Delta I \sin (2I-60) + l\Delta I \tan (75-I) \sin (150-2I) \right]$$

These terms account for successively the movement of the prism as a whole, the change in the angle of incidence on the prism, the changed air path between the prism and the mirror and the movement of the mirror. Simplifying and collecting terms

$$L = x\Delta I - t\Delta I \sin (I-30) - l\Delta I \sin (2I-60) - l\Delta I$$

For there to be no lateral movement on rotation, L = 0,

$$\text{i.e.} \quad x = t \sin (I-30) + l \sin (2I-60) + l$$

Thus a suitable choice of x, t and l allows the wavelength whose incidence angle at minimum deviation is I to be focussed on the axis of the telescope lens, the aperture of this lens being filled with light at all wavelengths.

5.2. Bandwidth of Monochromator.

There will be a finite band of wavelengths in focus at each point in the exit slit of the monochromator, due to the finite width of the entrance slit S_1. The width of the

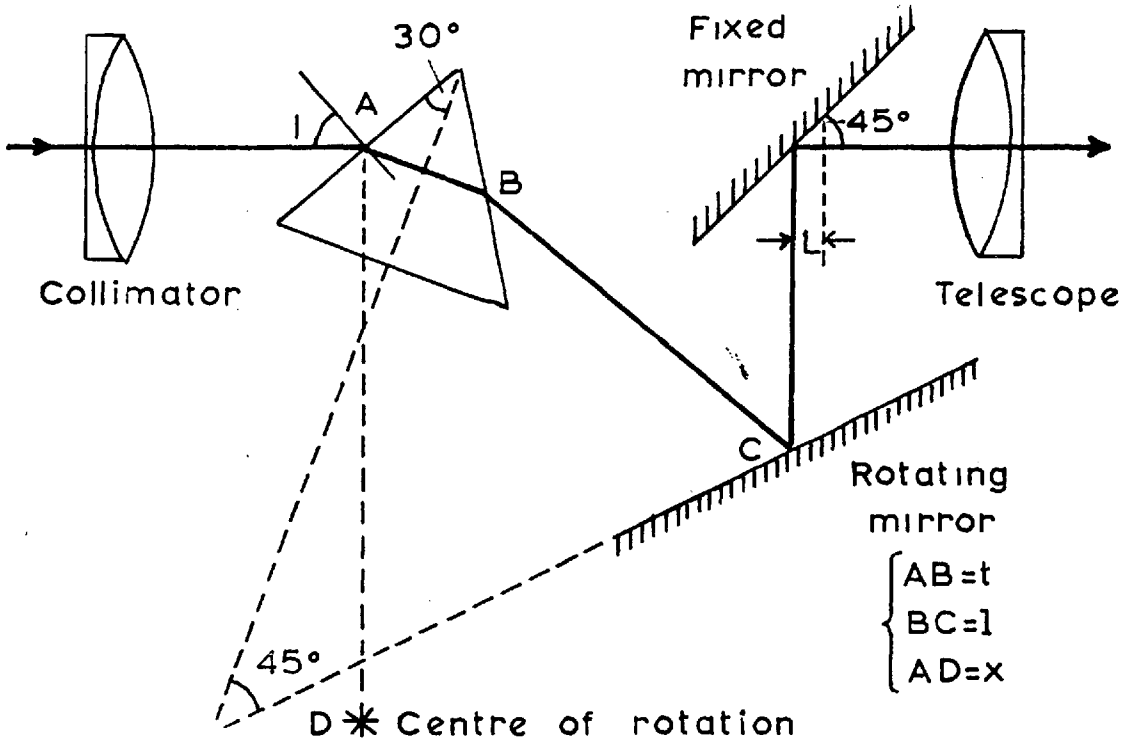

FIG. 5.1 DESIGN OF MONOCHROMATOR

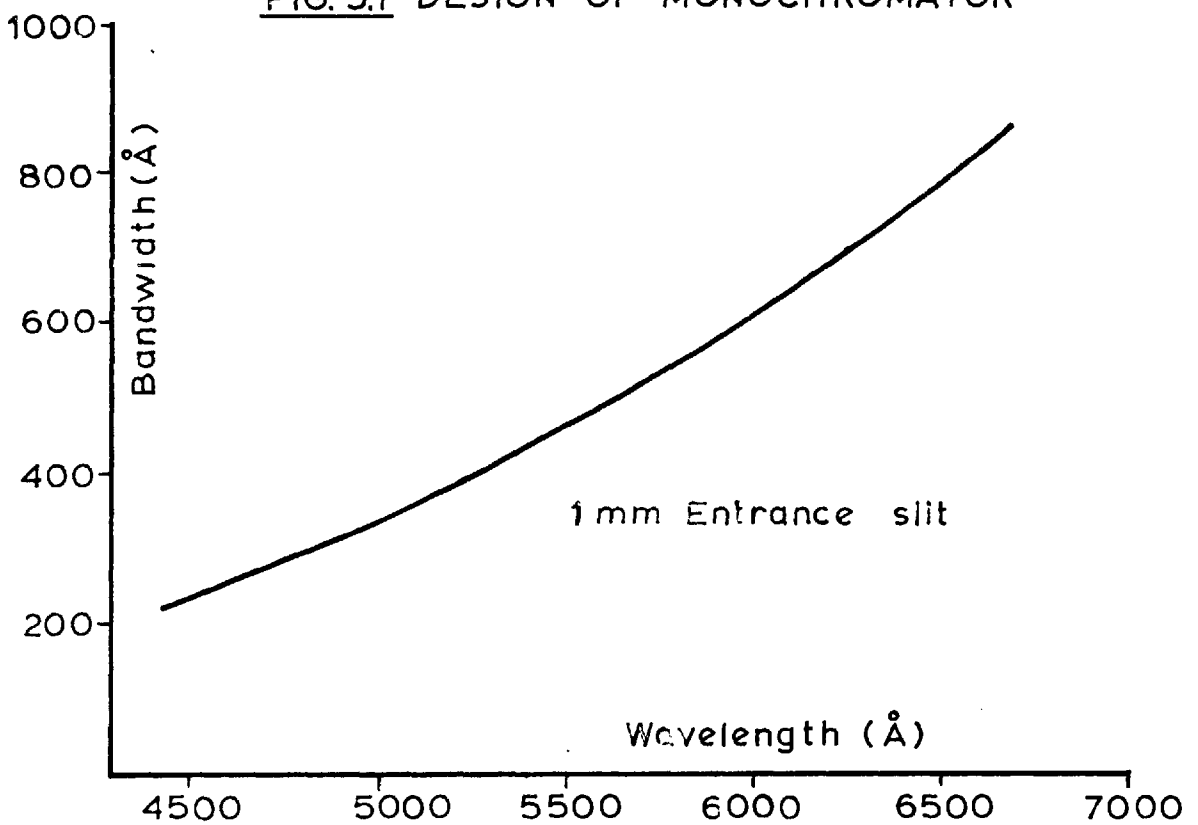

FIG. 5.2 VARIATION OF BANDWIDTH WITH WAVELENGTH

exit slit S_2 will lead to a further spreading of the band-width of the light incident upon the microscope condenser.

If f_1 and f_2 are the focal lengths of the monochromator collimator and telescope lenses respectively, the width of the image of the entrance slit in the plane of the exit slit is

$$S_1' = \frac{f_2}{f_1} S_1$$

The angular separation δD between wavelengths of λ and $\lambda + \delta\lambda$ incident upon the telescope lens is given by

$$\delta D = \delta\lambda \left(\frac{dD}{d\lambda}\right)_\lambda$$

where $\left(\frac{dD}{d\lambda}\right)_\lambda$ is the rate of change in the angle of minimum deviation with wavelength . Thus the bamd of wavelengths, $\Delta\lambda_1$, in focus at each point in the exit slit of the monochromator is given by

$$\Delta\lambda_1 \left(\frac{dD}{d\lambda}\right)_\lambda f_2 = \frac{f_2}{f_1} S_1$$

$$\text{i.e.} \quad \Delta\lambda_1 = \frac{S_1}{f_1} \Big/ \left(\frac{dD}{d\lambda}\right)_\lambda$$

where λ is the mean wavelength of the band. The range of wavelengths, $\Delta\lambda_2$, passing through the entire width of the exit slit is such that

$$\Delta\lambda_2 = \frac{S_1}{f_1} \Big/ \left(\frac{dD}{d\lambda}\right)_\lambda + \frac{S_2}{f_2} \Big/ \left(\frac{dD}{d\lambda}\right)_\lambda$$

The focal lengths of the collimator and telescope lenses were determined with a foco-collimator, while the relationship for the prism between the angle of minimum deviation D and the wavelength λ was plotted using a

Hilger-Watts spectrometer, the slope of the curve at a wavelength λ giving $(dD/d\lambda)_{\lambda}$. The bandwidth for various sizes of exit and entrance slits could thus in principle be calculated.

Only the bandwidth due to the finite width of the entrance slit is of experimental significance however, since in the apparatus the microscope condenser is focussed to give an image of the exit slit of the monochromator in the plane of the object, under these conditions the back apertures of both the condenser and objective being evenly filled with light. With the variables having the values found in the apparatus, a 1 mm exit slit has a wavelength variation of 190 Å across its width when the central wavelength is 5300 Å and the entrance slit is assumed to be infinitely thin. For the focal length of the microscope condenser and the distance of the exit slit from the condenser used, a 1 mm exit slit width gives an image approximately 30 microns in width in the plane of the object. The object diameters which are of experimental interest never exceed 5 μ, so that the variation in the mean illuminating wavelength across their width is less than 30 Å, it being virtually negligible for objects less than 1 μ in diameter. The illuminating bandwidth due to the finite width of the entrance slit, which amounts to about 100 Å for a 1 mm slit width in the green region of the spectrum is clearly far more important. Thus when considering the range of wavelengths illuminating the test objects, only that due

to the width of the entrance slit need be taken, the variation in bandwidth with wavelength when the monochromator has a 1 mm entrance slit being shown in fig. 5.2.

There will however be a wavelength variation across the full width of the illuminated field, so that measurements are always performed at the centre of this field, this being the point for which the wavelength calibration is made. Although the minimum possible bandwidth of illuminating wavelengths is desirable, in practice neither the imaging properties of the objective nor the visual properties of the eye vary significantly with a bandwidth of the order of 2% of the mean wavelength. Any uncertainty introduced into the results by a bandwidth of this order is no greater that due to the uncertainties in the size of the test objects and the inaccuracies in the measuring techniques employed. Hence bandwidths of about 100 Å are generally used, the entrance slit being adjusted accordingly. The monochromator was calibrated by inserting successively mercury, sodium and cadmium lamps in place of the normal tungsten source. The micrometer setting necessary to bring each line of known wavelength of the various spectra into the centre of the field of view of the microscope was noted, from which a calibration curve could be plotted for use with the tungsten lamp.

5.3. The Testing of the Microscope Objective.

The objective used in the experiments must be of sufficiently good quality to ensure that the general applicability of the results is not invalidated by the lens aberrations. Although observation of the usual diatom test objects revealed that the Beck objective had a resolution for periodic objects of the standard to be expected with the numerical aperture available, the more stringent star and interferometer tests were used to give explicit information on the aberrations present.

The star test, whose application has been described by Slater (1957), has been estimated by Welford (1960b) to be capable of detecting aberrations of the order of $\lambda/20$, depending upon the type of aberration present. It consists essentially in the examination of the in and out of focus images of circular pinholes whose diameter is less than half the resolution limit of the objective employed, these being illuminated by a condenser having an aperture at least as large as that of the objective. With perfectly corrected objectives, identical circular diffraction images are given at equal distances on either side of the best focal plane, the in focus image being an Airy diffraction pattern. The aberrations present in an objective may be deduced from the variation from these ideal conditions of the images obtained.

The objective to be used was star-tested in position on the apparatus, so that any aberrations introduced by

the scanning blocks could also be detected. Thus, by focussing the image in the plane of the eyepiece graticule, the objective was tested under its normal working conditions. Since all experimental observations are made at the centre of the field, the off-axial aberrations are not important, an aberration-free field 20 microns in diameter being quite adequate.

The star-test showed that the field of the Beck objective at full aperture was free of coma and astigmatism over a sufficiently large area, this field also being flat. Present however was some spherical aberration, this being minimised when the optical distance between the flange of the objective and the eyepiece graticule, or mechanical tubelength, was 180 mm. Changing the tubelength by $\pm$ 10 mm from this value had little effect, a small amount of under-corrected zonal aberration persisting at the optimum setting. This disappeared on stopping down the numerical aperture of the lens to about 1.1 when the objective was used with green light. The correction for spherical aberration worstened a little at the extremities of the spectrum but was still of far better quality than for an average objective.

The presence of the scanning blocks in the image space appeared to have no detrimental effect upon the quality of the image, no detectable additional aberrations being introduced when the angle of incidence on the blocks was altered. The only visible adverse optical effect of the scanning blocks was the introduction of faint secondary images

caused by reflections between the block faces, these moving with respect to the main image as the blocks were rotated. Their luminance and brightness were too low compared with the main image to necessitate the anti-reflection coating of the blocks however, a more important source of stray light being scattering from inhomogeneities in the fluorite components and reflections between the various lenses of the objective.

The results of the star-test were confirmed when the objective was tested on a modified Twyman-Green interferometer. The interferogram (fig. 5.3) shows the contour of the emergent axial wavefront when the objective is working at its optimum tubelength with light of wavelength 5461 Å. It can be seen that the correction is nearly perfect up to a numerical aperture of 1.1, but that at full aperture there is about one wavelength of zonal spherical aberration.

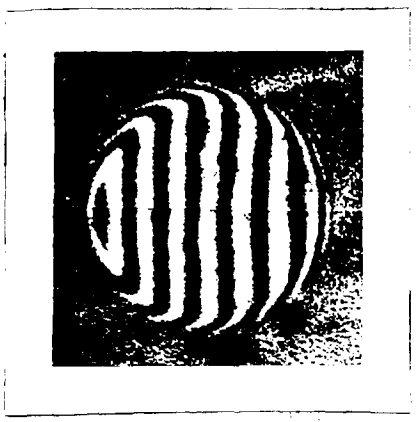

Fig. 5.3. Interferogram of Beck objective at λ = 5461 Å

Although a substantially perfectly corrected objective could be obtained by stopping down the aperture to 1.1, the experimental work was carried out with the full numerical aperture of 1.28. This was used because of the great practical interest of work at the highest apertures, but the presence of the outer zone of spherical aberration must be borne in mind when considering the experimental results obtained.

5.4. The Properties of the Scanning Blocks.

The two scanning blocks must be of such dimensions and form that, when rotated, they can move the image in two mutually perpendicular directions by an amount corresponding to the diameter of the image of the largest size of test object. This motion must be linear to within the limits of accuracy set by the other experimental conditions. The aberrations introduced by the insertion of the blocks into the image-forming wavefront should be within the Rayleigh tolerance or better, and no additional degradation in the image or the linearity of the image movement should be caused by imperfections in the blocks themselves.

The blocks were selected from a series of 1 cm squares of $\frac{3}{8}$" thick Pilkington plate glass of refractive index 1.52, this area of the faces being sufficiently large to intercept the rays from all parts of the objective pupil over the image field in use. The faces of the various blocks were tested against an optical flat to determine

their contour and with an auto-collimator for parallelism, the homogeneity of the blocks being assessed using a Twyman Green interferometer. Those selected had faces whose maximum surface variation in height was less than $\lambda/4$ for green light, these variations being gradual over the surface of the blocks. Opposite faces were parallel to less than $\frac{1}{5}'$, the optical thickness of the blocks being constant to within $\lambda/4$ over the full area of the faces.

Using such flat, parallel-sided blocks therefore, it must be considered whether their rotation results in a sufficiently linear image movement, whether the aberrations they introduce are within the Rayleigh tolerance and the quality of their geometrical finish is sufficiently high.

5.5. Linearity of Image Movement.

The insertion of a parallel-sided glass plate into a beam of light results in the light beam being displaced by an amount depending upon the angle of incidence upon the plate. Thus, in the apparatus, on rotation of the scanning blocks the image will be displaced laterally, the rotation of each block being controlled by a lever and micrometer head as described previously. It is required that equal changes in the position of the micrometer head produce equal image displacements at all points of the micrometer movement.

Consider the flat parallel sided plate ABCD, fig. 5.4., of thickness t and refractive index n, light being incident

normally on its face AB. If the block rotates about its centre O by an angle θ, the emergent light is displaced by an amount $\underline{d}$ as shown. If θ' is the angle of refraction in the block then

$$d = \frac{t}{\cos \theta'} \sin (\theta - \theta')$$

$$= t (1 - \sin^2\theta')^{-\frac{1}{2}} \left[\sin \theta (1 - \sin^2\theta')^{\frac{1}{2}} - (1 - \sin^2\theta)^{\frac{1}{2}} \sin \theta' \right]$$

Expanding this expression in terms of sin θ, taking θ to be sufficiently small for terms involving $\sin^4\theta$ and higher powers to be negligible, and collecting terms

$$d = \frac{t \sin \theta(n - 1)}{n} + \frac{t \sin^3\theta}{2n^3} (n^2 - 1) \quad \text{—5 (i)}$$

In the apparatus the lever and micrometer are arranged so that sin θ is a linear function of the micrometer reading. The image movement will therefore be directly related to the micrometer reading providing the value of the second term of equation 5(i) is very much smaller than that of the first, that is, providing sin θ is small.

The maximum image movement required is $\frac{1}{2}$ mm, corresponding to 5 μ in the object space with a primary magnification of x100, this being adequately greater than the largest size of test object. The blocks are arranged so that in the middle of their rotary movement their faces lie perpendicular to the axis of the microscope, the required maximum image movement being produced by a rotation of 2β where β is the maximum angle of incidence of the principal ray of

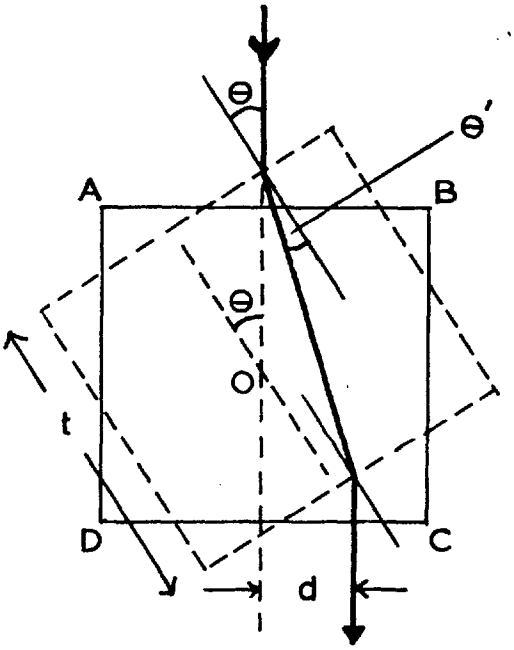

FIG. 5.4 DISPLACEMENT PRODUCED BY A PLANE PARALLEL PLATE

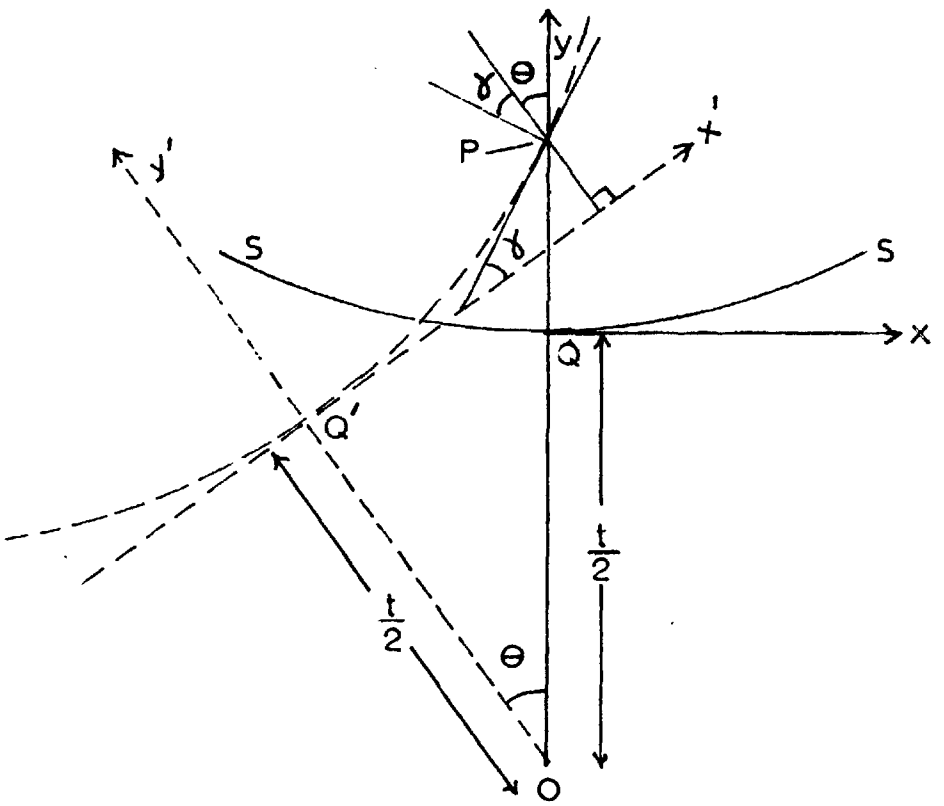

FIG. 5.5 THE EFFECT OF CURVATURE OF THE PLATE FACES

the image pencil on the block faces.

Then approximating $n = 1.5$, $t = 10$ mm, $d = \frac{1}{4}$ mm and substituting in the first term of equation 5 (i)

$$\frac{1}{4} = 10 \sin\beta \left(\frac{1}{2}\right) \left(\frac{2}{3}\right)$$

$$\therefore \sin\beta = .075$$

$$\text{i.e. } \beta = 4^{\circ}\ 18'$$

The second term of equation 5(i) now yields a small increment δd in the image displacement,

where

$$\delta d = \frac{10\ (.075)^3}{2\ (3/2)^3} \left(\frac{5}{4}\right) \text{ mm}$$

$$= 0.8\ \mu$$

$$\text{i.e. } \frac{\delta d}{d} = \frac{0.8}{250}$$

Thus the largest proportional error in the linearity of the image movement with micrometer movement over the range required is less than $1/3\%$, which is negligible compared with the standard deviation of the test objects themselves, smaller rotations of the blocks giving even smaller deviations from linearity.

5.6. Aberrations Introduced by the Blocks.

When a converging spherical wavefront from the objective is incident on one of the scanning blocks, its form after refraction by the block is no longer spherical. For their use to be acceptable, the total wavefront aberration introduced by the blocks into an image-forming pencil of rays must be within the Rayleigh tolerance, that is, the

aberrated wavefront must not depart by more than $\lambda/4$ from a reference sphere centred at the Gaussian image point.

Hopkins (1950) has given the aberration coefficients for a plane parallel plate as

$$S_I = -\frac{(n^2-1)}{n^3} u^4 t \quad - \text{ spherical aberration}$$

$$S_{II} = \left(\frac{U_{pr}}{u}\right) . S_I \quad - \text{ coma}$$

$$S_{III} = \left(\frac{U_{pr}}{u}\right)^2 . S_I \quad - \text{ astigmatism}$$

$$S_{IV} = 0 \quad - \text{ Petzval curvature}$$

$$S_V = \left(\frac{U_{pr}}{u}\right)^3 . S_I \quad - \text{ distortion}$$

where $\underline{n}$ and $\underline{t}$ are the refractive index and thickness of the plate, U_{pr} is the angle that the principal ray of the pencil makes with the normal to the surface of the plate and $\underline{u}$ is the semi-aperture angle of the pencil. The total wavefront aberration referred to the Gaussian image is

$$W = \tfrac{1}{8} S_I + \tfrac{1}{2} S_{II} \cos \phi + \tfrac{1}{2} S_{III} \cos^2 \phi + \tfrac{1}{4} S_{III} + \tfrac{1}{2} S_V \cos \phi \quad - \quad 5(ii)$$

ϕ being the angle that the plane containing the marginal ray and principal ray makes with that containing the principal ray and the normal to the plate face. It can be seen that at normal incidence, when $U_{pr} = 0$, only spherical aberration will be introduced but that when the incidence angle is finite the wavefront will become affected by coma and astigmatism. The distortion term S_V can be ignored,

since this merely represents a lateral movement of the image perpendicular to the optical axis, this being the movement already considered in section 5.5.

The aberrations introduced by each plate will be largest when the angle of incidence of the principal ray of the image pencil is largest, that is, when the normal to the face of the scanning block makes the greatest angle with the microscope axis. This maximum angle of incidence will correspond to the value found in section 5.5 for the case where the greatest image displacement is required. Thus $(U_{pr})_{max} = .075$, while the maximum value of u represents the numerical aperture of the image pencil, which with the 1.28 N.A, x100 objective in use is approximately .013. Thus substituting $n = 1.5$, $t = 10$, $U_{pr} = .075$, $u = .013$.

$$S_I = -\left(\frac{5}{4}\right)\left(\frac{8}{27}\right)(.013)^4 .10 \text{ mm}$$

$$= -1.1 \times 10^{-7} \text{ mm.}$$

In the sagittal section $\cos \phi = 0$ and from equation 5(ii)

$$= \tfrac{1}{8} S_I + \tfrac{1}{4}\left(\frac{.075}{.013}\right)^2 S_I$$

$$= -93 \times 10^{-8} \text{ mm}$$

In the tangential section, taking $\cos \phi = +1$,

$$= \tfrac{1}{8} S_I + \tfrac{1}{2}\left(\frac{.075}{.013}\right) S_I + \tfrac{1}{2}\left(\frac{.075}{.013}\right)^2 + \tfrac{1}{4}\left(\frac{.075}{.013}\right)^2 S_I$$

$$= -308 \times 10^{-8} \text{ mm}$$

With cos $\emptyset$ = - 1 the wavefront aberration is reduced slightly, all other values of cos $\emptyset$ yielding smaller wavefront aberrations, so that the above figure represents the maximum wavefront aberration for one scanning block. With both blocks in the path of the wavefront the aberrations introduced by the two blocks will be cumulative and will have a maximum value when the normals to the block faces make their largest angles with the microscope axis. Since, however, the axes of rotation of the two blocks are at right angles to one another, the sagittal section of wavefront for one block becomes the tangential section for the other. Hence the maximum wavefront aberration produced by the two blocks is given by

$$= - 93 \times 10^{-8} - 308 \times 10^{-8} \text{ mm}$$

$$\simeq - 4 \times 10^{-6} \text{ mm}$$

Although this is strictly only the primary wavefront aberration, the higher order aberrations will be negligible in comparison. Thus the total wavefront aberration throughout the visible spectrum is always well within the Rayleigh tolerance of a maximum $\lambda/4$ departure of the wavefront from the reference sphere.

5.7. Geometrical Quality of the Scanning Blocks.

The flatness and parallelism of the faces of the scanning blocks must be of sufficiently high quality to cause no degradation in the linearity of the image movement.

Suppose the two block faces are flat but are inclined

at a small angle $\delta\alpha$, this being measured in the plane perpendicular to the axis of rotation of the block, an inclination in a plane containing the axis of rotation merely giving a constant image displacement. This inclination is equivalent to an equal small change in the angle of incidence $\delta\theta$. From equation 5(i) the image displacement d for an incidence angle θ is given by

$$d = t \sin\theta \left(\frac{n-1}{n}\right) + \frac{t \sin^3\theta}{2n^3}(n^2 - 1)$$

$$\therefore \frac{d(d)}{d\theta} = t \cos\theta \left(\frac{n-1}{n}\right) + \frac{3t \sin^2\theta \cos\theta}{2n^3}(n^2 - 1)$$

Substituting $n = 1.5$, $t = 10$.

$$\delta d = \left[\frac{10}{3} + \frac{50}{9}\sin^2\theta\right] \cos\theta . \delta\theta$$

For the small values of θ used experimentally, $\cos\theta = 1$ and $\sin\theta = \theta$

$$\therefore \delta d = \left[\frac{10}{3} + \frac{50}{9}\theta^2\right] \delta\theta \qquad - 5(iii)$$

The first term gives a constant image displacement and therefore will not affect the linearity of the image movement. For the blocks selected, $\delta\theta$ has a value of less than $\frac{1'}{5}$ and the maximum incidence angle is $\theta = .075$. Substituting these values to give the maximum value of the varying component $\delta d'$ due to the second term of equation 5(iii)

$$\delta d' = \frac{50}{9} . (.075)^2 . (.00006) \text{ mm}$$

$$= .1875 \times 10^{-5} \text{ mm.}$$

This is negligible compared with the main deviation of $\frac{1}{4}$ mm and hence the parallism of the block faces is more than adequate.

If the block surfaces are parallel but not plane the result is that the change in the angle of incidence of the light upon the block when the block is rotated will not be the same as the angle of rotation. Consider, fig. 5.5, a ray of light incident normally on the block face SS so that it passes through the centre of rotation O of the block. Assuming that, over the area of the surface where the ray is incident, the curvature of the surface is uniform and that opposite faces of the block are parallel, the curvature of the face SS may be expressed by

$$y = bx^2$$

where the x and y axes are as shown and b is a constant. If now the block rotates through an angle θ, the effect of the curvature is to alter the angle of incidence slightly as compared with that for a flat surface. If x' and y' are the axes of the revolved coordinate system

$$y' = bx'^2$$

and the angle of incidence θ_1 is given by

$$\theta_1 = \theta + \gamma$$

where $\gamma = \frac{dy'}{dx'}$ at the point of incidence P of the ray. The x' coordinate of P is given by $(\frac{t}{2} \tan \theta)$ if the curvature is small, and

$$\frac{dy'}{dx'} = 2bx'$$

Hence, at the point P

$$\left(\frac{dy'}{dx'}\right)_P = \frac{2bt}{2} \tan \theta$$

The blocks selected had a maximum variation of surface height from the mean of less than $\lambda/4$ for green light, these variations in height being gradual over the 1 cm square block surface. This gives a maximum value for the coefficient $\underline{b}$ of the order of 10^{-4}, so that γ has a maximum value of about $\frac{1}{4}'$ when θ has its greatest value of approximately 4°. An angular error of this amount produces a proportional error in the image movement of less than .1%, so that again the quality of the geometrical finish of the blocks is more than adequate.

CHAPTER 6

THE IMAGES OF CIRCULAR APERTURES

6.1. General.

A series of experiments is described in this chapter in which the forms of the image intensity distributions of circular apertures of various sizes were determined. Preliminary experiments were made to investigate the influence of optical tubelength on the images, the effect of variations in the numerical aperture of the condenser also being studied. The main body of the experiments concerned the images obtained under 'full-cone' illuminating conditions, where the numerical apertures of the condenser and objective were the same, these results being compared with the predictions of scalar diffraction theory.

In all the experiments an illuminating wavelength of 5300 $\mathring{A}$ with a bandwidth of 100 $\mathring{A}$ was used, this wavelength being convenient for the visual sizing work to be described in the succeeding chapter, the aberration correction of the objective also being best in the green region of the spectrum. A further advantage is that the output of the lamp and the sensitivity of the photomultiplier are high at this wavelength, enabling a good signal-to-noise ratio to be maintained.

In determining the image intensity profile under a particular set of optical conditions, the image is first focussed and centred visually using the viewing eyepiece.

The mirror is then removed and the scanning blocks are adjusted to centre the image on the photomultiplier pinhole. A complete scan is then made across a diameter of the image using one scanning block only, the galvanometer signal being recorded at regular intervals as the reading of the controlling micrometer is varied. An unobstructed area of slide is then brought into the centre of the field and the galvanometer reading given is recorded as the clear signal. The ratio of the galvanometer reading at any point in the image to the clear signal thus gives the intensity of that image point normalised in terms of the intensity of the image of a completely transparent uniform object, it being convenient to specify this as a percentage transmission. Hence, knowing by calibration with a periodic object the lateral movement produced by the scanning blocks, the intensity profile of the image can be expressed as a transmission profile.

6.2. Causes of Error in the Experimental Image Profile.

Before discussing the experimental results obtained, it will be convenient to consider briefly some further limitations and causes of error in the apparatus, other than those discussed in previous chapter, which will lead to differences between the image intensity distributions found experimentally and those predicted by scalar diffraction theory.

We may note first that each size group of test objects will exhibit a variation in size equal to that of the original spheres from which they were produced. This means

that the form of the image profiles obtained will show a corresponding variation for different individual apertures. The problem thus arises of specifying the image intensity profile that corresponds to an aperture having the mean diameter of the size group, knowing the profiles for a representative smaple of individual apertures, usually about twelve. If the standard deviation in diameter, and hence the difference between the individual profiles, is small, then it is reasonably valid to take the transmission at each point in the image of the aperture of mean diameter as corresponding to the mean of the transmissions at similar points in the images of the various individual apertures. This is the basis on which the mean transmission curves referred to in the succeeding sections have been plotted.

For the larger sizes of apertures, and especially for those of 2.79 μ diameter where the standard deviation of the diameters is particularly large, this process is less valid. This may be easily understood by reference to fig. 6.4, where it can be seen that the profile for such apertures contains a large region of uniform transmission at the centre, a change in aperture diameter effecting primarily the extent of this region and not the gradient at the edge of the image. Thus the mean of the image profiles of large apertures having diameters which differ significantly from one another will yield an 'average' profile having an intensity gradient at its edge which is lower than that in the image of an actual aperture. For this reason when

discussing the results for the 2.79 μ apertures the profile shown is that of an individual aperture having a maximum transmission and a halfwidth, or diameter at half the maximum transmission, corresponding to the mean of these quantities for a number of individual apertures of the size group.

The focussing of the objective is of great importance in its effect upon the image profile. The focus normally chosen was that which gave the highest intensity at the centre of the image and it was found that, using this initial criterion, the focussing mechanism of the microscope was good enough to give reasonably consistent results, no significant defocussing occurring during the scanning process. A small defect of focus of about 0.1 μ however will in general cause a drop in the central transmission of the order of 1 or 2%, the other characteristics of the image profile being, within the limits of experimental error, unaffected. With most sizes of apertures it is impossible to distinguish whether such variations in central transmission are due to defocussing or to variations in size amongst the individual apertures of the size group. Thus the results probably include some of these slightly defocussed image profiles, resulting in the mean central transmissions being slightly lower than they would be if all the images were exactly in focus. Occasionally a manifestly defocussed curve was obtained with a markedly lower central transmission and broader halfwidth, such

curves being rejected.

An experimental defect which limits the general applicability of the results to a more serious extent is the presence of light reflected between the lenses of the objective, and, to a lesser extent, between the scanning blocks. The existence of such light means that each object point, in addition to its conjugate image point gives several faint out-of-focus images in the same plane, the exact configuration depending upon the position of the object point relative to the optical components. Thus the measured intensity in the image of an isolated aperture in a dark field is reduced by an amount depending upon the degree of scattering and reflection in the optical system. When the clear signal is measured however, the object field is normally completely transparent, so that, at the particular point in the image field where the intensity is recorded, contributions in intensity are made by light reflected and scattered onto that image point from non-conjugate object points, other than that given by pure diffraction effects. This means that the clear signal measured is too high in proportion to the image signal, so that the calculated transmissions are too low. Little can be done to remedy this defect except by blooming during the manufacture of the objective, although the scanning blocks could be coated. A large clear field must be used to give the clear signal in order that the signal measured should not be reduced, as it is with smaller areas, by diffraction effects occurring at the

edges of the areas.

A further source of error lies in the possibility that the intensity profile may be measured along a chord rather than along a diameter. This would yield a lower halfwidth and edge transmission gradient. With the smaller apertures this is unlikely to occur since the maximum intensity is confined to a very small area of the image, allowing it to be very precisely centred, so that the subsequent scan is certain to be across a diameter. With the larger apertures however the considerable area of uniform transmission at the middle of their images makes it impossible to centre them by their maximum intensity alone. The technique used in centring such an image is to scan along a chord with one scanning block, having first centred the image approximately, the two micrometer readings on opposite edges of the image where the galvanometer readings are the same being noted. If the micrometer is then adjusted to the mean of these two readings and the other scanning block moves the image in a direction perpendicular to that of the first block, then the second micrometer block should scan a diameter of the image past the photomultiplier pinhole. Since the scan can be made so that its nearest approach to the centre of the image is about 10% of the true halfwidth of the image before a 1% difference in the scanned halfwidth is given, in practice the errors due to this cause are likely to be small.

Finally it may be noted that the calibration of the

image movement produced by the blocks as measured using different stage micrometers and gratings is only accurate to within about ± 1%, so that a permanent calibration error of this order may exist in the image dimensions.

Some idea of the net result of these various factors upon the image intensity profile of a particular size of aperture can be gained from fig. 6.1, which shows the distribution for 0.814 μ apertures under the conditions indicated. The vertical lines represent the standard deviations in the transmission at each recorded point in the image, as derived from scans of twelve different apertures of the size group. The scale of the variation in transmission, halfwidth and other properties of the image profile is typical of all sizes of test object and it should be borne in mind that, although the mean intensity distributions only are normally shown, all the profiles in the succeeding sections show a similar variation in transmission.

6.3. The Effects of Tubelength Variation.

In section 5.3 the results for the optimum tubelength as found by the star and interferometric tests were discussed. Since at this optimum tubelength the spherical aberration of the objective is a minimum, the concentration of light at the centre of the image at the best focus should be a maximum. Experiments were conducted, using 0.814 μ apertures as objects, to see whether in fact this was the case.

The procedure was to centre the image of the aperture

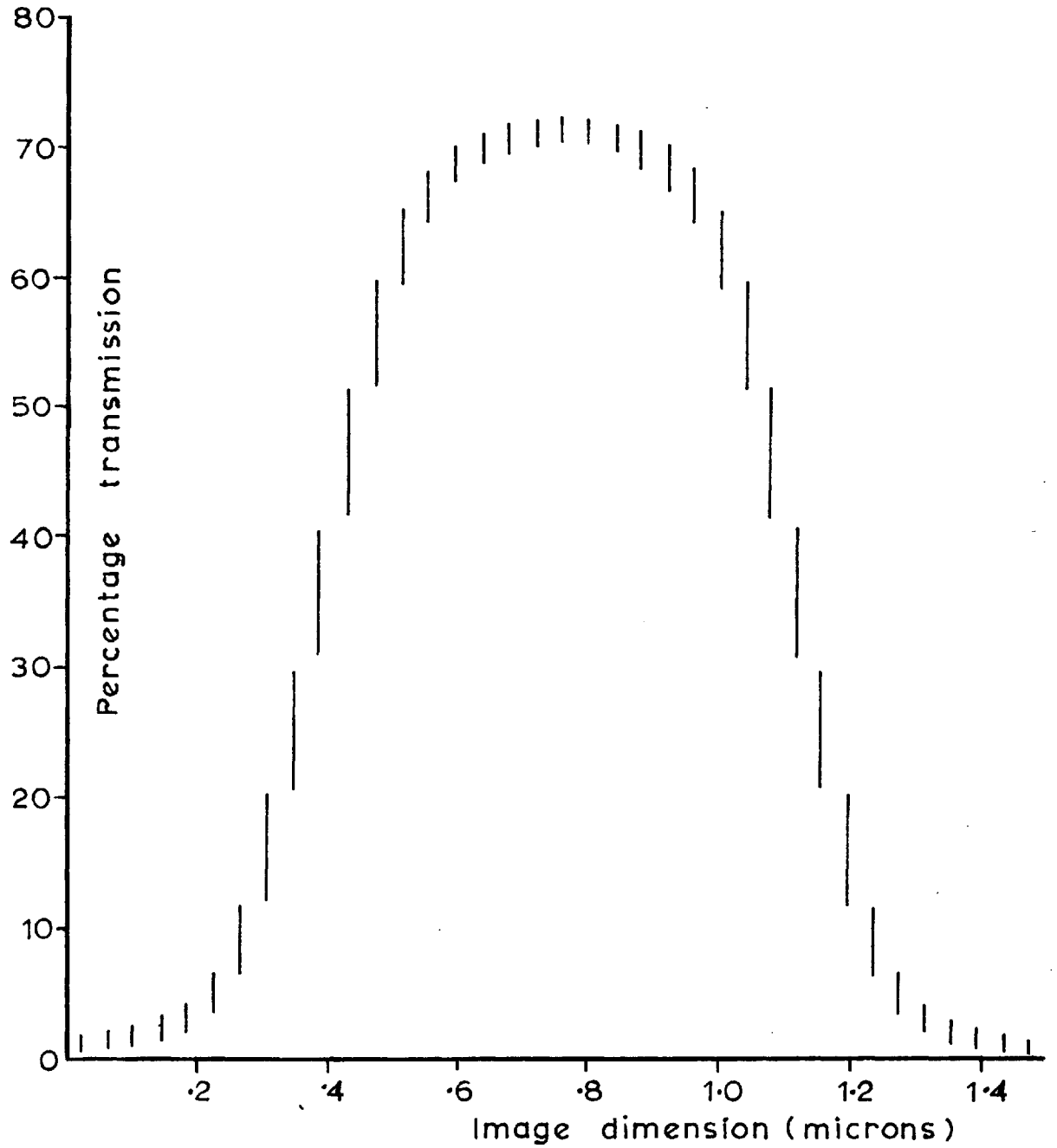

FIG. 6.1 STANDARD DEVIATIONS OF AN EXPERIMENTAL IMAGE TRANSMISSION PROFILE

0·814μ Apertures, $\lambda = 5300$ Å, $\delta\lambda = 100$ Å,
$(N.A.)_{o.g.} = (N.A.)_{cond.} = 1{\cdot}28$, T. L. = 180 mm

on the photomultiplier pinhole and to adjust its centration and focus until the maximum galvanometer signal was given. The clear signal was then recorded and hence the maximum central transmission at that particular tubelength calculated. The mechanical tubelength was varied between 160 and 225 mm, the numerical apertures of the objective and condenser being 1.28 and 1.30 respectively, while the wavelength and bandwidth were 5300 Å and 100 Å.

The results obtained are shown in fig. 6.2(a), the means and standard deviations for ten different individual apertures being plotted against the mechanical tubelength. It can be seen that at the previously determined optimum tubelength of 180 mm, the central transmission is in fact higher than at other tubelengths. The results also show that the central transmission at best focus is relatively insensitive to changes in tubelength, this agreeing well with the conclusions of the star and interferometer tests regarding the spherical aberration present at the various tubelengths.

The reduction of the intensity at the centre of the image in the presence of spherical aberration at the more extreme tubelengths is accompanied by an increase in the light intensity in the outer parts of the image. This is shown in fig. 6.2(b) for the case of the images of 0.511μ apertures at tubelengths of 180 and 220 mm, the curves representing the mean transmission profile at the best focus for ten different apertures, the other optical condi-

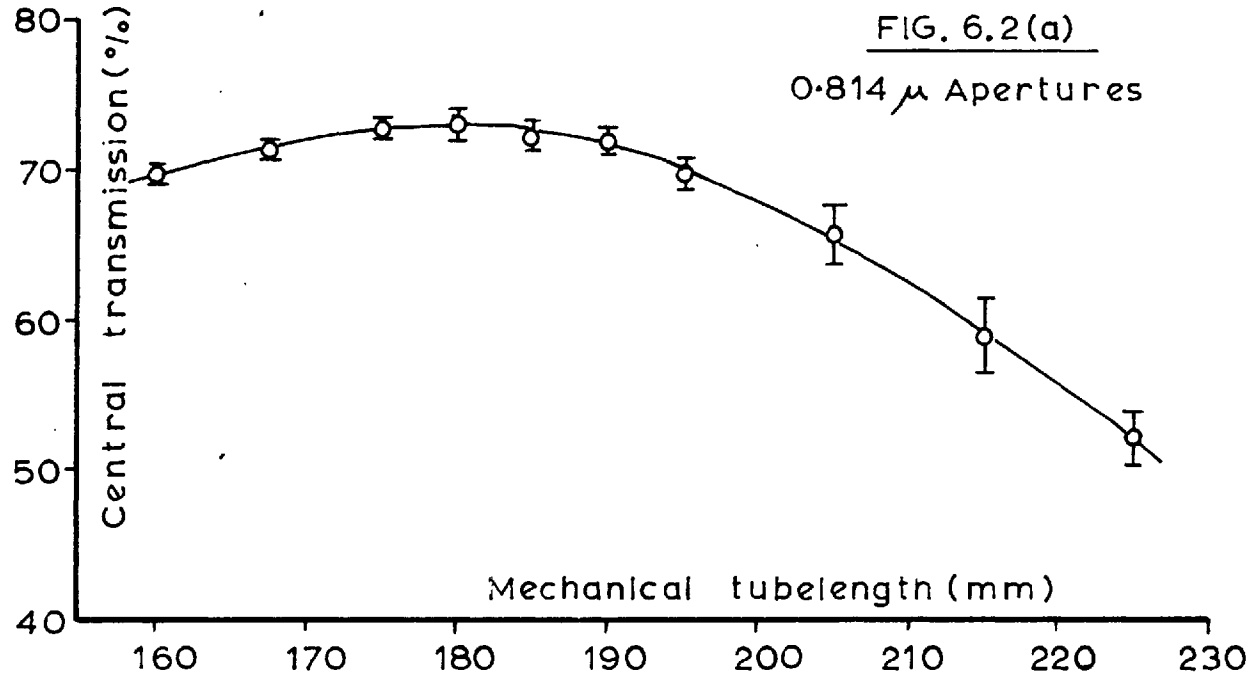

FIG. 6.2(a)

0·814 μ Apertures

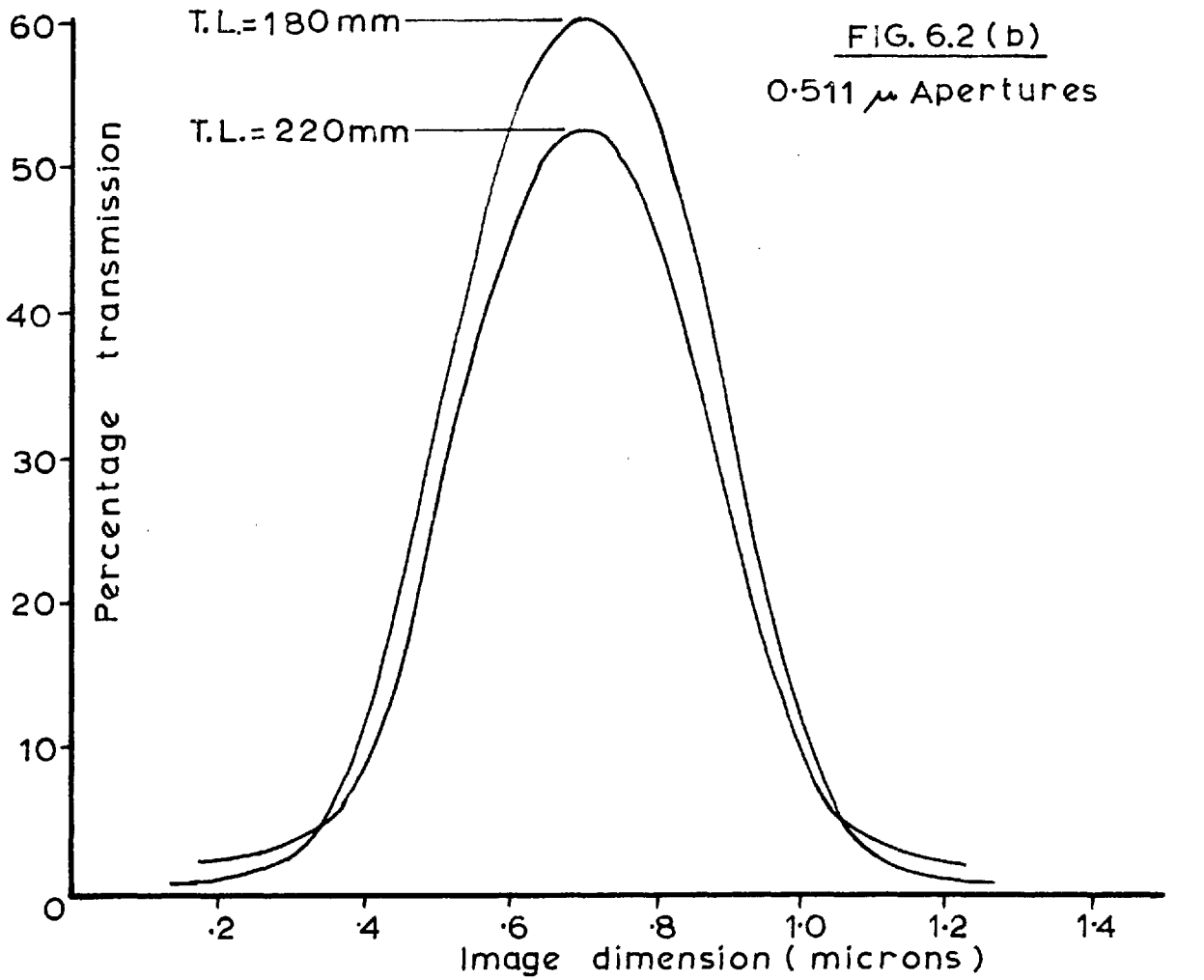

FIG. 6.2(b)

0·511 μ Apertures

tions being the same as in the previous experiment. Visually, this broadening of the intensity profile of the image was observed as a noticeable deterioration in the sharpness of the edge of the image. It may also be noted that the visual width of the image, making appropriate allowance for the differences in magnification, was significantly larger at the longer tubelength, a fact that emphasises the importance of using objectives of good spherical correction in high-resolution visual sizing work. The conclusions of Spinell and Loveland (1960) regarding the importance of correct cover-glass thickness in reducing spherical aberration are also relevant in this respect.

6.4. The Influence of Condenser Aperture.

It was pointed out in the discussion of theoretical results in chapter 2 that, in general, increasing the coherence of the illumination in a microscope by reducing the numerical aperture of the condenser results in images of greater contrast being given. In the case of objects consisting of circular holes this results in a higher central transmission and steeper transmission gradient at the edges of the image.

To verify experimentally that this was the case, the forms of the image intensity profiles of 0.814 μ apertures were determined when the numerical aperture of the condenser was set at various values, the numerical aperture of the objective being kept constant at 1.28 and the wavelength and bandwidth at 5300 $\mathring{A}$ and 100 $\mathring{A}$ respectively.

The images were focussed to give the maximum intensity at their centres.

The continuous curves in fig. 6.3. show the form of the image transmission profiles for this 'photoelectric' focus, the ratios of the numerical aperture of the condenser to that of the objective for the curves shown being 1.0, 0.91, 0.55 and 0.28, this being the 'S' value of Hopkins and Barham.

The curves, each of which is the mean of five scans, demonstrate markedly the enhancement of the central transmission at low S values, there being a corresponding decrease in the halfwidth of the images. Surprisingly however, this best photoelectric focus, where the central transmission is a maximum, no longer corresponds to the best visual focus for small values of S. The broken curves in fig. 6.3 show the transmission profile of the image when this is focussed visually, the halfwidths of the visual focus curves being indicated. The profiles at the best visual and photoelectric foci are the same for S = 1 and S = 0.91. The difference between the two profiles for S = 0.28 throws considerable light on the criteria whereby the image is judged visually to be 'in focus'. It is clear that the main desiderata are that the image should have lateral dimensions that are as small as possible and that the intensity gradient at the edge should be high. On the other hand, the value of the central transmission at the visual focus is obviously relatively unimportant. The

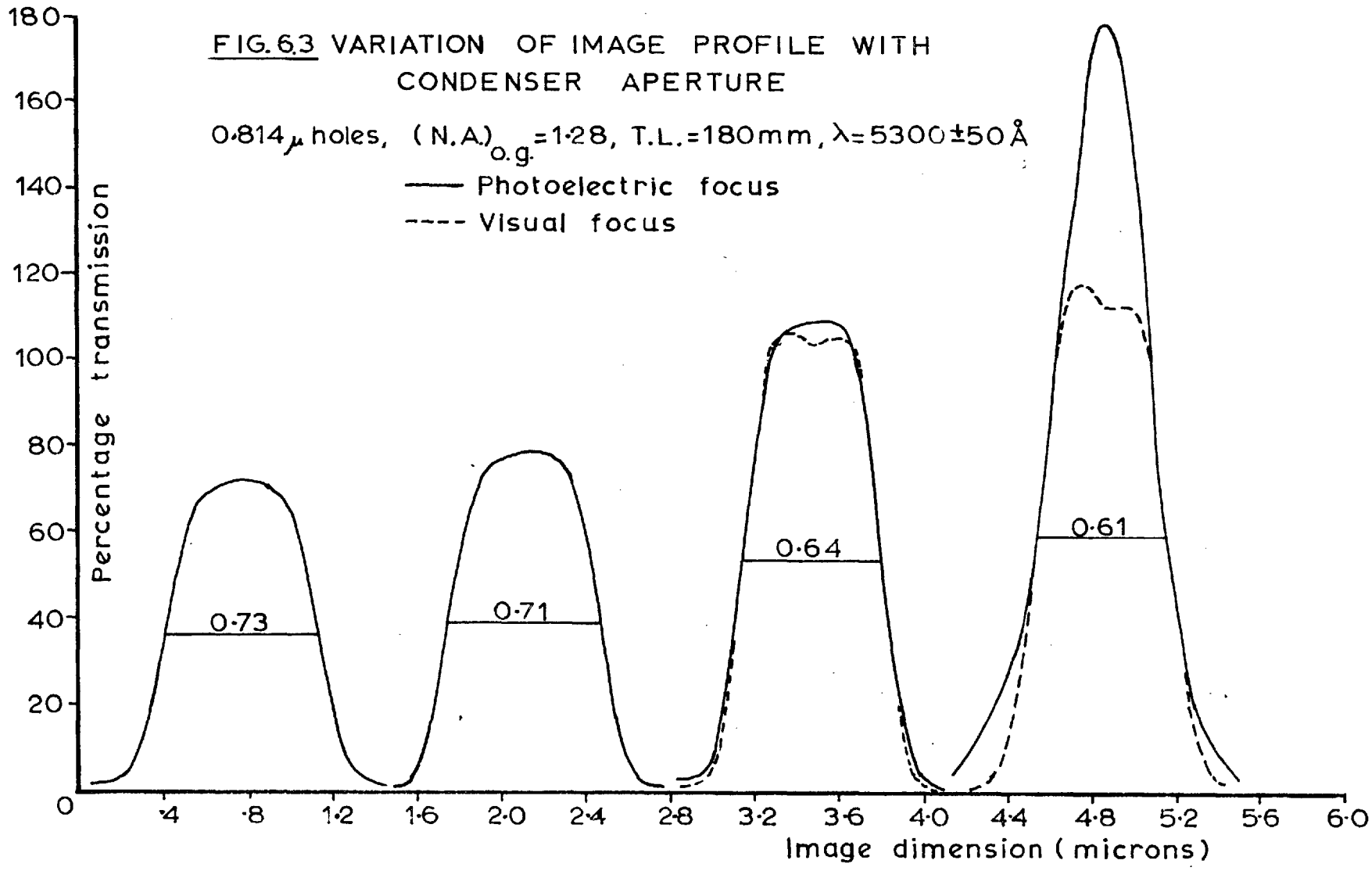
FIG. 6.3 VARIATION OF IMAGE PROFILE WITH CONDENSER APERTURE
0·814 μ holes, (N.A.)o.g. = 1·28, T.L. = 180mm, λ = 5300 ± 50 Å
Photoelectric focus
Visual focus
Percentage transmission
180
160
140
120
100
80
60
40
20
0
0·73
0·71
0·64
0·61
·4
·8
1·2
1·6
2·0
2·4
2·8
3·2
3·6
4·0
4·4
4·8
5·2
5·6
6·0
Image dimension (microns)

fact that, when S = 1, the focal position giving the minimum image dimensions and steepest edge transmission gradient also happens to give the highest central transmission is, from the visual point of view, fortuitous.

The exact relationship between the focus at which the highest central transmission occurs and the best visual focus certainly depends critically upon the size of the test object when this approaches the resolution limit of the objective. With the 0.814 μ apertures used, a higher central transmission was given at approximately symmetrically placed positions on either side of the best visual focus, the image profiles at these two photoelectric foci only differing slightly due to the small amount of residual spherical aberration in the objective.

Broadly speaking however the results may be taken as confirmation of the theoretical prediction that increasing the coherence of the illumination in a microscope gives images of greater contrast, a fact that is of course widely made use of in practical microscopy.

6.5. The Images of Circular Apertures under Full-cone Illumination.

As was stated in the previous section, when the condenser has the same numerical aperture as the objective (S=1), the intensity at the centre of the image at its best visual focus is a maximum. Using this focussing criterion, the transmission profiles of the full range of aperture objects were determined for the case where the numerical apertures

of the objective and condenser were both 1.28, the tube-length being 180 mm and the wavelength 5300 Å. The image distributions found in this way are shown in fig. 6.4, the radial variation of transmission only being given.

Table 6(i) below summarises these results; columns 1 and 2 give the actual size and standard deviation of the apertures, these being in fact the diameters of the spheres from which the apertures were made; columns 3 and 4 give the percentage transmissions at the centres of the images and their standard deviations derived from the profiles of twelve different apertures; columns 5 and 6 give the half-width in microns and its standard deviation, i.e. the width of the scan at a transmission equal to half that in column 3.

Table 6.(i). Scan profiles of circular apertures.

1 True aperture Diameter (μ)	2 S.D. (μ)	3 Max. Trans. %	4 S.D. %	5 Half-width (μ)	6 S.D. (μ)
0.138	.0062	7.8	1.7	0.26	.014
0.264	.0060	26.2	0.9	0.27	.010
0.365	.0079	47.5	1.3	0.31	.010
0.511	.0074	59.9	1.4	0.42	.010
0.557	.0108	62.1	1.8	0.44	.017
0.814	.0105	71.5	1.0	0.725	.020
1.171	.0133	79.6	2.5	0.975	.032
1.83	.018	90.0	2.3	1.61	.030
2.79	.15	98.5	0.6	2.45	.024

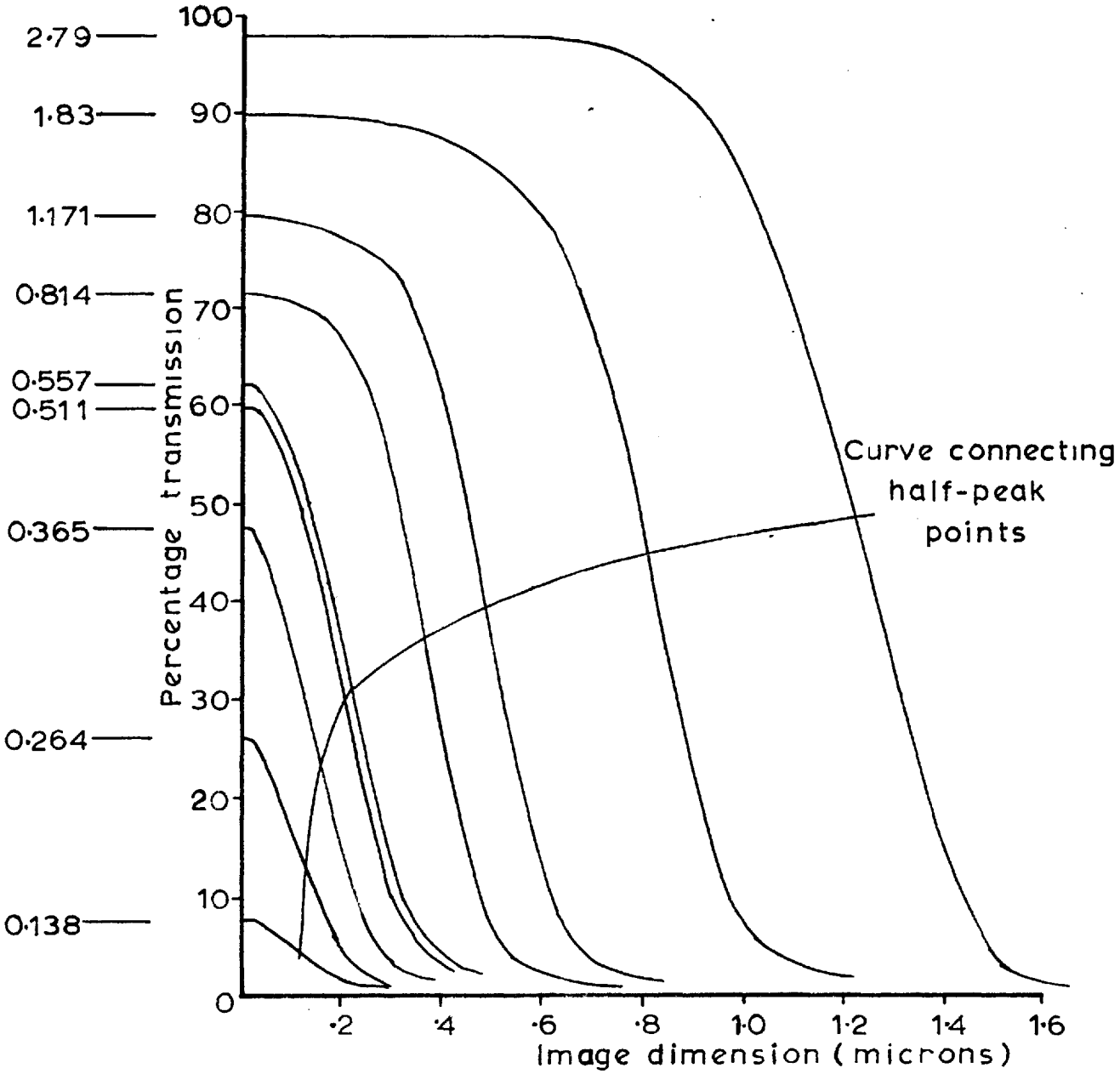

FIG. 6.4 RADIAL TRANSMISSION PROFILES FOR THE APERTURES INDICATED

$(N.A.)_{o.g.} = (N.A.)_{cond.} = 1{\cdot}28$, $TL = 180\,mm$, $\lambda = 5300 \pm 50\,Å$

It will be recalled that the scalar diffraction theory results obtained by Osterberg and Smith discussed in section 2.4 included intensity distributions for apertures whose sizes overlapped this range, so that it is possibel to make a comparison between the experimental results found when using high values of numerical aperture and the results of scalar diffraction theory. This comparison is made in fig. 6.5 (a) and (b), the abscissa in both cases being the true aperture diameter in Z units, these being the dimensionless diffraction units defined in section 2.3. Fig. 6.5(a) shows the variation of the transmission at the centre of the image with this parameter, while in fig. 6.5(b) the ordinate is the halfwidth of the image in Z units, the broken line being drawn at 45° to the axis and passing through the origin.

Although, for the reasons outlined in the discussions of the limitations of scalar diffraction theory and of the experimental technique, exact agreement between the theoretical and experimental results cannot be expected, it is evident that there is a close qualitative similarity between the two sets of results, the disagreements being in the directions expected. We may note also that, in addition to the lower experimental transmissions forecast for the reasons discussed in section 6.2. Andrejewski (1952) has shown, in a rigorous application of Maxwell's equations to the case of a plane wave incident upon a circular aperture, that the intensity in the aperture fluctuates violently

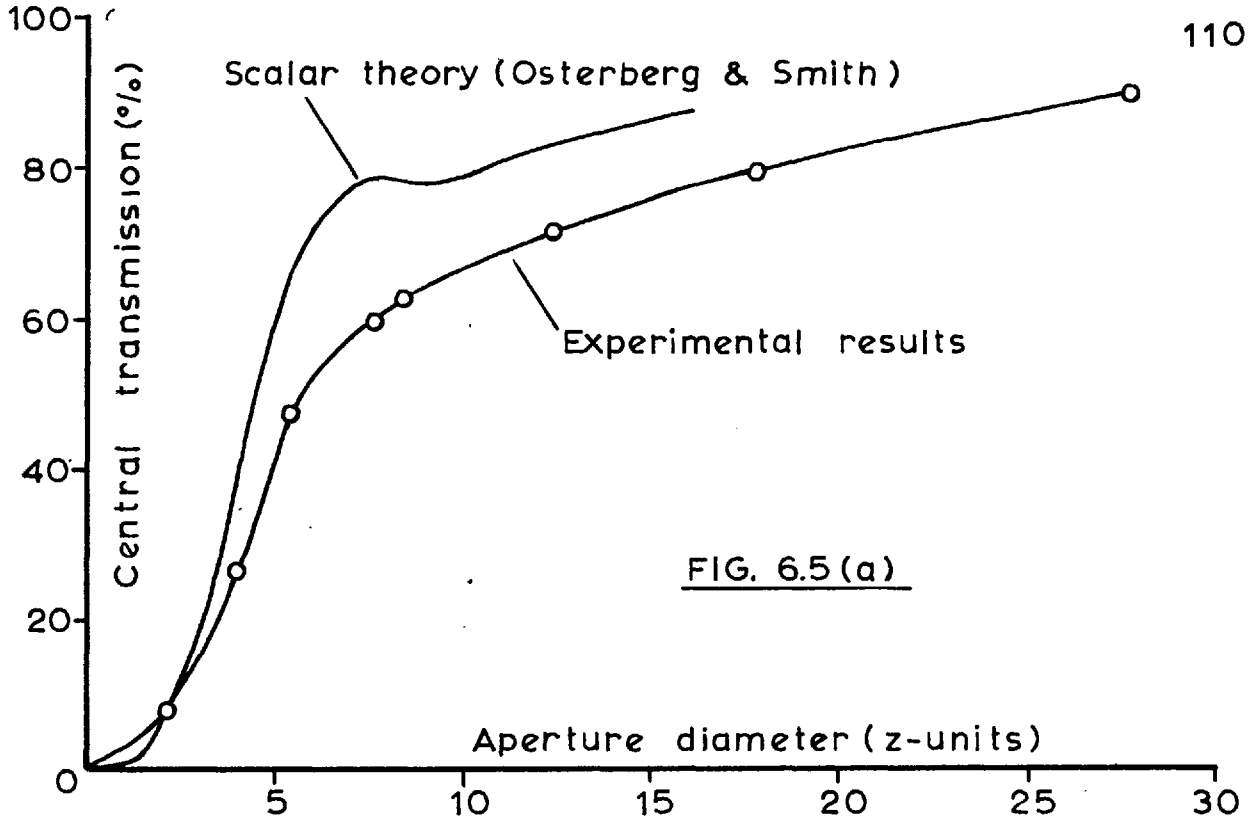

FIG. 6.5 (a)

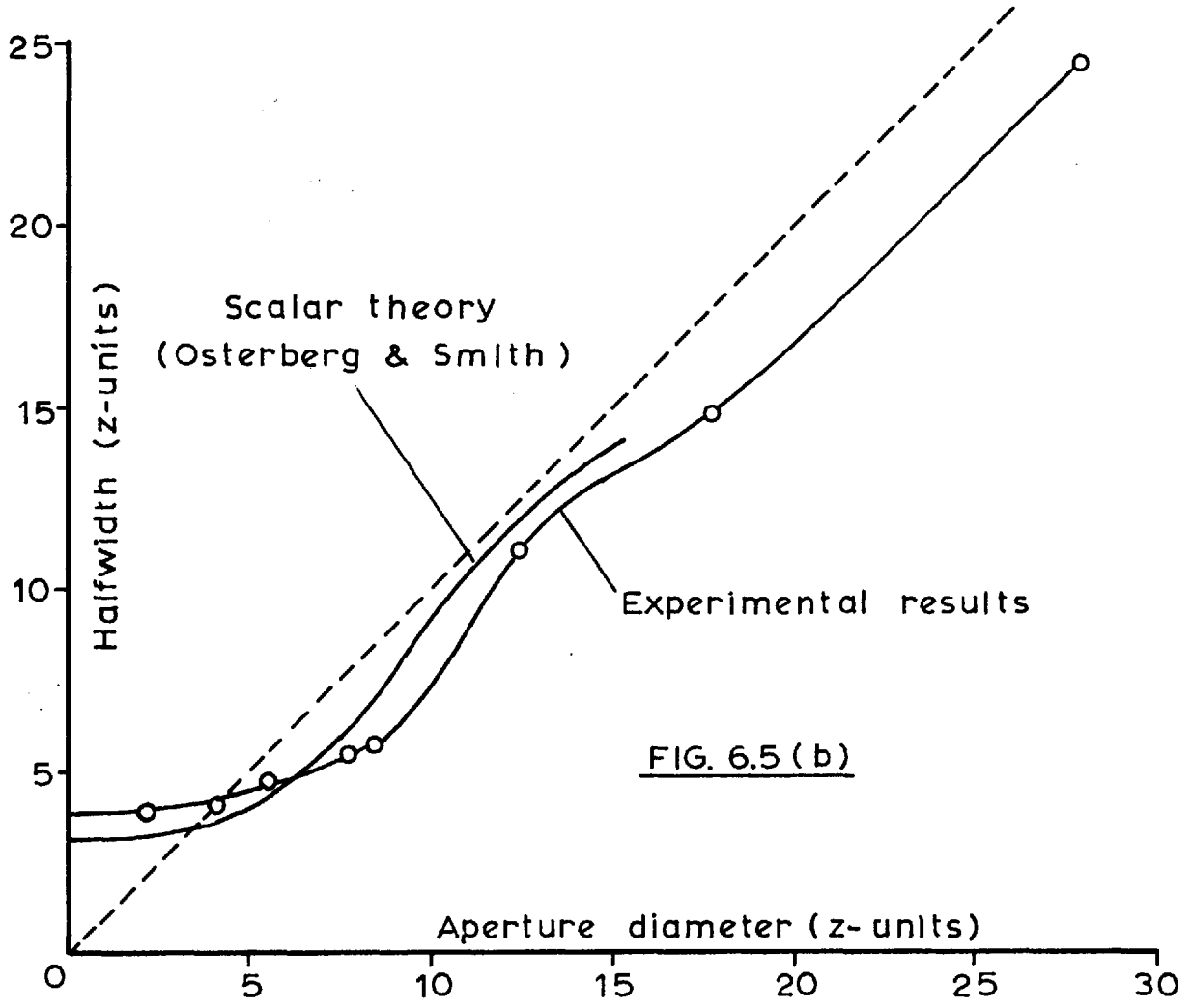

FIG. 6.5 (b)

(ca. 100%) across the aperture and with diameter, whereas in the approximate theory used by Osterberg and Smith it is assumed to be constant. Further, it appears from Andrejewski's work that apertures of about a wavelength in diameter scatter considerable amounts of energy not predicted by scalar theory, which helps in accounting for the experimental transmissions for apertures of diameters 3 to 15 Z units being up to 20% lower than those predicted by Osterberg and Smith (fig. 6.5(a)).

A further quantity of interest in the experimental image transmission curves of fig. 6.4 is the transmission at the point corresponding to the geometrical image of the edge of the object. The variation of this transmission with the diameter of the aperture, measured in Z units, is shown in fig. 6.6, the values predicted by Osterberg and Smith being shown for comparison. Also indicated is the $33\frac{1}{3}\%$ level derived by Welford for the case of a straight edge, as described in section 2.3.

Since the geometrical image of the edge falls at a part of the image profile where the transmission gradient is high, the standard deviation of the experimental results, indicated by the vertical lines, is large. However it would appear that experimentally the transmission at the geometrical edge under conditions of equal objective and condenser numerical aperture is tending towards a transmission of the order of 20% rather than the $33\frac{1}{3}\%$ level derived from scalar diffraction theory. Although the

experimental limitations can account for this discrepancy in part, it seems probable that the greater part of this difference is due to the inadequacy of the scalar theory for high aperture systems.

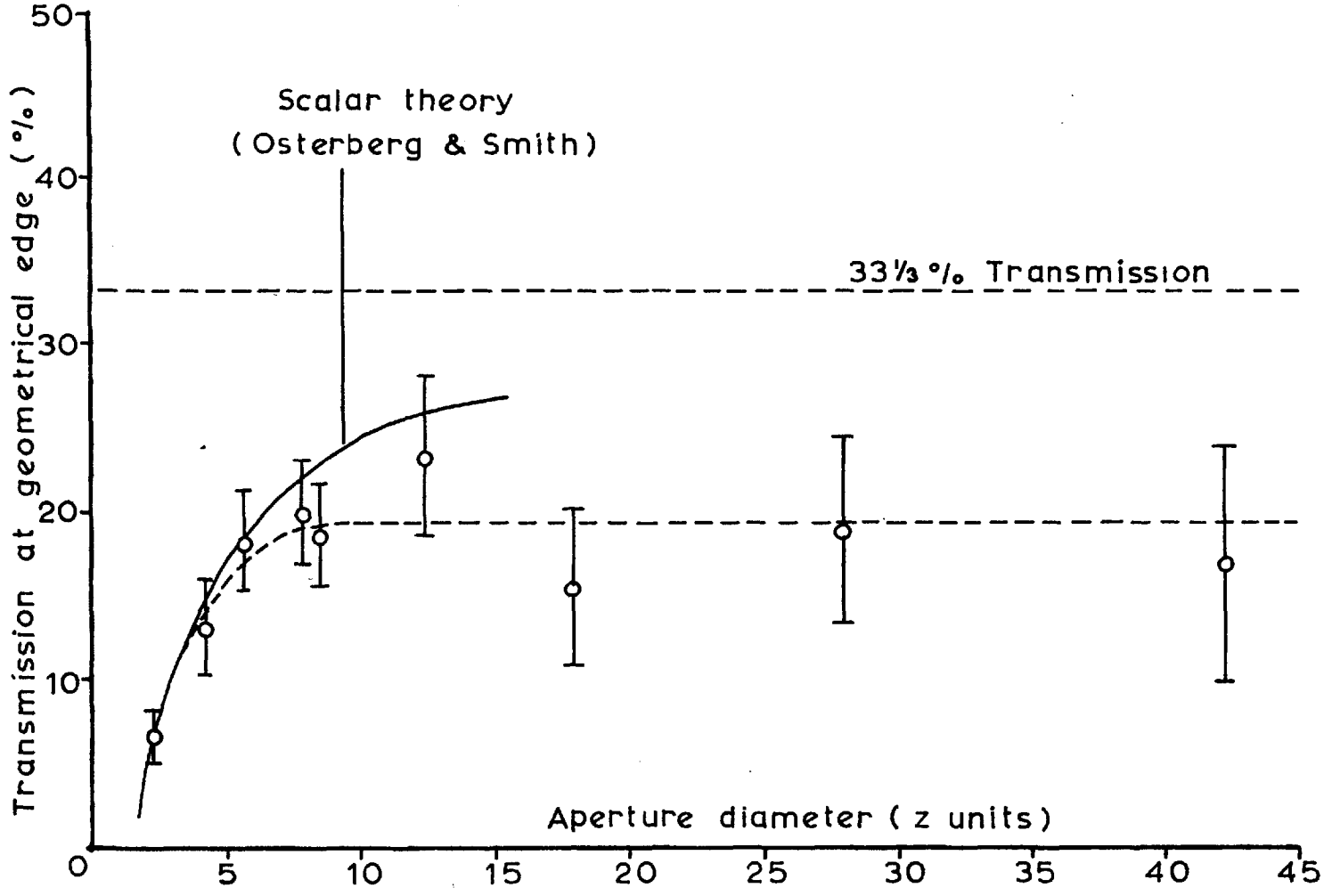

FIG. 6.6 VARIATION OF TRANSMISSION AT GEOMETRICAL EDGE WITH SIZE OF APERTURES

CHAPTER 7

THE VISUAL SIZE OF APERTURE IMAGES.

7.1. General.

It was pointed out in section 2.3. that no single simple relationship exists between the intensity profile in the primary image of a circular hole and the subjective brightness distribution seen when observing such an image with an eyepiece. However, it is found that, on measuring the apparent diameter of the visual image with a filar eyepiece, consistent results are given which can be directly related to the intensity profile in a way which depends upon the instrumental and visual conditions at the time of measurement.

Although the primary image has a continuous luminance distribution corresponding to those in fig. 6.4, the eye sees the aperture image as effectively a disc of light, whose subjective brightness may vary across its diameter but whose edges are fairly sharply defined. The sharpness of the image edges is probably due in part to the Mach effect, which is discussed more fully in section 8.3. One or more rings of light may be seen around the central disc, depending upon the instrumental and visual conditions, but these are less bright and have no effect upon the appearance of the centre of the image. In measuring the visual diameter, the edges used are those of the central bright disc, where the image brightness is just noticeably greater than that

of its dark surround. The eyepiece crosswire is first set tangentially to one side of the image, that is the position marked (i) in fig. 7.1, and is then traversed across the image disc until the small bright area towards which the crosswire is moving in the position (ii) of the figure just vanishes. The same edge of the crosswire is thus used in both cases, eliminating the effect of its finite width. The difference between the eyepiece micrometer readings in these two positions multiplied by a calibration factor gives the 'visual size' of the image.

The majority of the experimental measurements concerned the case where the objects were illuminated under 'full-cone' conditions, the effect on the visual size of the adaptation state of the eye, the magnification of the optical system and the luminance of the image being investigated. A brief study of the influence of the numerical aperture of the condenser was also made.

7.2. The Effect of the Adaptation of the Eye.

The illumination on the retina of the observer when making visual sizing measurements on a particular size of aperture corresponds closely to the form of the transmission profiles of the primary images described in the previous chapter. The eyepiece aberrations are negligible for a monochromatic image viewed axially and the chief differences between the retinal and primary images are due to the imaging properties of the observer's eye, these largely being controlled by the size of its entrance

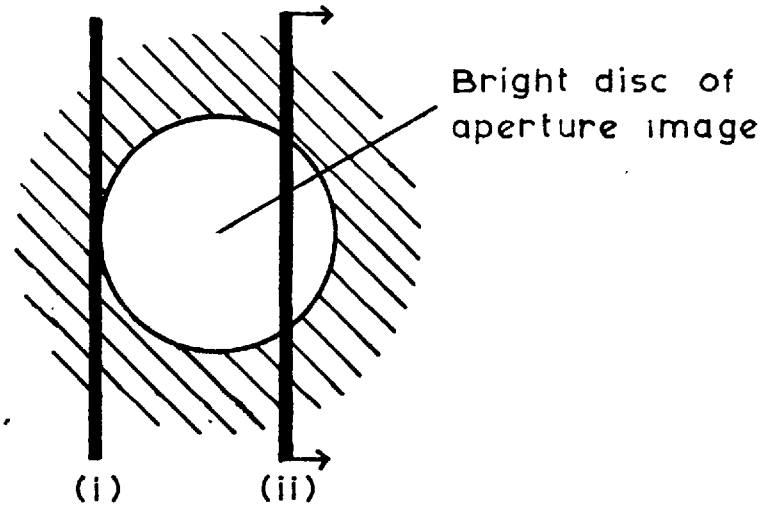

FIG. 7.1 MEASUREMENT OF VISUAL SIZE

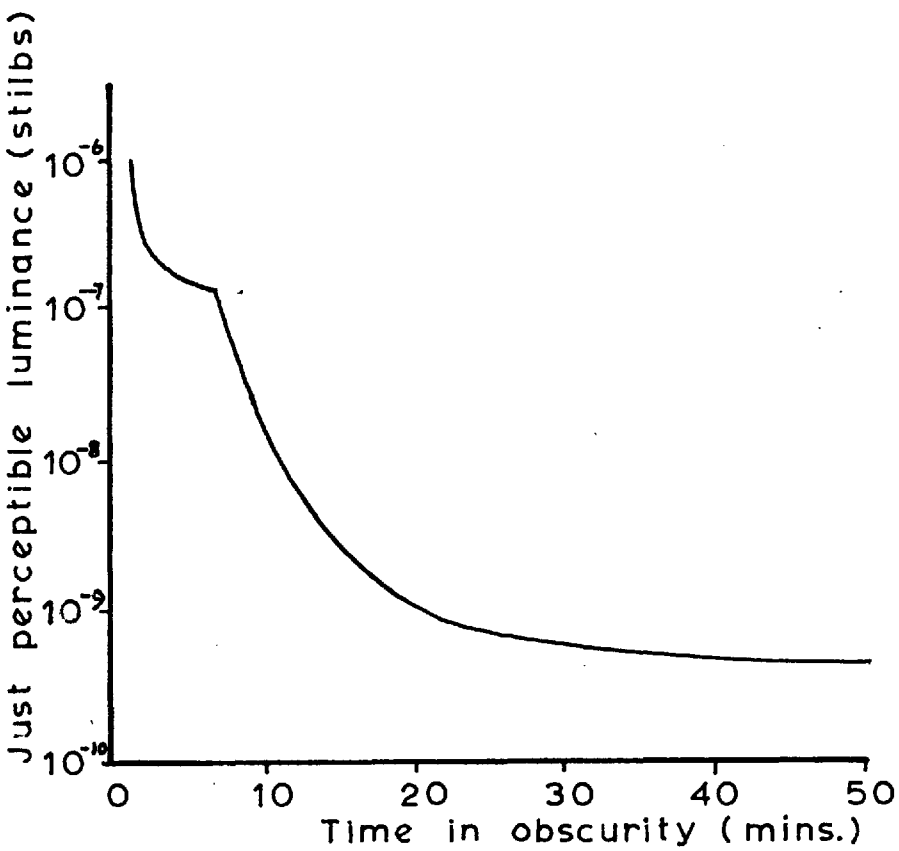

FIG. 7.2 THE COURSE OF DARK ADAPTATION
(AFTER WALSH)

pupil. This is effectively limited by the size of the exit pupil of the eyepiece, except when the eyepiece is of very low power. For example, a 10x eyepiece when used with the Beck objective has an exit pupil about $1\frac{1}{3}$ mm in diameter, whereas the natural pupillary diameter under normal conditions of luminance is about 3 mm, values lower than 2 mm only being reached at very high levels of luminance. The width of the eyepiece exit pupil only exceeds 2 mm when the eyepiece power is less than about 7x, so that, for the powers used experimentally (8x to 37x) the eye pupil was always limited by the exit pupil of the eyepiece.

Nothing can be done to control the exact response of the eye of a single observer to a particular visual stimulus presented under fixed conditions and viewed through a fixed pupil except to change the level of illumination to which the eye is adapted before observations are made. Thus, for what is effectively a constant distribution of light on the retina, the subjective brightness distribution that the observer 'sees' will vary according to the state of adaptation of his eye, the image appearing brighter the greater his degree of dark adaptation.

The course of adaptation to complete darkness after gazing at a bright field of view is shown in fig. 7.2, taken from Walsh (1953, p.65), the ordinates being the minimum luminance just perceptible after the eye has been in complete darkness for the time indicated by the corresponding abscissae. The first part of the curve shows the combined

recovery of both rods and cones while the part following the discontinuity represents the slower rod adaptation. Since the visual sizing technique involves, in effect, fixation upon the aperture image, this being of small angular subtense (ca. 1^{o}), the measurement is essentially a foveal one, so that only the first part of the curve, showing cone adaptation, is of interest. It can be seen from the curve that cone dark adaptation is virtually complete after about 5 minutes, although the exact time will depend upon the luminance to which the eye is originally adapted, reduction of this luminance resulting in a general shift of the adaptation curve of fig. 7.2 to the left and downwards.

The important feature of the curve for our purposes is that the light adapted eye is less sensitive to small luminances, of the type which occur in the outer parts of the aperture image, than is a dark-adapted eye. It was therefore expected that a greater luminance difference would be required before the image appeared noticeably brighter than its surround when the eye was light adapted, leading to a smaller visual size being given under these conditions.

To verify first that the visual size did vary with adaptation, preliminary experiments involving three different states of adaptation were made. In these the visual sizes of the images of 1.171 μ apertures were measured using a 20x eyepiece giving a total magnification of about 1900x, the retinal illumination at the centre of the image,

calculated from the exit pupil size of the eyepiece and the luminance of the field as deduced from the photomultiplier signal, being about 3×10^4 trolands; the other optical conditions were the same as were used in determining the image intensity profiles. Before each measurement, the eye was adapted as follows:

a) The used eye was allowed to observe for three minutes a uniform field of luminance approximately 0.04 stilbs and angular subtense 30°, this being the luminance of a white screen 1 metre from a 100 W filament lamp. Adaptation to this level of luminance was therefore complete and the images were sized immediately afterwards, further periods of adaptation being allowed between subsequent measurements.

b) The eye was allowed to adapt naturally to the mean luminance of the microscope field during measurements, these being recorded under equally low illuminating conditions. The level of adaptation was thus determined primarily by the angular subtense and luminance of the aperture images.

c) Complete dark adaptation of the used eye was secured by covering it with an eye patch for 5 minutes before measurements, after initially adapting it to the luminance level described in (a), further periods of dark adaptation being allowed between subsequent measurements.

The results obtained are given in table 7(i) below

Table 7(i). Effect of adaptation on sizing of 1.171 μ apertures.

Adaptation	Visual Size (μ)	S.D. (μ)	No. of results
a) Light adapted	1.309	.035	120
b) Field adapted	1.476	.086	120
c) Dark adapted	1.444	.056	60

It can be seen that the light adapted visual size is markedly lower, while those for the other states of adaptation are effectively the same. Under these conditions the angular subtense of the aperture image is about 40', and it would appear that a bright disc of this subtense does not greatly affect the dark adaptation of the eye, since if this were the case the field adapted results would lie between those obtained under conditions (a) and (c). This correspondence between the dark and field adapted sizes will be lost for increasing sizes of image however, since images of greater subtense will lead to an appreciable amount of light adaptation in the retina. It may be deduced that the use of lower luminance fields for the initial light adaptation in (a) would yield visual sizing results which more closely approached those obtained under the dark and field adapted conditions.

In normal sizing work the observer may either be

working in well-lit external conditions, so that his adaptation will correspond to state (a) or in semi-darkness, where the luminance of the microscope field excercises a greater control on his adaptation, i.e. state (b). Complete dark adaptation never occurs in practice and therefore no further experiments were performed under these conditions.

Using the same eyepiece power, retinal illumination and other conditions as before, the visual sizes of the whole range of apertures were measured under the conditions of adaptation defined in (a) and (b). The results are given in table 7(ii) below.

Table 7(ii) Visual sizing of apertures.

Aperture size (μ)	(a) Light adapted			(b) Field Adapted		
	Vis. size (μ)	S.D. (μ)	No. of readings	Vis. Size (μ)	S.D. (μ)	No. of readings
0.138	Measurements Impracticable			.518	.061	480
0.264				.552	.068	480
0.365				.577	.076	480
0.511	.738	.046	240	.747	.074	480
0.557	.806	.051	240	.780	.080	480
0.814	1.034	.038	480	1.104	.087	480
1.171	1.321	.048	960	1.489	.087	480
1.83	1.956	.054	240	1.997	.066	120
2.79	2.815	.062	240	2.863	.080	240

Fig. 7.3 shows the visual size plotted against the true size of the apertures, the broken line being drawn at 45° to either axis. The oversizing which occurs at all aperture

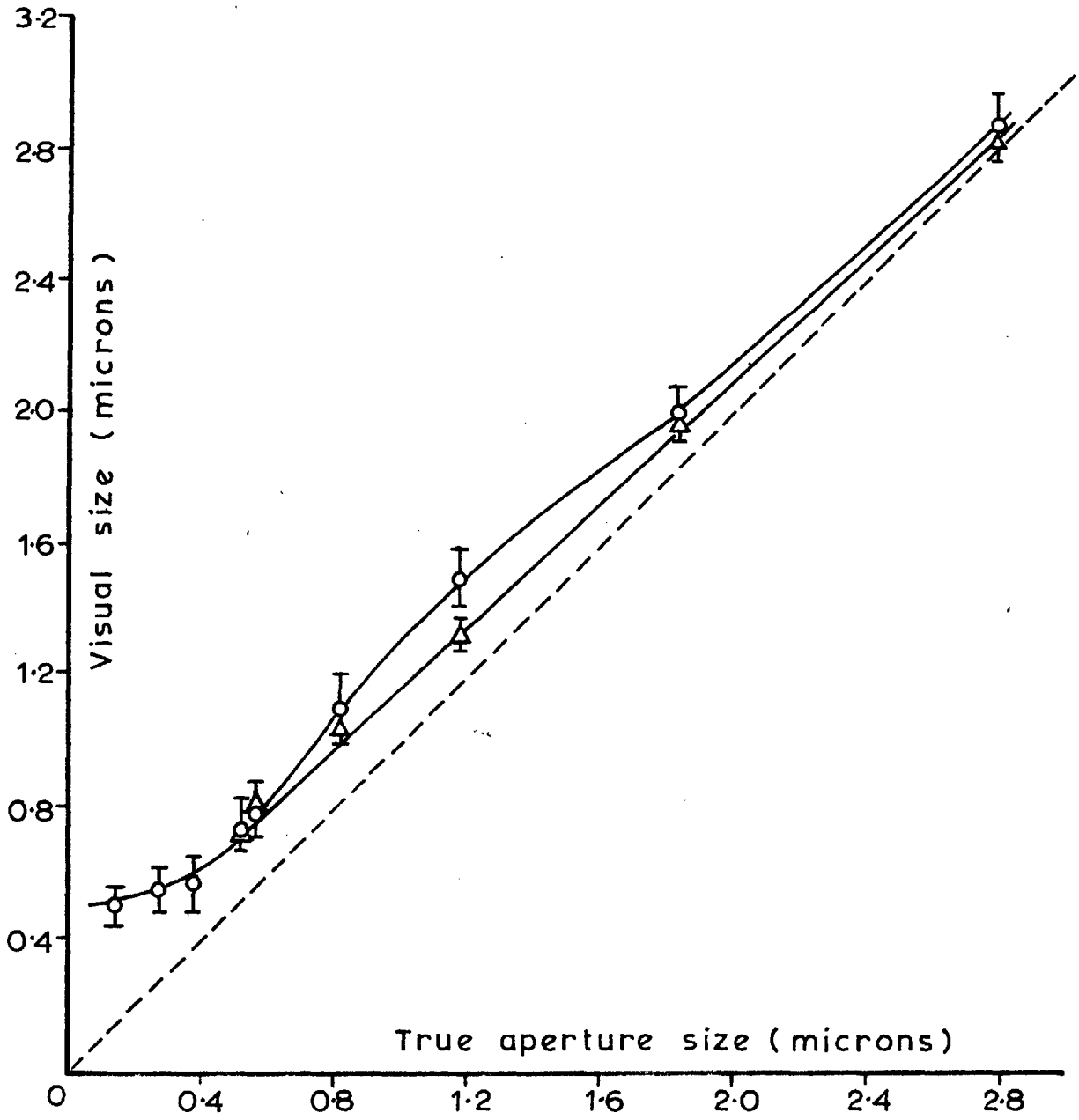

FIG. 7.3 VARIATION OF VISUAL SIZE WITH TRUE APERTURE DIAMETER

$(N.A)_{o.g.} = (N.A.)_{cond.} = 1{\cdot}28$, T.L. = 180mm, $\lambda = 5300 \pm 50$ Å

20 x Eyepiece

Δ Light adapted visual sizes

o Field adapted visual sizes

diameters is apparent. It is interesting that the greatest discrepancies between the two states of adaptation occur when the true aperture size is about 1 μ. The similarity between the results for the more extreme sizes can be explained by noting that with full light adaptation the subjective brightness of the images of the smaller apertures is too low for their visual size to have any meaning, some measure of dark adaptation being necessary before the images can be seen clearly enough for measurements to be made. On the other hand, the larger sizes of aperture yield retinal images of considerable angular diameter ($>1^{o}$) so that the eye, in performing its scanning movements across the image and the area immediately surrounding it, becomes substantially light adapted. Hence the visual sizes obtained in the field adapted state approach those given under light adapted conditions.

When the visual sizes are plotted on the transmission curves for the images the results shown in fig. 7.4 are obtained. Although exact quantitative deductions are impossible due to the comparatively large standard deviations involved, it would appear that the transmission at the light adapted visual edge is an approximately constant fraction of the central transmission (ca. 9% of T max) whereas the field adapted eye, until substantial light adaptation starts to occur with the larger aperture sizes, sets the visual edge at a point related to the sharp change in slope at the lower part of the transmission curves.

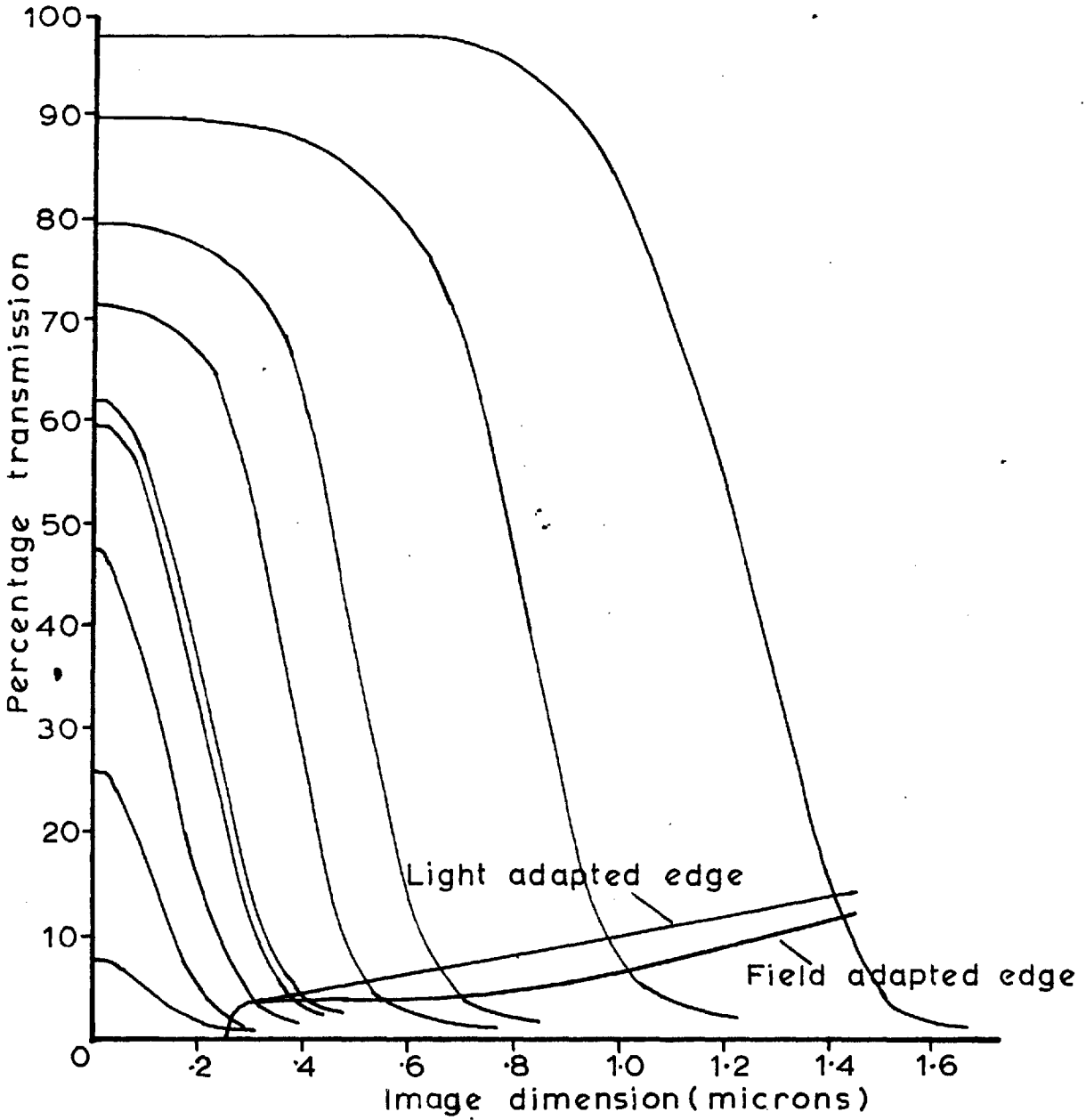

FIG.7.4 RELATION OF THE VISUAL EDGE TO THE TRANSMISSION PROFILES OF THE APERTURE IMAGES

20X Eyepiece, Retinal illum. = 10^4 trolands

This latter point occurs at approximately the same transmission (ca. 4%) in the images of all the apertures having diameters greater than about 0.3 μ . The transmissions at the visual edges for the two states of adaptation, and hence the visual sizes, approach one another as the transmission at the centre of the image decreases, that is as the aperture size decreases.

One interesting feature of the results given in table 7(ii) which can easily be explained in relation to the image transmission profiles is the smaller standard deviation of the light adapted results as compared with those under field adapted conditions. Assuming that the eye sets the visual edge at a particular transmission whose value depends upon the adaptation of the eye, the variations in visual size will be due primarily to fluctuations in the observer's 'transmission appreciation' of the image. Thus, although the mean transmission at the visual edge will differ according to the adaptation of the eye, the standard deviation of the visual edge transmission will be about the same in all states of adaptation. Hence the variation in the visual size will be less where the transmission gradient at the visual edge if high, that is for the light adapted state, than for the lower gradient found at the field adapted visual edge. The reduced standard deviations are probably also due in part to the more rigidly defined adaptation conditions used in (a) as compared with (b) where the adaptation may vary with the number and distribution of the aperture

images in the field of view.

The results obtained with a single observer will of course vary somewhat due to slight variations in the way he applies the setting criterion, fatigue and other factors. Some idea of the effect of these upon the results can be gained from fig. 7.5, each histogram representing the visual sizing results for the particular date indicated, the apertures all being 0.814 μ and the observing conditions, except for adaptation, being kept constant. The ordinates in each histogram represent the number of apertures measured as having visual size lying within the ranges indicated by the abscissae. The strong vertical lines represent the mean visual size and the dashed lines the limits of the standard deviation, each histogram containing 120 results. These means and standard deviations are given in table 7(iii) below.

Table 7(iii) Visual sizing of 0.814 μ Apertures.

a) Light Adapted			b) Field Adapted		
Date	Mean V.S. (μ)	S.D. (μ)	Date	Mean V.S. (μ)	S.D. (μ)
14.7.59	1.042	.039	12.3.59	1.093	.093
16.7.59	1.031	.037	4.5.59	1.104	.078
17.7.59	1.027	.035	11.5.59	1.126	.089
24.7.59	1.036	.038	15.5.59	1.093	.066

It is apparent from the histograms and table that the results for the mean visual size under particular conditions can be reproduced with a high degree of consistency, but that under light adaptation the variation of the individual

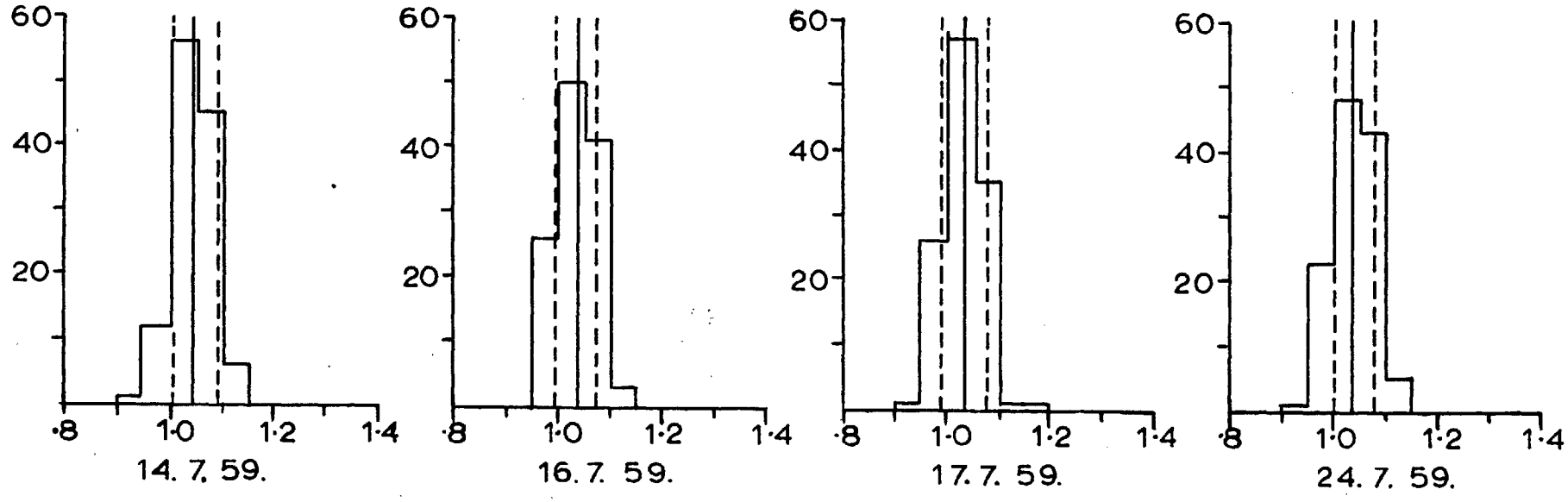

(a) Light adapted

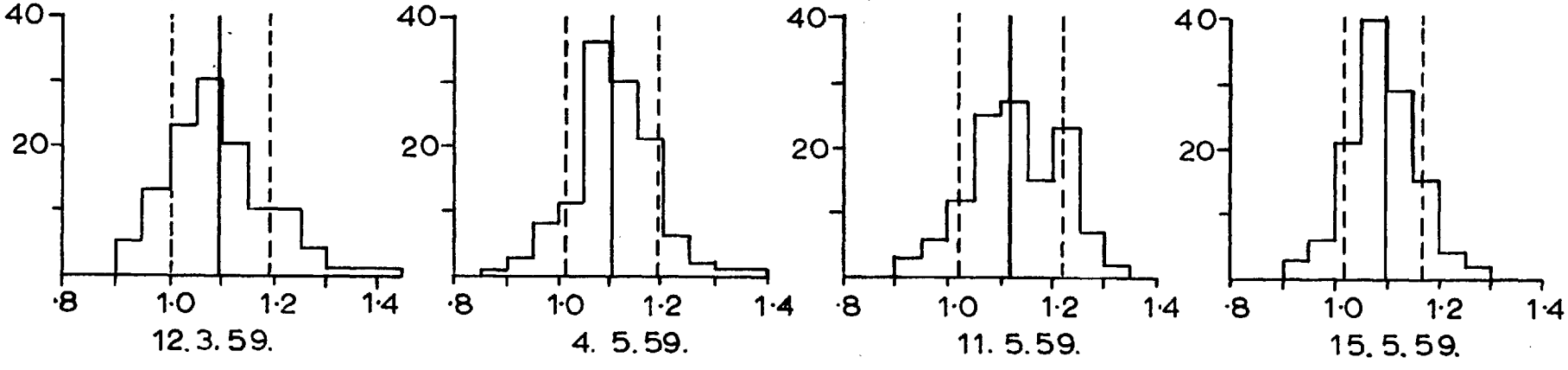

(b) Field adapted

FIG. 7.5 VISUAL SIZING HISTOGRAMS

results from the mean is far less than with field adaptation.

7.3. The Dependance of Visual Size upon Magnification.

The higher the overall magnification used in the microscope system the larger will be the image formed on the retina of the observer for a given object. It will be recalled from fig. 2.6 that the luminance discrimination of the eye improves as the visual subtense of the area of interest increases. Thus it may be expected that the visual size, which depends essentially upon the luminance discrimination of the eye, will vary with the magnification at which the image is viewed, assuming that other conditions are kept constant.

Experiments were therefore carried out to investigate the effect of varying the magnification by using eyepieces of different powers. Apertures of diameter 0.814 μ were used as test objects, the wavelength and bandwidth being 5300 Å and 100Å, while the tubelength was 180 mm; the objective and condenser both had numerical apertures of 1.28. The retinal illumination at the centre of the aperture images was standardised at 3×10^4 trolands, a value which, according to the results to be described in section 7.4 below is well above the region where this is a critical factor. Six Ramsden eyepieces, ranging in power from 8x to 37x, were used and 120 visual sizings were made with each power, using the usual sizing criterion and filar eyepiece. The eye was allowed to adapt naturally to the

microscope field, the results obtained being given in table 7(iv) below.

Table 7(iv) Dependance of visual size on magnification for 0.814 μ apertures.

Eye-piece power	Visual Size (μ)	% Trans. at visual edge (Tv.s)	$\frac{Tv.s}{Tmax}$ as per-centage	Angular subtense of V.S. ($'$)
x37	1.089$\pm$.044	4.1$\pm$0.7	5.7$\pm$1.7	50.1$\pm$2.0
x25	1.093$\pm$.045	4.0$\pm$1.05	5.6$\pm$1.45	35.0$\pm$1.4
x20	1.083$\pm$.034	4.3$\pm$0.85	6.0$\pm$1.15	29.2$\pm$0.9
x15	1.046$\pm$.050	5.1$\pm$1.85	7.1$\pm$2.6	19.9$\pm$1.0
x10	1.024$\pm$.065	6.3$\pm$2.95	8.8$\pm$4.15	13.3$\pm$0.8
x8	0.926$\pm$.088	12.0$\pm$7.1	16.8$\pm$9.95	8.8$\pm$0.8

The range figures correspond to the standard deviations and the percentage transmissions at the visual edge positions are derived from the photoelectric scan curve for the 0.814 μ apertures given in fig. 6.4.

The visual size is plotted against its angular subtense i.e. effectively against magnification in fig. 7.6. It can be seen that, with eyepiece powers above 20x, the visual size remains, within the limits of experimental error, constant, but with lower eyepiece powers it falls sharply, a value of about 85% of its original value being given when an 8x eyepiece is used. Based on the classical considerations of resolving power, an eyepiece magnification of between 5 and 15x should be used with a 95x, 1.3 N.A. objective at

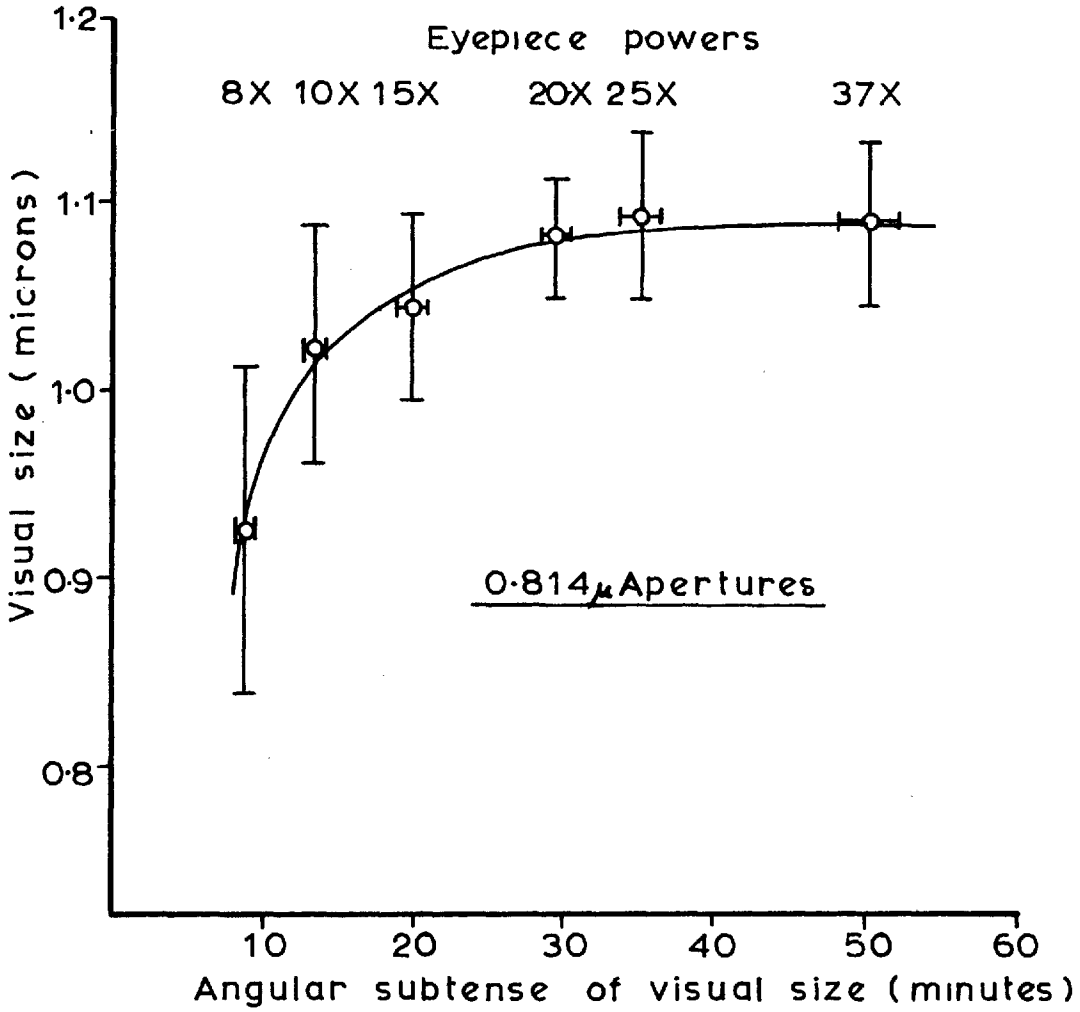

FIG. 7.6 VARIATION IN VISUAL SIZE WITH EYEPIECE POWER

Field adaptation, Ret. illum. = 10^4 trol.

$(N.A.)_{o.g.} = (N.A.)_{cond.} = 1{\cdot}28$, $\lambda = 5300 \pm 50$ Å

this wavelength. Thus, if we consider that consistency and, as far as possible, independance of the individual characteristics of the optical system used, are the desiderata in visual sizing, then it is clear that, for this aperture size at least, a higher eyepiece power than that normally recommended is desirable.

Fig. 7.7 shows the transmission at the 'visual edge' (Tv.s.) as a percentage of the transmission at the centre of the image (T_{max}) plotted against the angular subtense of the visual size. It is clear that the 'visual edge' is moving progressively inwards towards the higher transmissions as the eyepiece power is decreased. At eyepiece powers above 20x however the visual edge is set at a constant transmission. This may be compared in fig. 7.8 with Hunt's results (shown originally in fig. 2.6) the ratio of the increase in luminance necessary to make a circular test patch distinguishable from its surround to the surround luminance being plotted against the angular diameter of the test patch. Although by no means identical they are clearly qualitatively similar.

The results for one size of aperture (0.814μ) alone however do not by themselves clarify the reasons for a constancy in size being reached above a certain magnification. This may depend on:-

a) The angular subtense of the whole image of the object, so that smaller objects demand larger magnification.

b) The angular subtense of the whole transmission gradient

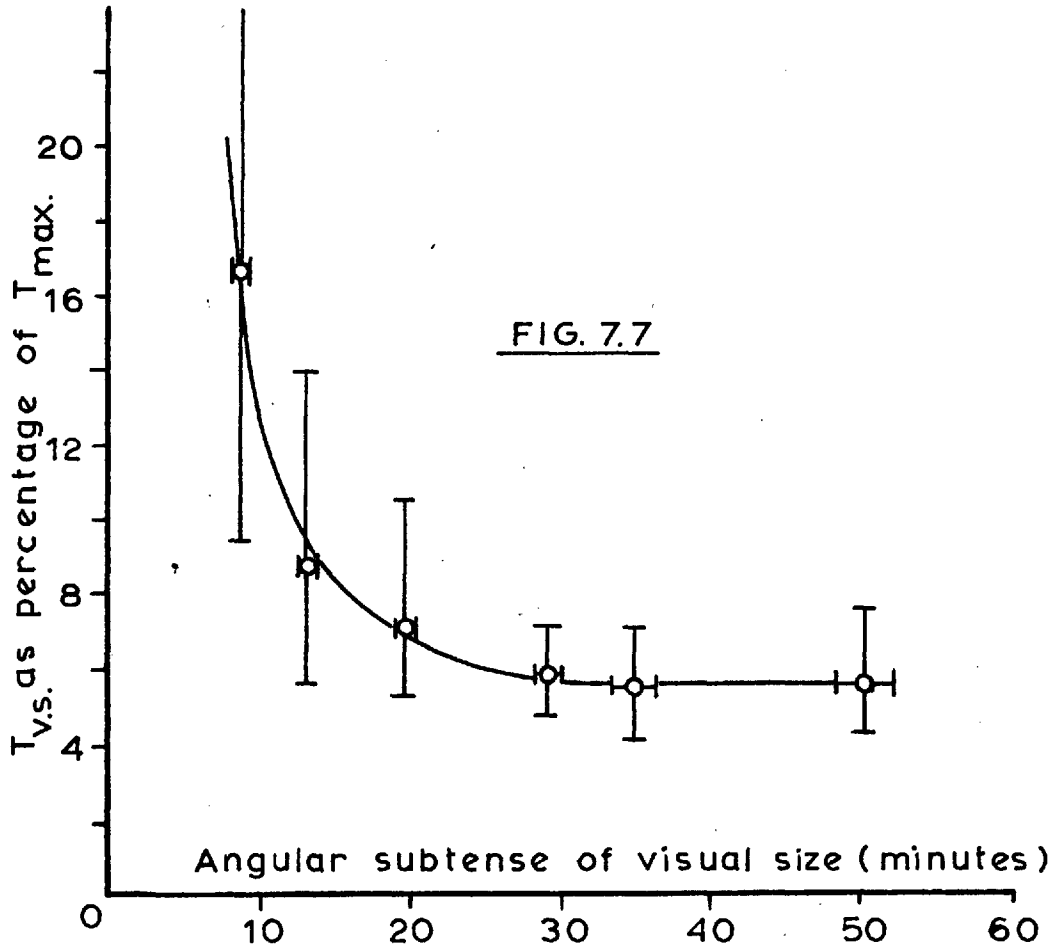

FIG. 7.7

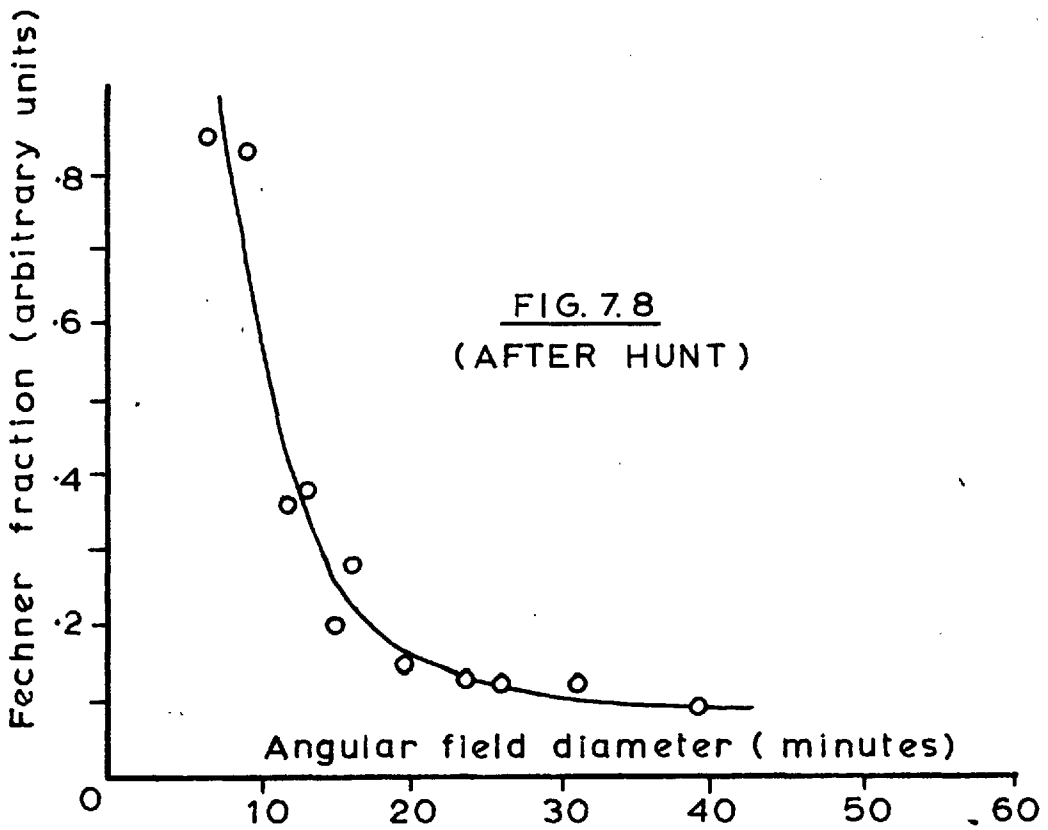

FIG. 7.8
(AFTER HUNT)

at the edge of the image, this again varying with object size.

c) The angular subtense of the lower part of the image gradient (below ca. 10%), the form of this region being approximately the same for all sizes of apertures.

To distinguish between these possibilities, 0.138μ apertures were used as objects and their visual sizes measured with different eyepiece powers under exactly the same optical and visual conditions as were used for the 0.814 μ diameter objects. The results obtained are given below, sixty sizings being performed at each eyepiece power.

Table 7(v) The effect of magnification on the visual size of 0.138 μ apertures.

Eyepiece power	Visual Size (μ)	Angular subtense of V.S. (min.)
10x	0.389 $\pm$ .060	5.1 $\pm$ 0.8
15X	0.446 $\pm$ .044	8.5 $\pm$ 0.8
20x	0.476 $\pm$ .061	12.9 $\pm$ 1.6
25x	0.491 $\pm$ .046	15.7 $\pm$ 1.5
37x	0.481 $\pm$ .041	22.1 $\pm$ 1.9

It is apparent from these results that constancy in visual size is again reached when the eyepiece power reaches about 20x. Since the angular subtenses of the whole image and edge gradient differ considerably from those for the 0.814μ apertures, it may be concluded that it is the subtense of the transmission gradient at the outer part of the

image which is of importance, the characteristics of this region being common to the images of all sizes of aperture.

It should be noted that the same differences between the light and field adapted visual sizes as were discussed in the previous section occur at all magnifications. This is illustrated below for the case of 0.814 μ apertures with eyepiece powers of 10x and 20x, the other conditions being equal. The means and standard deviations are based on 120 results in each case.

Table 7(vi).

Eyepiece power	Light-adapted visual size (μ)	Field adapted visual size (μ)
x10	0.978 $\pm$ .053	1.024 $\pm$ .065
x20	1.034 $\pm$ .038	1.104 $\pm$ .078

In the foregoing discussion it has been assumed that the retinal illumination is directly proportional to the area of the entrance pupil of the eye and hence to the exit pupil area of the eyepiece. Although for large pupil areas the occurrence of the Stiles-Crawford effect prevents this from being the case, for the pupil diameters used ($<$ 1 mm) this is a valid assumption.

More seriously, it could be objected that the visual size might go on increasing with magnification above the limits found were it not for the marked diffraction effects occurring in the retinal image due to the very small

effective eye pupils used. In fact however, consideration shows that the form of the intensity relationships in different parts of the aperture image on the retina is unchanged by the variations in the pupil size as the eyepiece power is varied, although the actual distances on the retina between those parts of the image are of course altered.

The geometrical magnification of the primary image given by the eyepiece is inversely proportional to its focal length, this ranging from about 7 to 30 mm for the eyepieces used. To a close approximation, the diameter of the exit pupil of the eyepiece, and hence the entrance pupil of the eye and its numerical aperture, is also inversely proportional to its focal length. This means that the dimensions of the diffraction images formed on the retina of any two points in the primary image will be changed in the same ratio as the distance on the retina between the images of the two points. Hence the form of the intensity relationships between different parts of the retinal image is preserved, only the dimensions or angular subtense of the image changing with eyepiece power, so that the basis of the conclusions regarding the effect of magnification is sound.

7.4. The Influence of Image Luminance.

In the discussion of the effect of magnification it was tacitly assumed that only the relative luminances in different parts of the images, i.e. their transmission

profiles] were of interest, not their absolute values. The possibility exists however that this is not justifiable and that the absolute values should be considered. This difficulty can be resolved by varying the luminance of the image, other conditions being kept fixed, and seeing if the visual size does in fact change. If there is a continuous variation of visual size with luminance, then we should be dealing with absolute values, if the results are constant when the luminance is changed, then it is the relative values that need to concern us.

In ascertaining which was the case, 0.814 μ apertures were again used as objects, and the same retinal illumination as before was taken as the normal value (3×10^4 trolands). Visual sizes were measured with 8x and 37x eyepieces (it being assumed that intermediate powers were unlikely to show any vastly different effects) at values of retinal illumination which bore a logarithmic ratio to the normal value. All other conditions were kept as constant as possible, the eye being allowed to adapt naturally to the eyepiece field. The total range of retinal illumination covered ($4\frac{1}{2}$ log units) was limited at its upper end by the output of the lamp and at the lower end by the sensitivity of the detector.

Sixty settings were made at each illumination level and the results obtained are tabulated below. The transmission at the visual edge was determined from the scan curve as before.

Table 7(vii) Effect of retinal illumination on the visual sizing of 0.814 μ apertures.

Retinal illumination (trolands)	Relative log. ret. illum.	x8 eyepiece			x37 Eyepiece		
		Visual size (μ)	Tv.s (%)	$\frac{Tv.s}{Tmax}$ as %	Visual size (μ)	Tv.s (%)	$\frac{Tv.s}{Tmax}$ as %
$3x10^5$	1.0	0.904 ±.110	13.7	19.2			
10^5	0.5	0.942 ±.087	10.8	15.1			
$3x10^4$	0	0.924 ±.073	12.0	16.8	1.076 ±.045	4.3	6.0
10^4	-015	0.908 ±.079	13.4	18.7	1.093 ±.037	3.9	5.5
$3x10^3$	-1.0	0.925 ±.083	12.1	16.9	1.068 ±.046	4.5	6.3
10^3	-1.5	0.879 ±.089	16.1	22.5	1.054 ±.038	5.0	7.0
$3x10^2$	-2.0	0.846 ±.088	19.7	27.6	1.019 ± .054	6.4	9.0
10^2	-2.5	0.828 ±.100	22.0	30.8	0.998 ±.047	7.5	10.5
30	-3.0				0.966 ±.060	9,1	12.7
10	-3.5				0.889 ±.070	15.1	21.1

When the mean visual sizes obtained are plotted against the retinal illumination for both eyepiece powers (figs. 7.9 and 7.10) it becomes apparent that the visual size remains constant over a wide range of retinal illumination, or image luminance, it only falling off at the lower end of

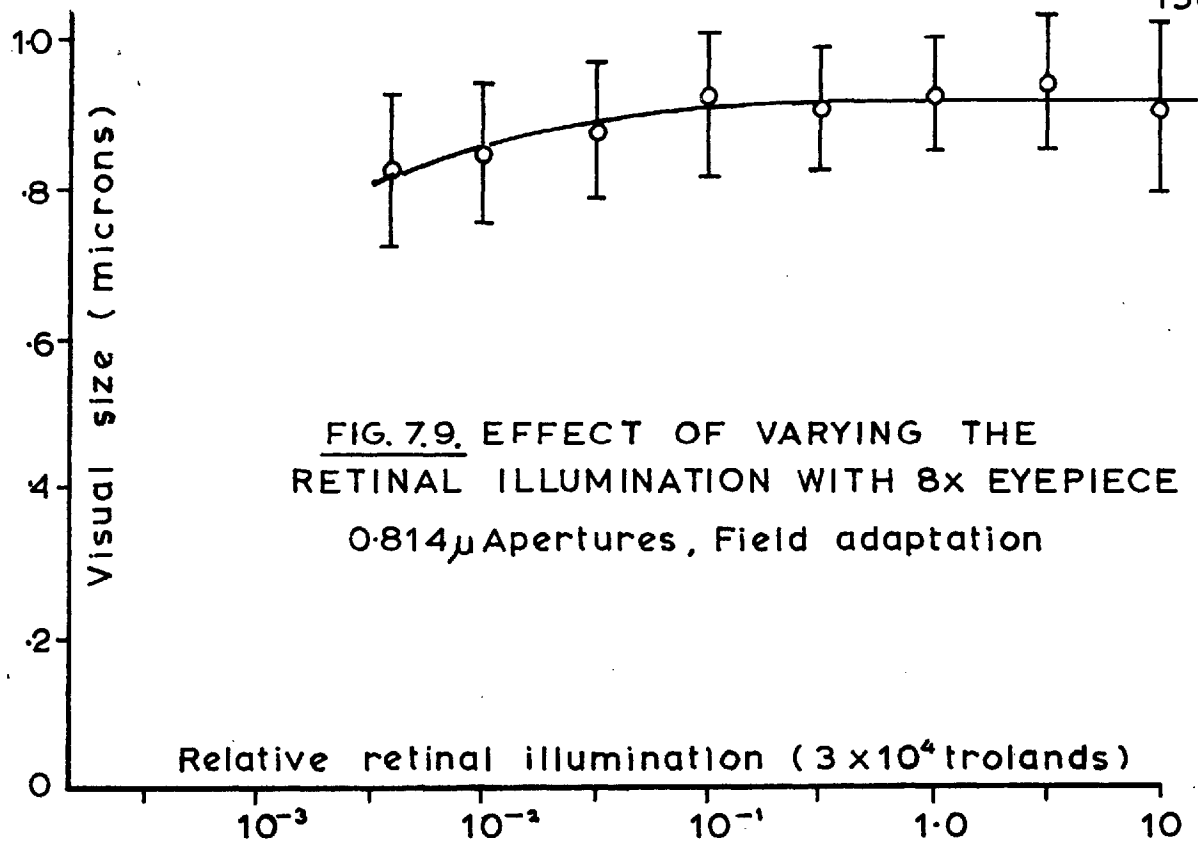

FIG. 7.9. EFFECT OF VARYING THE RETINAL ILLUMINATION WITH 8x EYEPIECE
0·814μ Apertures, Field adaptation

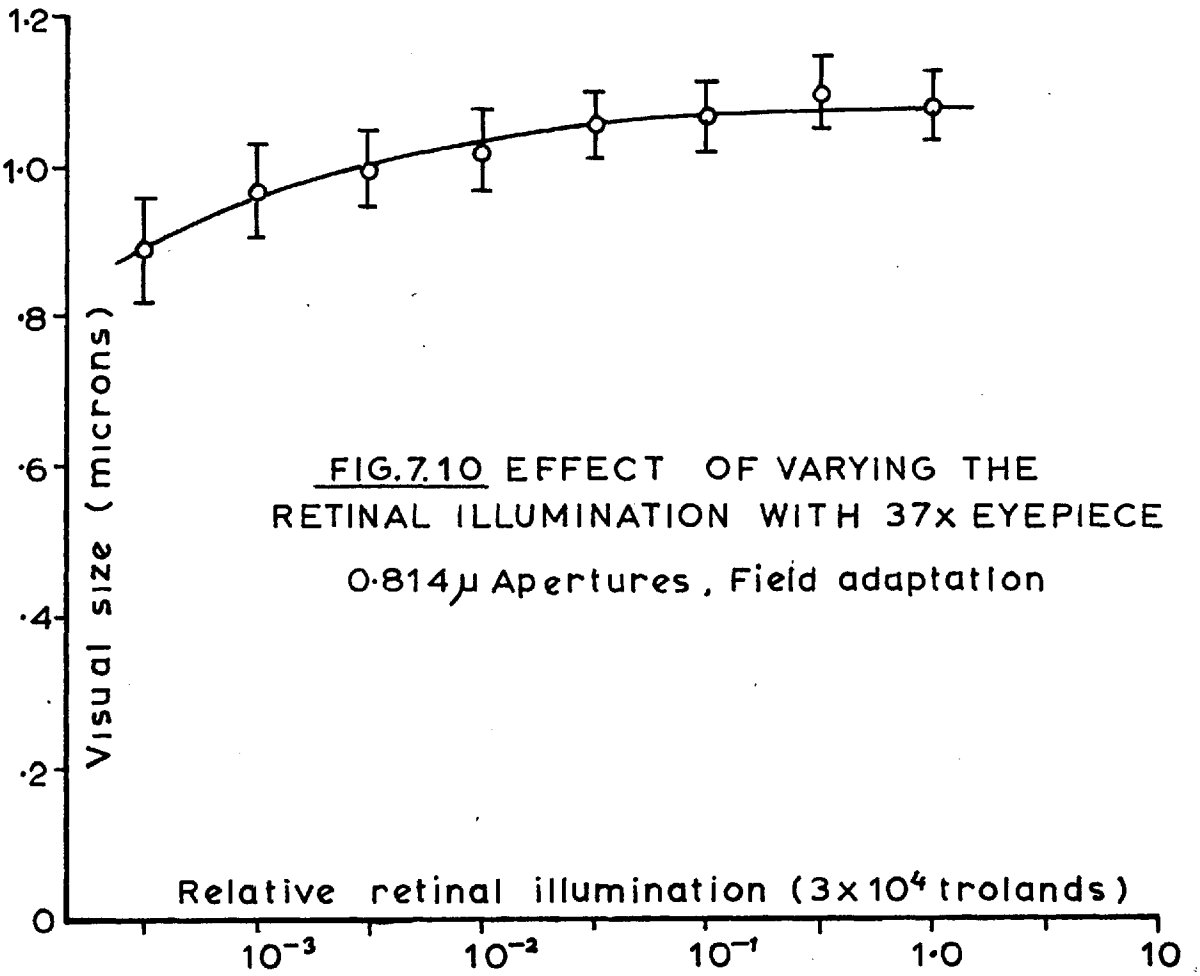

FIG. 7.10 EFFECT OF VARYING THE RETINAL ILLUMINATION WITH 37x EYEPIECE
0·814μ Apertures, Field adaptation

the range. The fact that a hundredfold increase in retinal illumination has no effect upon the visual size rules out the possibility that we are concerned with absolute values of luminance (i.e. threshold effects) and indicates that the ratio of the luminances in different parts of the image is the important factor (i.e. the transmission profile). When we reduce the luminance still further however the visual size does fall off rapidly, and a plot of Tv.s/T max shows a rapid rise (figs. 7.11 and 7.12). This is clearly comparable to the rise in the Fechner fraction with decreasing field luminance that was shown in fig. 2.5.

At the top of the range (ten times the normal illumination) a certain amount of glare was present, this being reflected by the larger standard deviation of the visual sizing results. In fact it appears that the range of retinal illumination over which the visual size remains constant corresponds remarkably closely to the range where the viewing conditions seem comfortable to the observer. Thus at low illumination levels the image is difficult to see while at high levels glare is present with its attendant inaccuracies.

7.5. The Effect of Condenser Aperture.

In section 6.4, fig. 6.3, photoelectric scan curves were given showing the form of the image transmission profile of 0.814 μ holes at the best visual focus for various ratios of condenser to objective N.A. It was pointed out that an increase in the coherence of the illumination

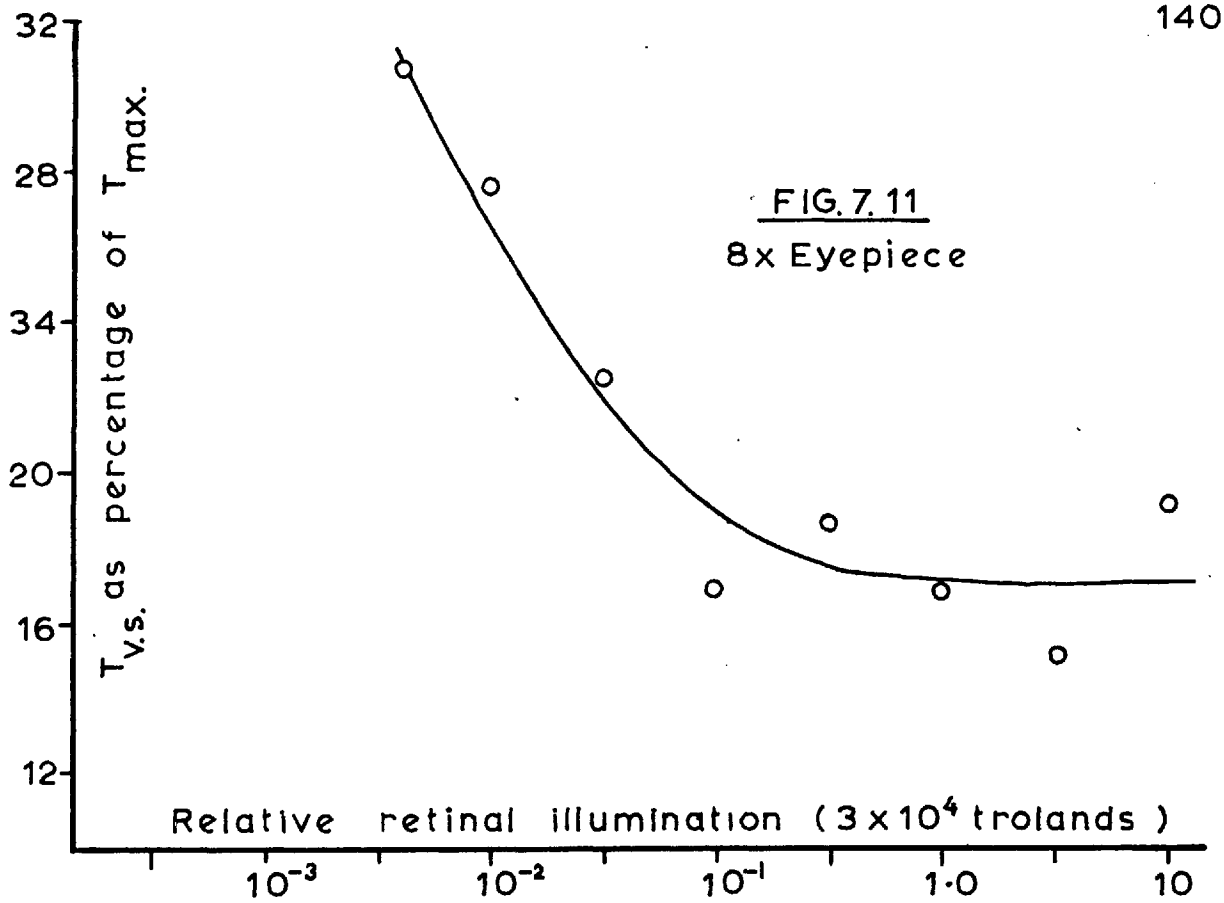

FIG. 7.11

8x Eyepiece

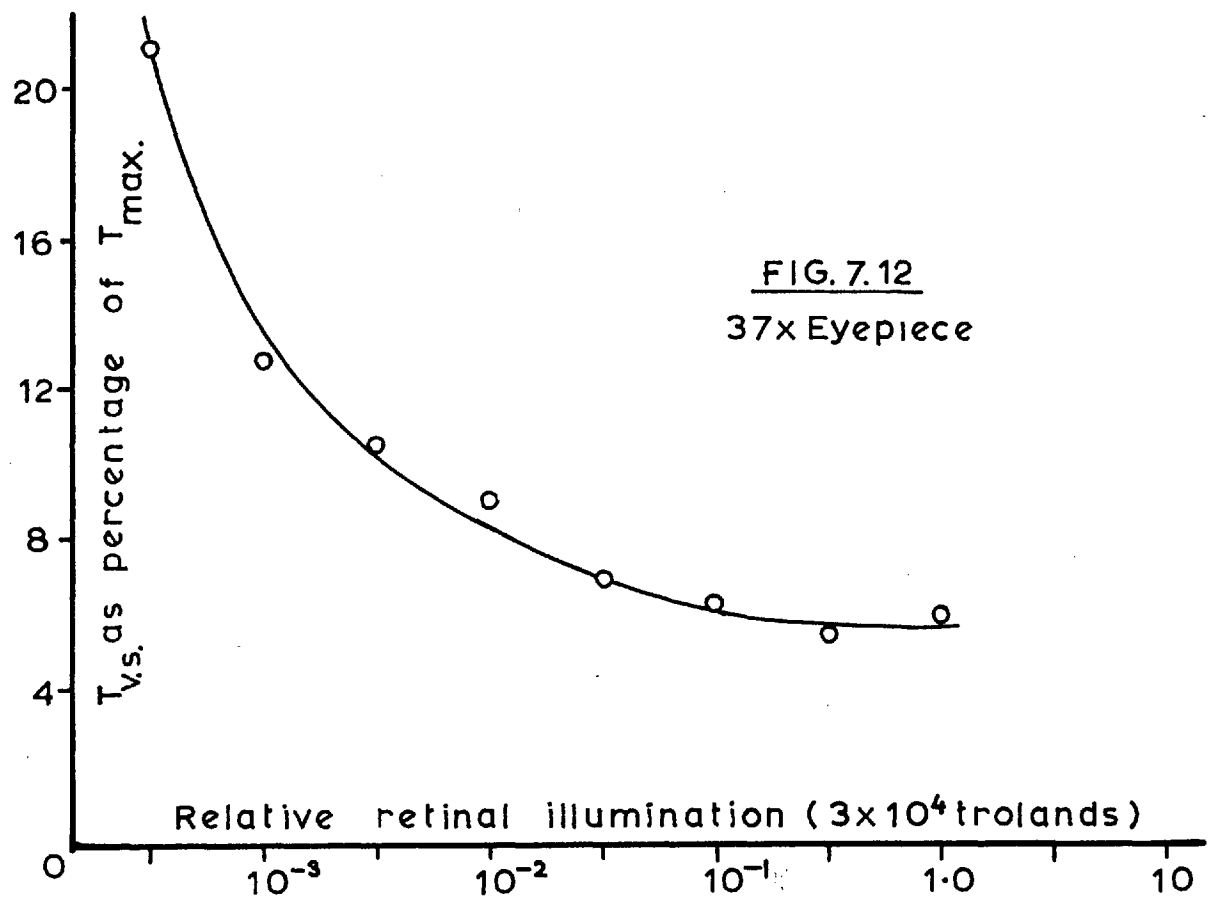

FIG. 7.12

37x Eyepiece

resulted in images of greater contrast and smaller lateral dimensions being given. To investigate whether this was reflected in the visual sizing results, the same objects and illuminating conditions were used in conjunction with a 20x eyepiece and a retinal illumination of 3×10^4 trolands. The eye was allowed to adapt naturally to the field and sixty results were obtained for each value of 'S', these being tabulated below.

Table 7(viii) Variation in visual size with condenser aperture.

N.A. of condenser	'S' value	Visual size (μ)
1.28	1.0	1.086 $\pm$ .042
1.17	0.91	1.096 $\pm$ .049
0.71	0.55	1.021 $\pm$ .037
0.36	0.28	0.997 $\pm$ .037

It is apparent that a reduction in the N.A. of the condenser leads to a reduction in the visual size as expected. The appearance of the image was considerably 'crisper' at the smaller S values, and even the small reduction in S from 1 to 0.9 perceptibly improved the image contrast.

CHAPTER 8

THE IMAGES OF OPAQUE DISCS

8.1. General.

No independant check by electron microscopy has yet been possible on the sizes of the opaque discs produced from the polystyrene spheres by the method described in section 3.3. However the double-shadowing technique used to make the discs is essentially a direct extension of that used to produce the apertures, this having been shown to give accurate reproductions of the sphere profiles, and there seems no reason why the discs should not be of the same quality. Certainly the results of measurements on the disc images with the apparatus exhibit approximately the same degree of consistency as is obtained with the well-proven aperture test objects and the agreement between the experimental and theoretical results is about equal for both types of object. Restrictions in the amount of time available have however limited the number of experimental results so far obtained with the discs, so that there is a correspondingly higher degree of uncertainty in the results as compared with those for the apertures, where the experimental measurements were more thorough.

In general, the form of the disc images and their subjective appearance are found to be affected by exactly the same variables as were of importance in the case of the apertures. The image transmission profiles and visual

sizes can be measured in the same way as those of the apertures, the point taken as the visual edge in measuring the visual size being that where the subjective brightness of the image is just lower than that of its surround. The adaptation level of the eye when measuring the size of the disc images is of course normally governed by the luminance of the microscope field, the distinction between the various adaptation states used with the apertures not being necessary in this case.

Studies have been made of the effect of variations in the condenser N.A. on the disc images, including a brief investigation of the occurrence and position of the Mach bands seen. Transmission profiles and visual sizes have been measured for discs having diameters ranging from 0.557 to 2.79 μ under full-cone illuminating conditions.

8.2. The Influence of Condenser Aperture.

It is to be expected that alterations in the coherence of the illumination produced by variations in the N.A. of the condenser will affect the form of the disc images.

To discover the exact nature of the changes occurring in the transmission profiles, scans were made of the images of 1.171 μ discs at four different values of condenser aperture, giving S values of 1.0, 0.91, 0.55 and 0.28. The illuminating wavelength was kept at the standard 5300 $\mathring{A}$, the tubelength at 180 mm and the objective N.A. at 1.28. The transmission profiles found for each S value are shown

in fig. 8.1, each profile being the mean of 10 scans. The halfwidths and central transmissions of the images are tabulated below.

Table 8(i). Variation in image profiles of 1.171 μ discs with condenser N.A.

Condenser N,A.	S	Half width (μ)	S.D. (μ)	Central transmission (%)	S.D. (%)
1.28	1.0	1.215	.035	18.2	2.6
1.16	0.91	1.235	.050	8.0	0.6
0.70	0.55	1.250	.030	6.0	1.1
0.36	0.28	1.255	.045	6.2	2.0

It is apparent that the halfwidth increases steadily as the condenser is stopped down, while the corresponding central transmission decreases. As may be expected, this is the exact reverse of the result found in the case of the aperture images. Noticeable in the transmission curves of fig. 8.1 are the heavy diffraction rings that are produced as the condenser N.A. approaches 0.3.

The visual sizes of the disc images were measured under thewe same conditions, the results being given below. A 20x eyepiece was used in conjunction with a retinal illumination of 3×10^4 trolands, 120 measurements being made for each value of S.

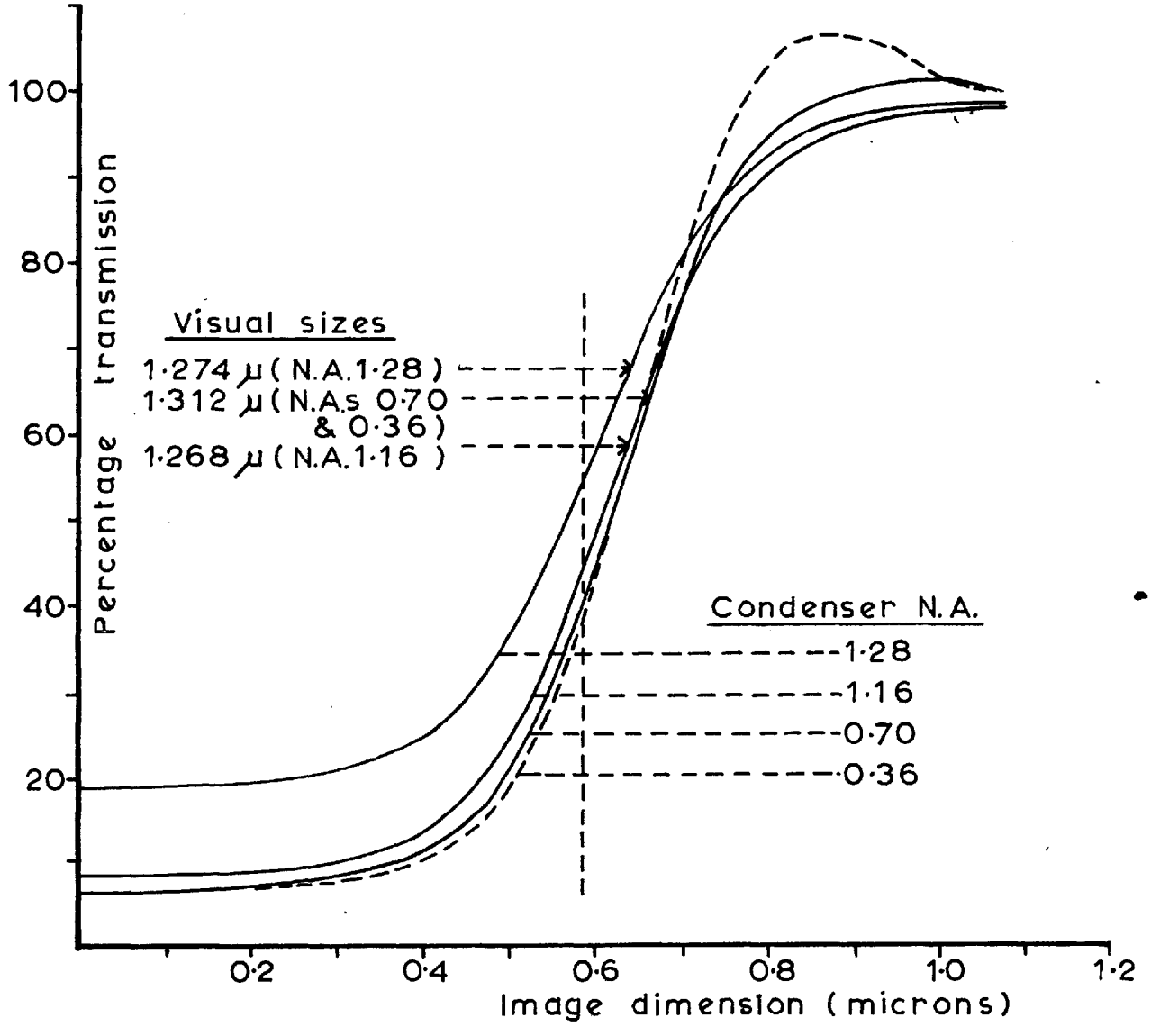

FIG. 8.1 VARIATION OF RADIAL IMAGE TRANSMISSION PROFILE WITH CONDENSER N.A. FOR 1·171μ DISCS

Objective N.A.=1·28, T.L.=180mm, λ= 5300±50Å

Table 8(ii). The variation of visual size of 1.171 μ discs with condenser N.A.

1 Condenser N.A.	2 S	3 Mean Visual Size (μ)	4 S.D.	5 Trans. at edge %	6 Variation (app.) %
1.28	1.0	1.274	.065	65	± 9
1.16	0.91	1.268	.063	58	± 9
0.70	0.55	1.312	.061	63	± 11
0.36	0.28	1.312	.070	63	± 13

The visual size clearly remains, within the limits of experimental error, remarkably constant. This is explicable when the visual sizes are compared with the corresponding transmission curves (see columns 5 and 6) which show that the visual edge in all cases is set at a transmission of approximately 60%. All the image transmission profiles have roughly the same width at this point and hence all the visual sizes are the same. The greater 'transmission difference' between the surround and the visual edge in the case of the disc images as compared with those of the apertures is of course to be expected from contrast considerations. It should be noted that the visual size still exceeds the true size under all conditions however.

Exact comparison with the theoretical results for disc images of Canals-Frau and Rousseau (1958) is impossible since the experimental results are for a disc diameter of 17.7 Z units, while their results extend only to a figure

of 4 Z units. However, they give some results (their fig. 6) for images of a straight edge between transparent and opaque fields with S values between 0.2 and 1.0 and with rectangular pupils; these results are reproduced in fig. 8.2. These may be compared qualitatively with the experimental results, when it can be seen that the fringes on the light side of the edge are very well reproduced. Qualitative agreement also exists with the theoretical results.for the variation in the central transmission with condenser N.A.

8.3. The Occurrence of the Mach Effect.

Although during the visual experiments with the circular apertures the Mach effect associated with the luminance gradients at the image edges probably accounted in part for the relatively sharp-edged images seen, no distinct bright or dark bands of the type normally associated with the effect were visible. With the discs however, especially those of larger diameter, a narrow bright band was generally observed inside the border of the dark disc image, other bright or dark bands also being seen depending upon the exact disc diameter and illuminating conditions.

The presence of dark or bright rings around a disc image may of course either be a subjective visual effect or a pure diffraction phenomenon. In order to verify that the former was the case, 1.83 μ discs were observed under constant conditions of wavelength and objective N.A., the luminance of the field being high enough to avoid any

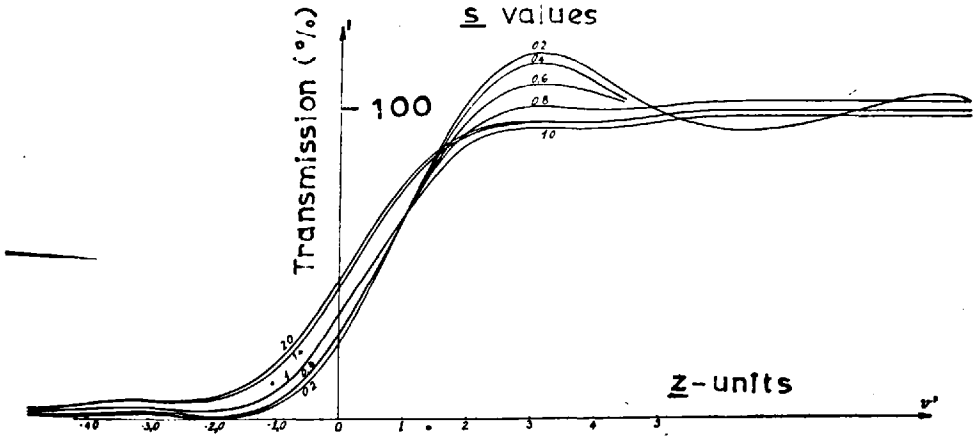

Fig. 8.2. The image of a straight edge (after Canals-Frau and Rousseau).

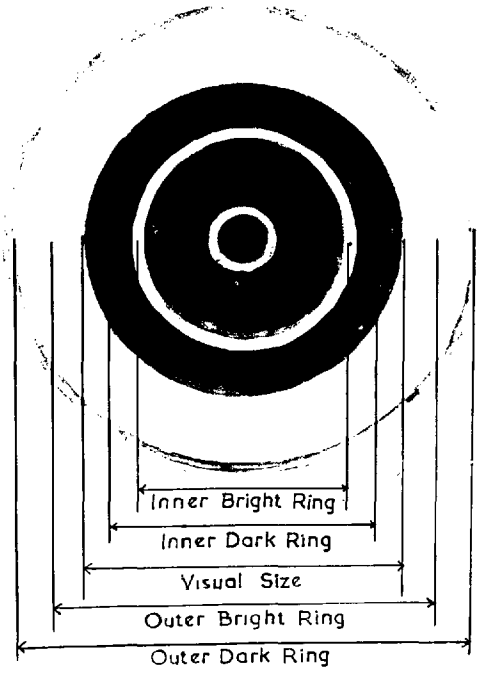

Fig. 8.3 The Mach effect seen with 1·83 μ discs

unwanted low-luminance effects. The subjective appearance of the image seen is shown diagramatically in fig. 8.3, the various diameters being measured in the usual way with a filar eyepiece, giving setting errors of the order of 0.04 μ. The following features governing the presence of the various bright and dark rings may be noted:

a) The outer dark ring was only detectable when the condenser N.A. fell below about 0.4, its diameter being apparently constant with varying condenser N.A. below this level.

b) The inner bright ring was visible at all condenser N.A.s, although its contrast was considerably enhanced when $\underline{S}$ fell below about 0.6. The position and width of the ring were, within the limits of experimental measurement, unaffected by the stopping down of the condenser.

c) The use of eyepiece powers varying from 5x to 37x had no apparent effect upon the presence and relative positions of the bands, although no exact measurements were made to verify this.

The subjective brightness distribution observed when the condenser N.A. was 0.36 is compared with the corresponding transmission profile in fig. 8.4. The broken line represents the brightness distribution, the ordinates being arbitrary and relative only. It is apparent that the bright and dark bands are seen at the junctions between the areas of approximately constant luminance and those where a steep luminance gradient exists. This corresponds exactly to the conditions under which the Mach bands are normally

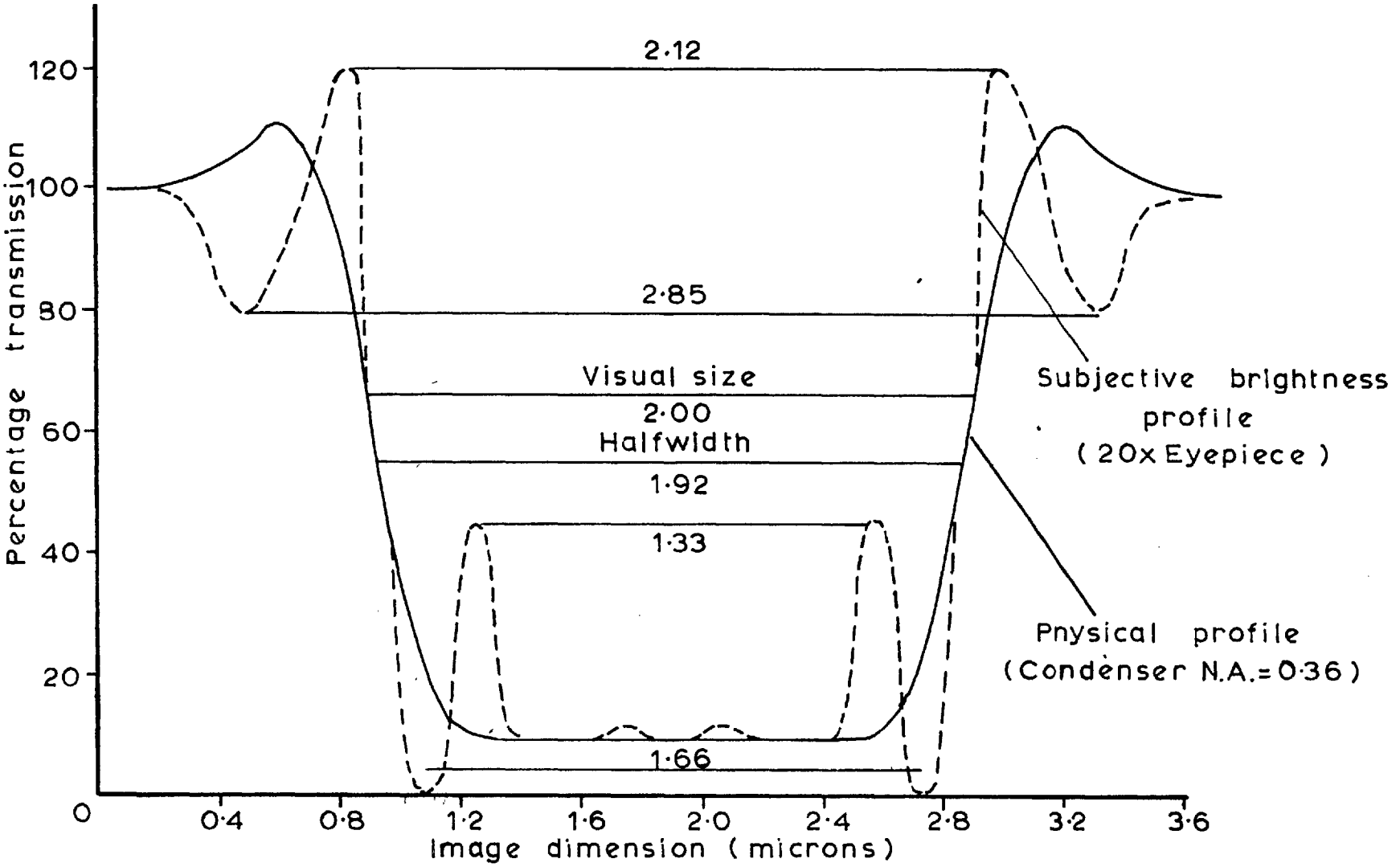

FIG. 8.4 COMPARISON BETWEEN THE PHYSICAL & SUBJECTIVE LIGHT DISTRIBUTIONS IN THE IMAGE OF A 1·83 μ DISC

seen. The increased visibility of the bands seen experimentally when the condenser aperture is decreased is directly related to the steeper edge transmission gradient given under these conditions. It is clear from fig. 8.4 that there is no possibility of the bands being diffraction rings, although the latter obviously do exist at very low condenser N.A.s.

The only anomalous effect observed in the images of the 1.83 μ discs was the presence, under some illuminating and observing conditions, of the very weak central bright ring of diameter 0.3 μ shown in fig. 8.3. This is not explicable in terms of the simple Mach effect and is probably a visual contrast effect related to the angular separation between the two opposite edges of the image, it only appearing with a 20x eyepiece, giving an angular visual size of about 54'. This suggestion is supported by the fact that no corresponding ring was observed with the images of larger or smaller discs with a 20x eyepiece, although the main bright and dark Mach rings continued to be visible.

Although from the visual sizing point of view it might be thought that the presence of these bright and dark bands could prove distracting, in practice this is not found to be the case. Indeed, the 'sharpening' of the visual edge by reason of the greater subjective contrast between the image and its surround undoubtedly allows more consistent visual sizing results to be obtained and is therefore of considerable benefit.

8.4. Disc Images Under Full-Cone Illumination.

The image transmission profiles for the full range of discs that have so far been prepared were measured in the usual way with equal objective and condenser apertures, the wavelength being 5300 Å and the tubelength 180 mm. The discs were focussed to give the minimum transmission at the centre of their images. The mean profiles obtained are shown in fig. 8.5, the central transmissions and halfwidths being given in table 8(iii) below.

Table 8(iii) The images of circular opaque discs.

Disc diameter (μ)	No. of Scans.	Mean half width (μ)	S.D. (μ)	Mean Central trans-mission %	S.D. (%)
0.557	5	0.69	.034	15.6	4.0
0.814	6	0.90	.010	19.5	0.5
1.171	10	1.215	.035	18.2	2.6
1.83	5	1.85	.040	11.9	1.2
2.79	3	2.92	.11	5.2	0.3

It is apparent that the halfwidth generally exceeds the disc diameter and that, unlike the apertures, the central transmission is relatively insensitive to changes in object diameter over this range.

The visual sizing results obtained under the same instrumental conditions with a 20x eyepiece and a field luminance giving a retinal illumination of 3×10^4 trolands

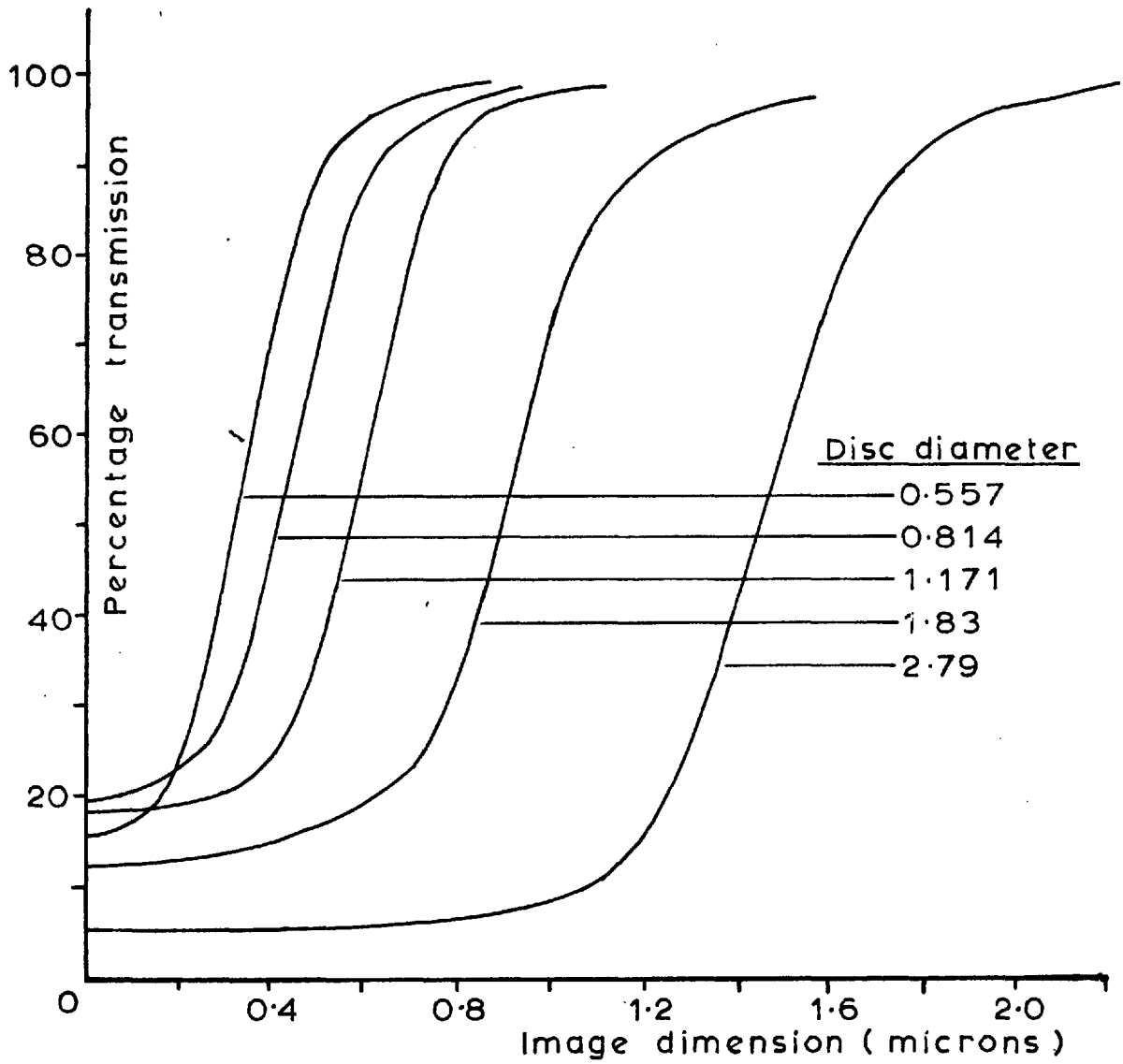

FIG. 8.5 RADIAL IMAGE TRANSMISSION PROFILES FOR THE OPAQUE DISCS INDICATED

$(N.A.)_{o.g.} = (N.A.)_{cond.} = 1{\cdot}28$, T. L. = 180 mm, $\lambda = 5300 \pm 50$ Å

are given below.

Table 8(iv) Visual sizing of opaque discs.

Disc diameter (μ)	Visual size (μ)	S.D. (μ)	No. of readings	Transmission at visual edge (%)	Variation (app.) %
0.557	0.712	.076	120	60	± 10
0.814	0.886	.052	60	58	± 7
1.171	1.274	.065	120	65	± 9
1.83	1.882	.093	60	60	± 10
2.79	3.093	.116	90	67	± 10

There is considerable oversizing at all sizes, the transmission at the visual edge being about 60% in every case, a value in agreement with that found in section 8.2.

Comparison of the experimental disc image profiles with the results of Osterberg and Smith is more difficult than in the case of the aperture images, since there is less overlap between the object diameters used for the theoretical and experimental results. Fig. 8.6 shows the half-widths found in both cases, measured with respect to the central transmission, plotted against the true disc diameter, the dimensions being in Z units. The broken line is drawn at 45° to either axis. It would appear that, within the limited range of overlap of size, the measure of agreement between the two sets of results is about the same as was found for the aperture images (see fig. 6.5(b)).

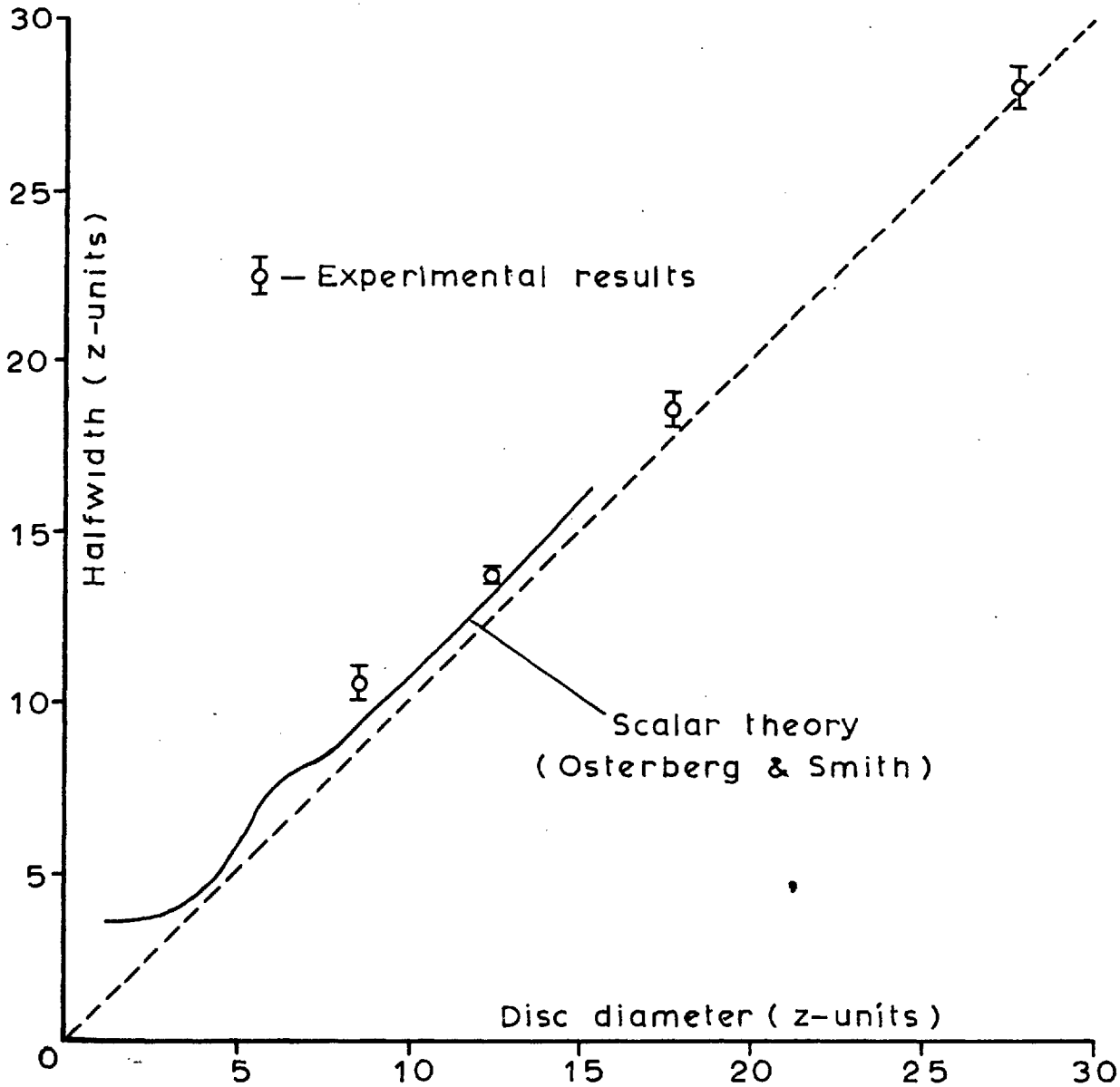

FIG. 8.6 VARIATION OF IMAGE HALFWIDTH WITH DISC DIAMETER

Since, unlike the apertures, the central transmission in the disc images does not vary markedly with object diameter when this exceeds about 4 Z units in either the experimental or the theoretical results, no comparison has been made of the variation of this quantity with disc size for the two cases. However, it is interesting to note that the theoretical prediction that smaller diameter discs may have smaller central transmissions appears to find substantiation in practice for those of 0.557 μ diameter (fig. 8.5), although, due to the limited number of the results, this must be treated with some reserve.

CHAPTER 9

DISCUSSION AND CONCLUSIONS

From the experimental results given in the previous chapters it is possible to compare the forms of the images of small objects found in practice with those predicted by scalar diffraction theory. In addition, the optimum conditions for visual sizing work may be deduced, together with an estimate of the limitations and errors inherent in such techniques.

9.1. The Diffraction Images of Small Objects.

It is apparent from the scanning results given in chapters 6 and 8 that significant quantitative differences exist between the form of the images predicted by scalar diffraction theory and those found in practice with a high-aperture objective. Although the optical and recording conditions used experimentally might be blamed in part for these discrepancies, there is little doubt that, in the main, they are due to the approximations of scalar diffraction theory being inapplicable to systems of high N.A.

The differences, which amount to about 10% of the parameter in the typical case of the halfwidth of the transmission profile of the image, are however sufficiently small to offer encouragement for the further development of such techniques as the variable phase-contrast method of measuring the size of objects below the resolution limit

of the objective, as described in section 1.9. The validity of such methods depends upon the correctness of the scalar diffraction theory on which they are based. The potential usefulness of the variable phase method deserves further emphasis in view of the conclusions reached in section 9.3. below regarding the impossibility of deducing the true diameter of an object, when this lies below the resolution limit of the sizing objective, from the visual size measured under normal bright-field conditions.

The fact that the transmission of clear apertures of diameter as large as ten times the resolution limit of the objective is found experimentally not to reach 100% and that that of similar opaque discs does not reach zero is of interest in its relevance to microspectrophotometric measurements on the absorption of small objects as described, for example, by Swift and Rasch (1956). Clearly if perfectly transparent and opaque particles of such comparatively large diameter give the 'false' readings found for their absorption, similar errors must be expected for partially absorbing objects, the errors being even larger for objects whose diameters approach the resolution limit more closely. Although the experimental results were for objects of very small thickness, the same effects may be expected for thicker objects and it is probable that, for even approximate accuracy in absorption measurements, the object must have a diameter of at least 40 $\underline{Z}$ units.

9.2. The Optimum Conditions for Visual Sizing.

The results of chapter 7 show that no unique value exists for the visual diameter of the image of an object formed under fixed conditions of condenser and objective aperture, the visual size varying widely with variations in the values of the parameters controlling the visual response of the eye. In general the size obtained is found to differ from the true size of the object.

The problem involved in making measurements of the size of objects by visual microscopy thus reduces to one of specifying the conditions under which the visually measured diameter of the image is consistent and as independant as possible of the exact visual conditions prevailing and the particular visual responses of the observer. Once having obtained a consistent visual size, a correction factor, appropriate to the values of numerical aperture in use, can be applied to give the true size of the object. What then are the conclusions that can be drawn from the experimental results regarding the conditions under which this consistency is given?

It will be recalled first, from the results described in section 7.3, that, for fixed values of retinal illumination and adaptation, the other instrumental conditions being constant, the visual size varied with the total magnification until the latter reached a value of about 1900x with the 1.28 N.A. objective in use. Magnifications above this value yielded a constant visual size, this constancy being

reached at approximately the same magnification whatever the adaptation state of the eye or the retinal illumination, although the actual value of the constant size varied with these quantities. Thus it appears that, for consistent visual sizing results with non-periodic objects illuminated with green light, a total magnification of at least 1500x the N.A. of the objective must be used, this being considerably more than that derived on the basis of Abbe theory.

Next we may note that the results of section 7.4 showed that, with other conditions constant, the visual size increased with the retinal illumination until this reached a value of about 3×10^3 trolands, when further increases yielded the same visual size. This retinal illumination corresponds to that produced by a field of luminance approximately 0.4 stilb when viewed through a pupil of 1 mm diameter, or 0.04 stilbs viewed through the natural pupil, which has a diameter of about 3 mm at this level of luminance. The magnification in use affected the magnitude but not the constancy of this visual size, while light adaptation necessitated a slightly higher level of illumination. In all cases, the condition for constant visual size reduced effectively to the image having to appear comfortably bright.

Although the results of sections 7.3 and 7.4 were obtained with the aperture type of test object and 'down-the-tube' viewing, experience suggests that similar results are given with other types of non-periodic object and

projection viewing.

Combining the results of varying the retinal illumination and magnification, it becomes possible to construct a diagram showing the conditions under which the visual size of the image of an object, for a fixed value of S and for a particular adaptation state for the observer, remains constant. This is shown in fig. 9.1. The ordinate represents the visual size, while the abscissae show the retinal illumination and total magnification. It is apparent that a 'plateau' of visual size is reached when the magnification and retinal illumination exceed certain critical values, failure of one of the variables to reach the critical value yielding smaller visual sizes. The useful upper values for the abscissae are set by glare in the case of the retinal illumination and by the available eyepieces in the case of the magnification, this restriction being paralleled in projection viewing by the lack of light at large screen magnifications. With aperture objects a higher initial state of light adaptation of the eye of the observer results in the whole plateau moving downwards parallel to the Z axis to give smaller visual sizes for the same values of the abscissae. With opaque objects this effect will not occur, since the adaptation level is normally governed by the retinal illumination given by the clear areas of the field and is hence no longer an independant variable.

Thus it is to be recommended that for visual sizing work with non-periodic objects the conditions should be

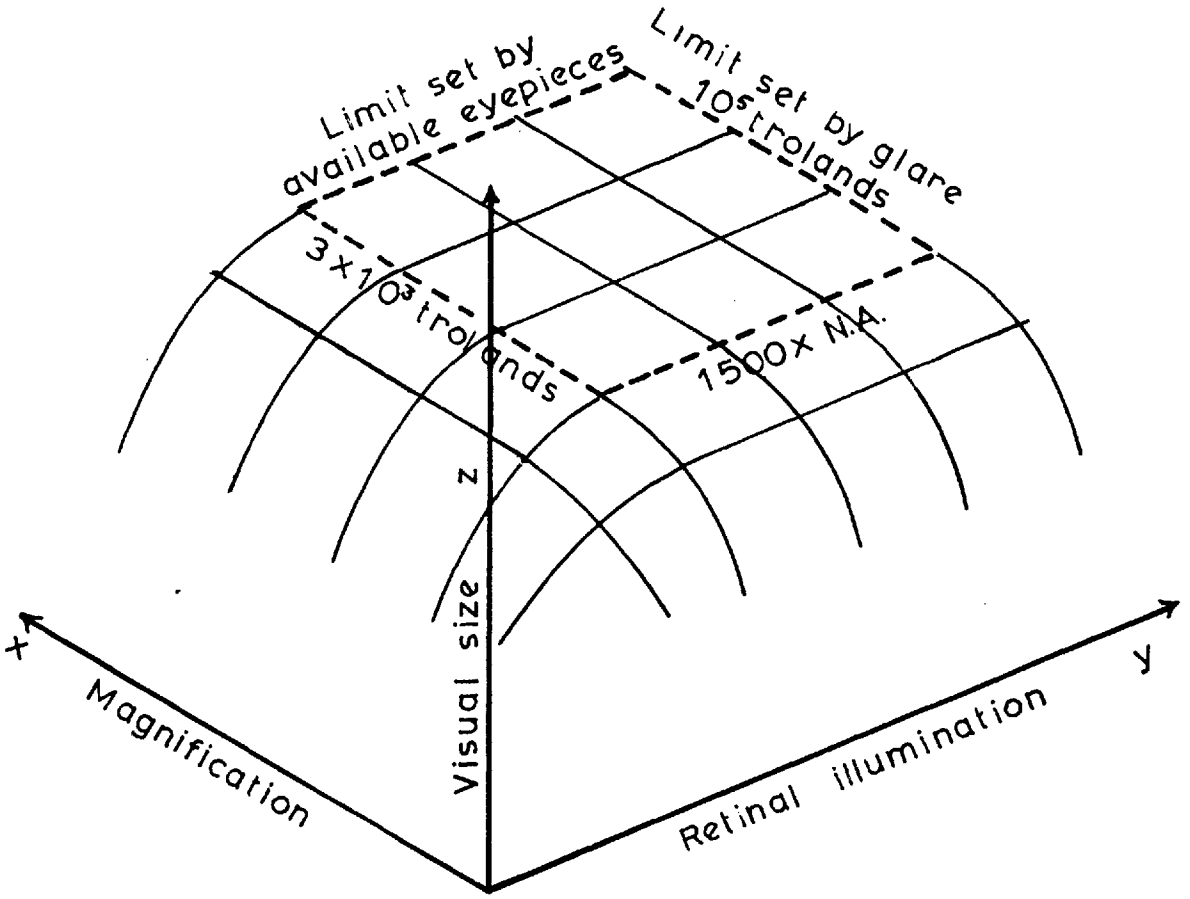

FIG. 9.1 VARIATION OF VISUAL SIZE WITH OBSERVING CONDITIONS

adjusted so that the observer is working well away from the edges of the sizing plateau, that is, the total magnification should be of the order of 2000x the objective N.A. and the retinal illumination should be about 10^4 trolands. It is preferable that the observer should work in well-lit external conditions so that his eyes remain light adapted. This will ensure that the results are more reproducable, a conclusion reached in section 7.2. There is no doubt that such conditions also reduce the fatigue involved in making measurements and there is a technical advantage in that it is easier to make notes and take readings.

9.3. The Limitations and Errors of Visual Sizing.

Using the optimum observing conditions detailed in the previous section, important conclusions may be drawn from the results found experimentally regarding the size range of objects that can be measured visually using bright-field microscopy and the relation between the measured and true sizes of the objects.

Considering first the size of the smallest object that can be measured using the simple visual sizing technique, the results given in table 7(ii) and fig. 7.3 show that, for bright objects in a dark surround, the visual sizing results start to become ambiguous when the object diameter falls below about 6 $\underline{Z}$ units, that is, between one and two times the resolution limit of the sizing objective. Although the experimental measurements, made on large numbers of objects all having the same size, continue to show a

slight fall of visual size with true size below this level, in practice such large numbers of measurements will not generally be possible, so that the small variation given in table 7(ii) will be lost. Thus objects whose diameter is less than this limit all give images having approximately the same visual size, although both the subjective brightness and physical luminance of the images diminish as the object size is reduced, assuming the illumination of the objects is kept constant. For such objects therefore, the true size cannot be deduced from the visual size, although it might be possible by comparing the subjective brightness of their images to say that one object is larger than the other.

The experimental results of table 8(iv) do not provide sufficient evidence for the case where the objects are opaque in a bright field, since the smallest test objects used were twice the resolution limit of the objective in diameter. The problem for such objects is somewhat different however, since, whereas a transparent object in an opaque surround can always be made visible, providing it is sufficiently intensely illuminated, the contrast of the image of an opaque object in a transparent surround may not be great enough for it to be detectable visually. The contrast of the image of a particular object will vary with the coherence of its illumination, while whether this contrast is larger enough for the image to be detectable by the observer will depend upon the luminance level, the

angular subtense of the image and the other visual factors discussed previously. It would appear, on the basis of experiments with 0.557 μ discs and a low power objective whose N.A. could be varied with a Davis diaphragm, that the diameter of the smallest opaque disc that can be seen with the microscope under the optimum sizing conditions is about $1/5$ of the resolution limit of the objective, that is about 0.75 $\underline{Z}$ units. As has been mentioned, the test objects used for the experimental results of chapter 8 have a minimum diameter of 8.5 $\underline{Z}$ units, but more recent work by Leifer (1961) with smaller sizes of test objects prepared by the same method seems to confirm that the results with opaque disc images are of the same form as those with circular apertures, that is, the measured visual size reaches an approximately constant value when the disc diameter falls below about 6 $\underline{Z}$ units, although for the same conditions of illumination the larger objects are seen in better contrast.

In general therefore, visual measurements of object size made with bright-field illumination can only be uniquely related to the true size of the objects where this exceeds about 6 $\underline{Z}$ units, a value slightly larger than the resolution limit of the objective (3.83 $\underline{Z}$ units). The measured visual size of objects smaller than this limit will approximate to a constant value (actually about twice the resolution limit of the objective) which is independent of the true size of the object.

For objects whose diameter is greater than this limit,

the results given in tables 7(ii) and 8(iv) show that with both transparent and opaque objects, viewed with full-cone illumination under the conditions specified in section 9.2, the visual size is larger than the true size of the object by about 0.1μ for the objective employed, that is, about 1.5 $\underline{Z}$ units. This oversize appears to be approximately independent of object size, although it should be remembered that the variation in individual measurements is of the same order of magnitude as the oversize itself.

The estimate of the oversize is only valid when the same sizing criterion as that used experimentally is applied. This is not necessarily the case, different criteria being used in some visual sizing methods. For example, where the area of the image of an opaque object is compared with that of a series of opaque areas on a graticule (see section 1.4) the eye probably estimates the image size in terms of the area whose contrast compared to its surround is about the same as that of the opaque graticule areas. This clearly is equivalent to setting the visual edge at a very low transmission and obviously results in a smaller visual size being given than would be obtained using the experimental criterion.

Stopping down the condenser will, according to the results of sections 7.5 and 8.2, decrease the visual size of transparent objects in an opaque surround and increase it slightly for opaque objects. The results show however that a modest reduction in condenser aperture, to give an

S value of about 0.8, has no significant effect upon the visual size but improves markedly the contrast of the image. Such a reduction is therefore to be recommended, since an improvement in image contrast considerably reduces visual fatigue in sizing work. This corresponds closely to the usual microscopist's rule that for visual work the best results are obtained when the condenser is stopped down until about $^2/_3$ of the area of the back aperture of the objective is filled with light. Further decreases in the condenser aperture are not desirable, since the visual size starts to vary with S, while diffraction rings round the images may become confusing.

It seems reasonable to suppose that similar results would be given in visual measurements of the dimensions of other objects which were not re-entrant in form and were of negligible thickness. It is, of course, impossible to generalise these results in a quantitative way to the case where the objects have a finite thickness. However, experiments conducted with the silver-coated spheres, produced during the attempts at disc preparation described in section 3.3 indicated that, after making appropriate allowance for the thickness of the silver layer the visual size again exceeded the true size for such objects.

There can be no doubt that considerable advantages accrue from the use of the shadowing technique of Hamilton and Phelps, described in section 3.2, when a particulate specimen is to be sized. This method, which gives trans-

parent profiles of the particles in an opaque film, is, of course, only usable when the size alone of the particles is required, since the features which allow a specimen to be separated, for example, into coal and stone dust are lost. The great advantage of the technique is that it not only allows images of high contrast to be obtained, but also removes all the problems of object thickness, refractive index and absorption, each of which will effect the image and hence the visual size under normal conditions. A further advantage is the improved ease of detection of particles below the resolution limit of the objective, although it must be remembered that such objects still cannot be sized.

9.4. The Influence of the Observer.

The possibility exists that the sizing results were strongly influenced by the acuity, thresholds and other visual responses of the observer (W.N.C.). This must be considered unlikely however.

Certain of the sizing experiments have been repeated by Leifer with an agreement that is well within the standard deviation of the results and the observations on, for example, the Mach effect, have been confirmed by several individuals.

It should be noted that the visual acuity of the observer, at 6/4, was slightly better than average, which might possibly mean that correspondingly higher magnifications than those quoted would be needed by some observers.

There is no reason to suppose that any significant differences in luminance discrimination or other properties occurred from those of the average eye. Since the measurements were all made in monochromatic green light, the complications of colour perception were absent.

It therefore seems reasonable to conclude that the sizing results obtained by other observers, providing they suffered from no marked visual defects, would not differ widely from those found by the present writer.

9.5. Conclusions.

From the experiments described in this thesis it is concluded that the optimum conditions for high-resolution visual sizing are that the observer should be light adapted, the image being viewed at a magnification greater than 1500x times the N.A. of the sizing objective. The image luminance must be high enough to give a retinal illumination of about 10^4 trolands. Under these conditions, the true size of the object may be deduced from the measured visual size by subtracting a factor of 1.5 $\underline{Z}$ units, providing that the object is thin and of high contrast and that its true size is not less than 6 $\underline{Z}$ units. The recommended sizing criterion must also be used. Single measurements of object size made in this way will have an accuracy of approximately $\pm$ 1 $\underline{Z}$ units.

REFERENCES

ANDREJEWSKI, W. (1952) Dissertation, Aachen.

A.S.T.M. STANDARDS (1951) E20-51T, 1539.

BACKUS, R.C. and WILLIAMS, R.C. (1948) J. Appl. Phys. 19, 1186.
(1949) J. Appl. Phys. 20, 224.

BARER, R. (1960) Nature 188, 398.

BECK, C. (1924) 'The Microscope', Part II, R. & J. Beck, London, p. 166.

BISHOP, D.L. (1934). J. Res. Nat. Bur. Stand. 12, 173.

BLACKTIN, S.C. (1946) Chem. & Ind. 65, 154.

BOND, W.L. (1954) J. Opt. Soc. Amer. 44, 429.

BRADFORD, E.B. (1952) J. Appl. Phys. 23, 609.
and VANDERHOFF, J.W. (1955) J. Appl. Phys. 26, 864.

BROWN, C.R. and YANT, W.P. (1935) U.S. Bureau of Mines Report 3289.

BRUMLEY, C.H. and RICHARDSON, D. (1950) J. Opt. Soc. Amer. 40, 800.

CANALS-FRAU, D. and Mme. ROUSSEAU, M. (1958) Optical Acta 5, 15.

CHAMOT, E.M. and MASON, W.L. (1958a) 'Handbook of Chemical Microscopy', Vol. 1. Chapman & Hall, 3rd ed. p.444.
(1958b) ibid, p.486.

CLENDINNEN, F.J. (1910) J. Roy. Micro. Soc. 1910, 368.

DELESSE, A. (1847) Comptes Rendus 25 (1847), 544.

DUNBAR, C. (1934) J. Sci. Instrum. 11, 85.

DUNN, E.J. (1930) Ind. & Eng. Chem., Analytical Ed. 2, 59.

DYSON, J. (1960) J. Opt. Soc. Amer. 50, 754.

ENGLAND, J.B.A. (1957) J. Sci. Instrum. 34, 208.

FAIRS, G.L. (1943) Chem. & Ind. 62, 374.
(1951) J. Roy. Micro. Soc. 71, 209.

FERET, L.R. (1931) Assoc. Int. l'Essai des Mat. 2, Group n.

FIORENTINI, A. et al., (1955) Optica Acta 1, 192

and ERCOLES, A.M. (1957) Optica Acta 4, 151.

FIORENTINI, A. (1958) Int. Coll. on Physical Problems of Colour Television, Optica Acta 5, 71.

FLEURY, P. (1951) 'Contraste de Phase et Contraste par Interferences', Ed. Rev. d'Optique, p. 15.

and MATHIEU, J.P. (1956) 'Images Optiques', Ed. Eyrolles, Paris, p. 458.

FRECHETTE, V.D. and SEPHTON, H.I. (1949) Bull. Amer. Ceram. Soc. 28, 496.

FRY, G.A. (1948). Amer. J. Optom., Monograph 45.

GALBRAITH, W. (1955). Quart. J. Micr. Sc. 96, 285.

GAMBLE, D.L. and PFUND, A.H. (1933) J. Opt. Soc. Amer. 23, 416.

GEHMAN, S.E. and MORRIS, T.C. (1932) Ind. & Eng. Chem., Analytical Ed. 4, 137.

GEROULD, C.H. (1950) J. Appl. Phys. 21, 183.

GREEN, H. (1921) J. Franklin Inst. 192, 637
(1927) J. Franklin Inst. 204, 713.

HALE, A.J. (1958) 'The Interference Microscope in Biological Research', Livingstone.

HAMILTON, R.J. et al., (1954) Brit. J. Appl. Phys. Suppl. 3, 101.

and PHELPS, B.A. (1956) Brit. J. Appl. Phys, 7, 186.

HARTRIDGE, H. (1954) J. Queckett Micro. Club Ser. 4, 4, 57.

HAWKSLEY, P.G.W. (1952) Bull. Brit. Coal. Util. Res. Council 16, 117.

HEYWOOD, H. (1937) Chem. & Ind. 56, 149.
(1945) Trans. Instn. Min. Metall. 55, 391.

HOLDSWORTH, J.F. et al. (1954) Brit. J. Appl. Phys., suppl. 3, 96.

HOOKE, R. (1655) 'Micrographia'

HOPKINS, H.H. (1950) 'Wave Theory of Aberrations' Oxford U.P. pp.86, 140.
and BARHAM, P.M. (1950) Proc. Phys. Soc. B, 63, 737.

HUITT, J.L. (1954) Amer. Aossoc. Petr. Geol. Bull, 38, 159.

HUNT, R.W.G. (1953) J. Phot. Sci. 1, 149.

LEIFER, I. (1961) Private communication.

LOVELAND, R.P. and TREVELLI, A.P.H. (1927) J. Franklin Inst. 204, 193, 377.

LOVELAND, R.P. (1952) A.S.T.M. Symp. on Light Microscopy, No. 143, 94.

MACADAM, F.A. and TAYLOR (1946) B.P. 592, 815.

MAINLAND, D, (1929) J. Anatomy 63, 345.

MARECHAL, A. (1953) Rev. d'Optique 32, 649.

MARTIN, G. et al. (1923) Trans. Brit. Cer. Soc. 23, 61.

MAY, K.R. (1945) J. Sci. Instrum. 22, 187.

MING FENG, I. (1951) J. Appl. Phys. 22, 820.

McDOUGALL, W. (1903) Proc. Physiol. Soc. 1, 19.

McGINN, J. H. (1956) U.S. Pat. 2, 730, 008.

NELSON, E.M. (1903) J. Roy. Micro. Soc. 1903, 579.
(1904) J. Roy. Micro. Soc. 1904, 269.

OSTERBERG, H. (1947) J. Opt. Soc. Amer. 37, 726.
and PRIDE, G.E. (1950a) J. Opt. Soc. Amer. 40, 14.
and PRIDE, G.E, (1950b) J. Opt. Soc. Amer. 40, 64.

and SMITH, L.W. (1960) J. Opt. Soc. Amer. 50, 362.

PATTERSON, H.S. and CAWOOD, W. (1936) Trans. Farad. Soc. 32, 1084.

PAYNE, B.O. (1950) J. Roy. Micro. Soc. 1950, 225.
(1954) J. Roy. Micro. Soc. 1954, 108.

RICHARDS, O.W. (1959) A.S.T.M. Symp. on Microscopy, No. 257, 6.

ROBINS, W.H.M. (1952) Nature 170, 583.
(1954) Brit. J. Appl. Phys. Suppl. 3, 189.

RONCHI, V. (1957) 'Optics - The Science of Vision', N.Y. Univ. Press, p. 258.
(1958) Int. Coll. on Physical Problems of Colour Television Optica Acta 5, 37.

SCAMMON, R.E. and SCOTT, G.H. (1927) Anat. Rec. 35, 269.

SCHEDLING, H. (1958) Acta Physica Austriaca 2, 13.

SCOTT, G.D. (1949) J. Appl. Phys. 20, 417.

SENNETT, R.S. and SCOTT, G.D. (1950) J. Opt. Soc. Amer. 40, 203.

SIEDENTOPF and SZIGSMONDY (1903) Ann. Phys. 4, 1.

SLANSKY, S. (1955) Optica Acta 2, 119.

SLATER, P.N. (1957) J. Queckett Micro. Club. Ser. 4, 4, 8.
(1958) Ph.D. Thesis, London.
(1960) 'Optics in Metrology' Pergamon Press, p. 269.

SMITH, L.W. (1960) J. Opt. Soc. Amer. 50, 369

SOPER, A.K. (1954) Brit. J. Appl. Phys. Suppl.3, 120.

SPENCER, C.J.D. and WELFORD, W.T. (1961) J. Sci. Instrum. (to be published)

SPINELL, E.M. and LOVELAND, R.P. (1960) J. Roy. Micro. Soc., 1960, 59.

SPITTA, E.J. (1920) 'Microscopy' Murray, 3rd. Ed., p. 265.

STEEL, W.H. (1953) Rev. d'Optique 32, 4.

STRONG, J. (1938) 'Modern Physical Laboratory Practice' Blackie, p. 380.

SWIFT, H. and RASCH, E. (1956) 'Physical Techniques in Biological Research' vol. III, Academic Press, N.Y., p. 353.

THOULESS, R.H. (1922) Brit. J. Psychol. 13, 310.

TIMBRELL, V. (1952) Nature 170, 318.

TOLANSKY, S. (1948) 'Multiple Beam Interferometry', Clarendon Press.

WADSWORTH, F.L.O. (1894) Astrophys. J. 2, 264.

WALSH, J.W.T. (1953) 'Photometry', Constable, 2nd. Ed.

WALTON, W.H. (1948) Nature 162, 329.

WATSON, H.H. (1952) Brit. Industr. Med. 9, 80.

and CRUISE, A.J. (1954) Engineering (Lond.) 177, 594.

and MULFORD, D.F. (1954) Brit. J. Appl. Phys. Suppl. 3, 105.

WEINSTEIN, W. (1955) J. Opt. Soc. Amer. 45, 1006.

WELFORD, W.T. (1960a) 'Optics in Metrology' Pergamon Press, p. 85.

(1960b) J. Opt. Soc. Amer. 50, 21.

(1961) J. Opt. Soc. Amer. (to be published)

WRIGHT, A.E. (1957) J. Sedim. Petrol. 27, 306.

ACKNOWLEDGEMENTS

My thanks are due to Dr. W.T. Welford for suggesting the problem and for much helpful guidance and encouragement, to Professor W.D. Wright for the use of the facilities of his laboratories and to other members of the Technical Optics Section, particularly Mr. C.J.D. Spencer, for their useful criticism and suggestions.

I am indebted to the National Coal Board for financing this research.